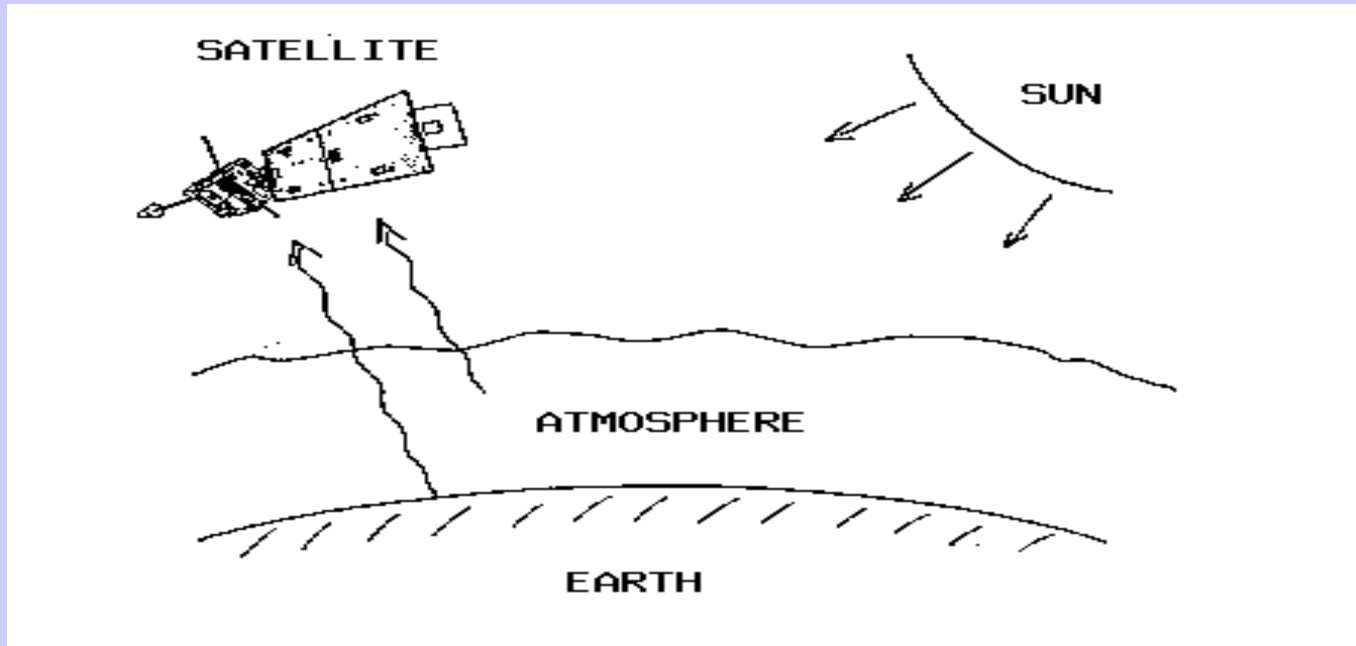


Summary of Satellite Remote Sensing Concepts

Madison
29 Mar 2013

Paul Menzel
UW/CIMSS

Satellite remote sensing of the Earth-atmosphere

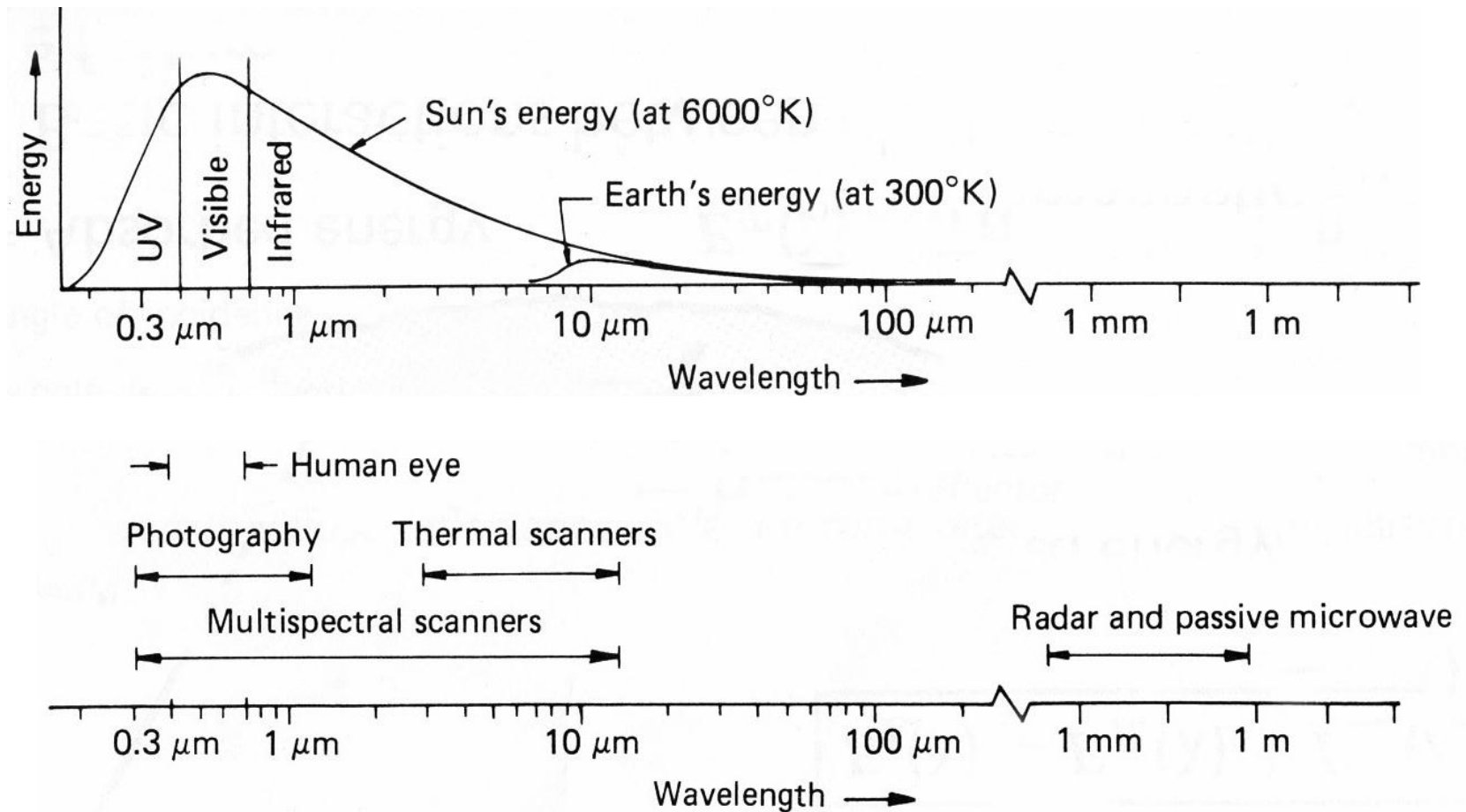


Observations depend on

- telescope characteristics (resolving power, diffraction)
- detector characteristics (signal to noise)
- communications bandwidth (bit depth)
- spectral intervals (window, absorption band)
- time of day (daylight visible)
- atmospheric state (T, Q, clouds)
- earth surface (Ts, vegetation cover)

Radiation and the Planck Function

Spectral Characteristics of Energy Sources and Sensing Systems



Terminology of radiant energy

**Energy from
the Earth Atmosphere**

over time is

Flux

which strikes the detector area

Irradiance

at a given wavelength interval

**Monochromatic
Irradiance**

over a solid angle on the Earth

**Radiance observed by
satellite radiometer**

is described by

The Planck function

can be inverted to

Brightness temperature

Definitions of Radiation

QUANTITY	SYMBOL	UNITS
Energy	dQ	Joules
Flux	dQ/dt	Joules/sec = Watts
Irradiance	dQ/dt/dA	Watts/meter²
Monochromatic Irradiance	dQ/dt/dA/dλ	W/m²/micron
	or	
	dQ/dt/dA/dν	W/m²/cm⁻¹
Radiance	dQ/dt/dA/dλ/dΩ	W/m²/micron/ster
	or	
	dQ/dt/dA/dν/dΩ	W/m²/cm⁻¹/ster

Using wavenumbers

$$B(\nu, T) = \frac{c_1 \nu^3}{e^{c_2 \nu / T} - 1}$$

(mW/m²/ster/cm⁻¹)

$$\nu(\text{max in cm}^{-1}) = 1.95T$$

$$B(\nu_{\text{max}}, T) \sim T^{**3}.$$

$$E = \pi \int_0^{\infty} B(\nu, T) d\nu = \sigma T^4,$$

$$T = \frac{c_1 \nu^3}{c_2 \nu / [\ln(\frac{c_1 \nu^3}{B_\nu} + 1)]}$$

Using wavelengths

$$B(\lambda, T) = \frac{c_1}{\lambda^5 [e^{c_2 / \lambda T} - 1]}$$

(mW/m²/ster/μm)

$$\lambda(\text{max in cm})T = 0.2897$$

$$B(\lambda_{\text{max}}, T) \sim T^{**5}.$$

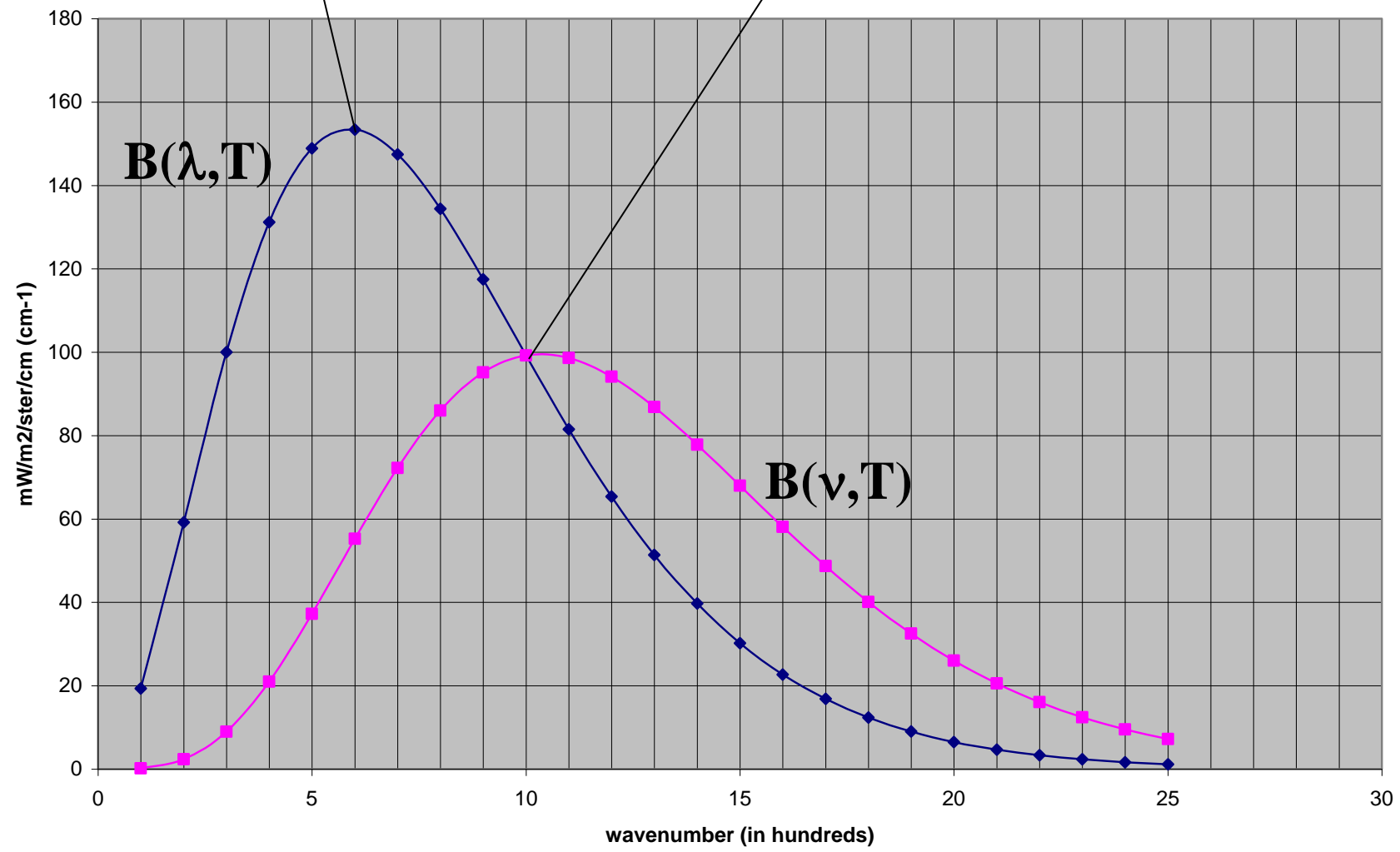
$$E = \pi \int_0^{\infty} B(\lambda, T) d\lambda = \sigma T^4,$$

$$T = \frac{c_1}{c_2 / [\lambda \ln(\frac{c_1}{\lambda^5 B_\lambda} + 1)]}$$

$$B(\lambda_{\max}, T) \sim T^5$$

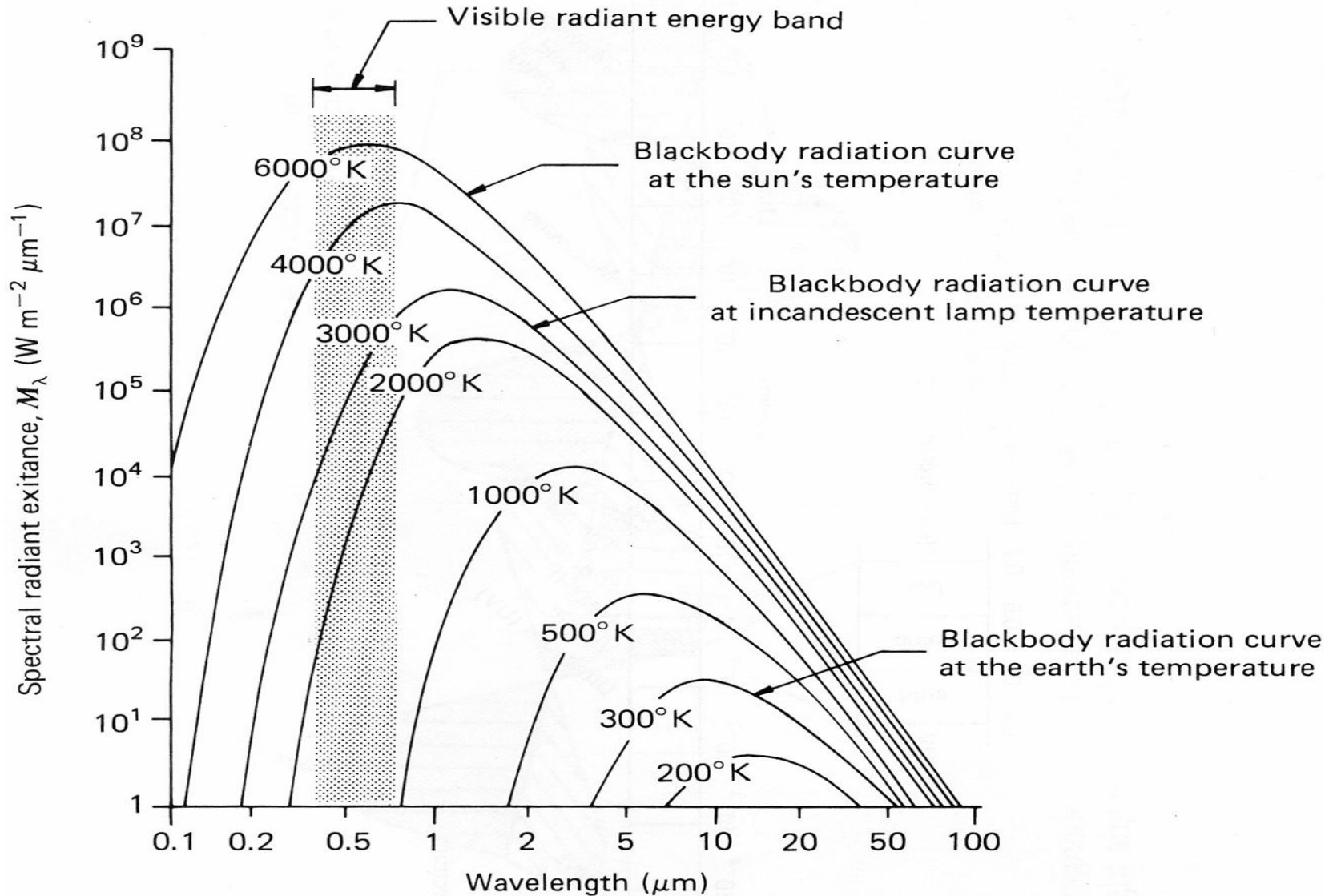
$$B(\nu_{\max}, T) \sim T^3$$

Planck Radiances



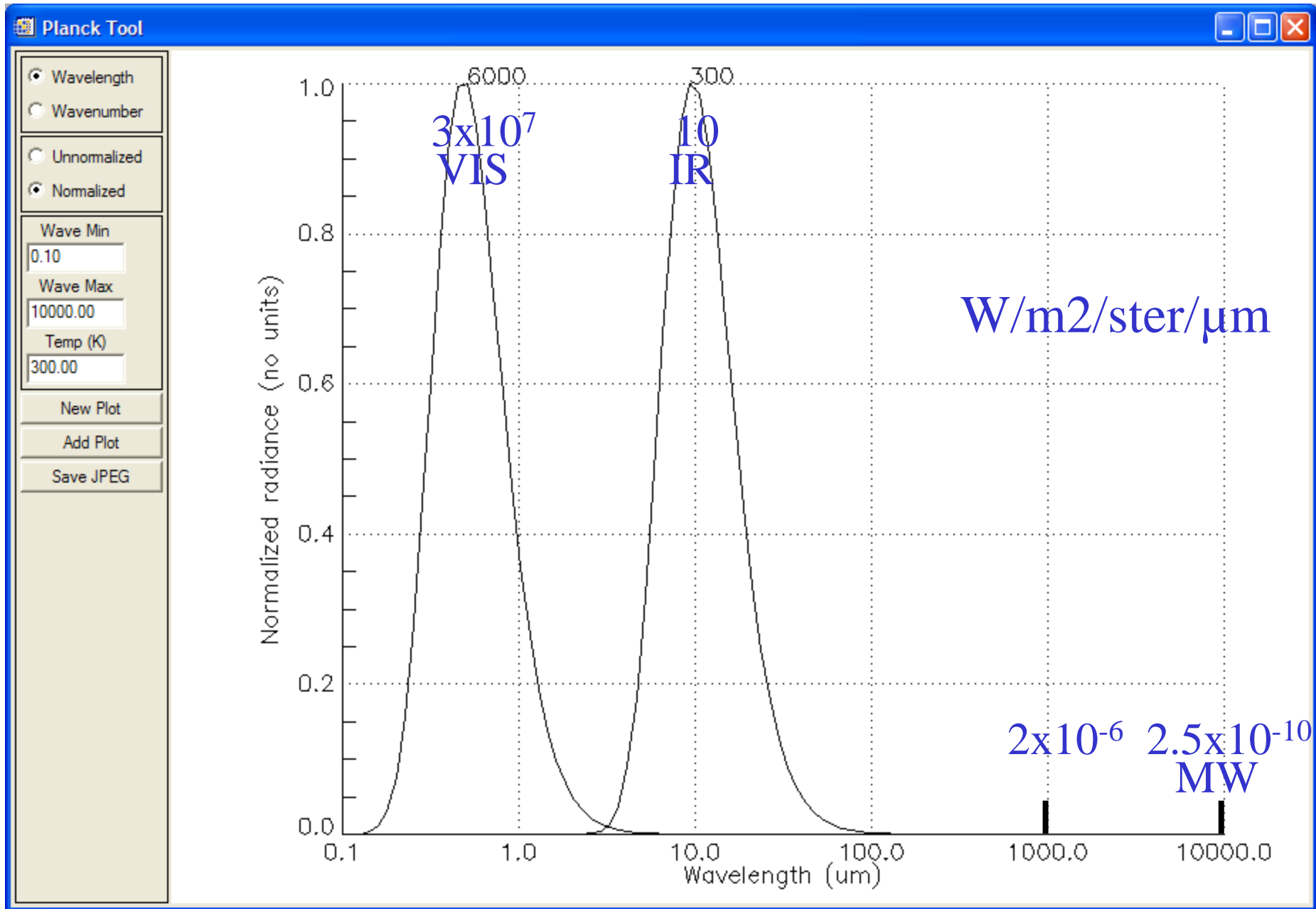
$B(\lambda, T)$ versus $B(\nu, T)$

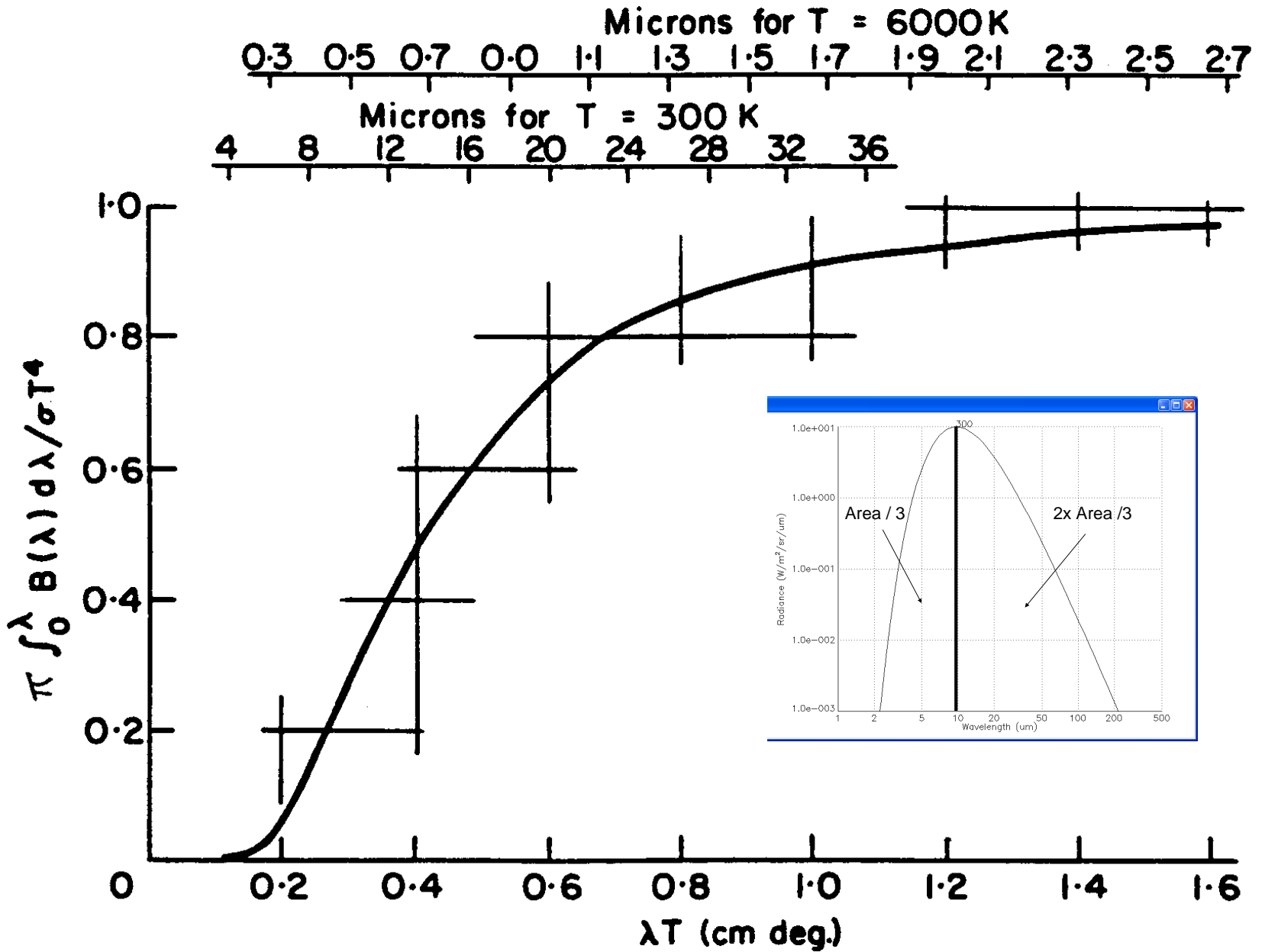
Spectral Distribution of Energy Radiated from Blackbodies at Various Temperatures



← Sun

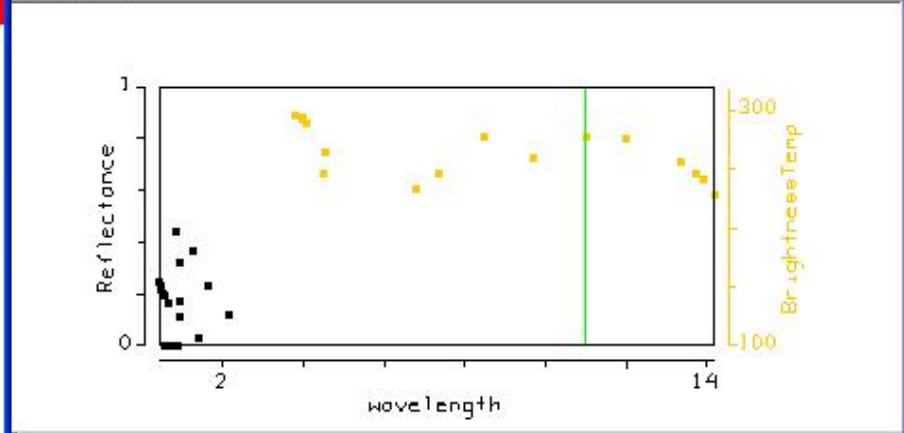
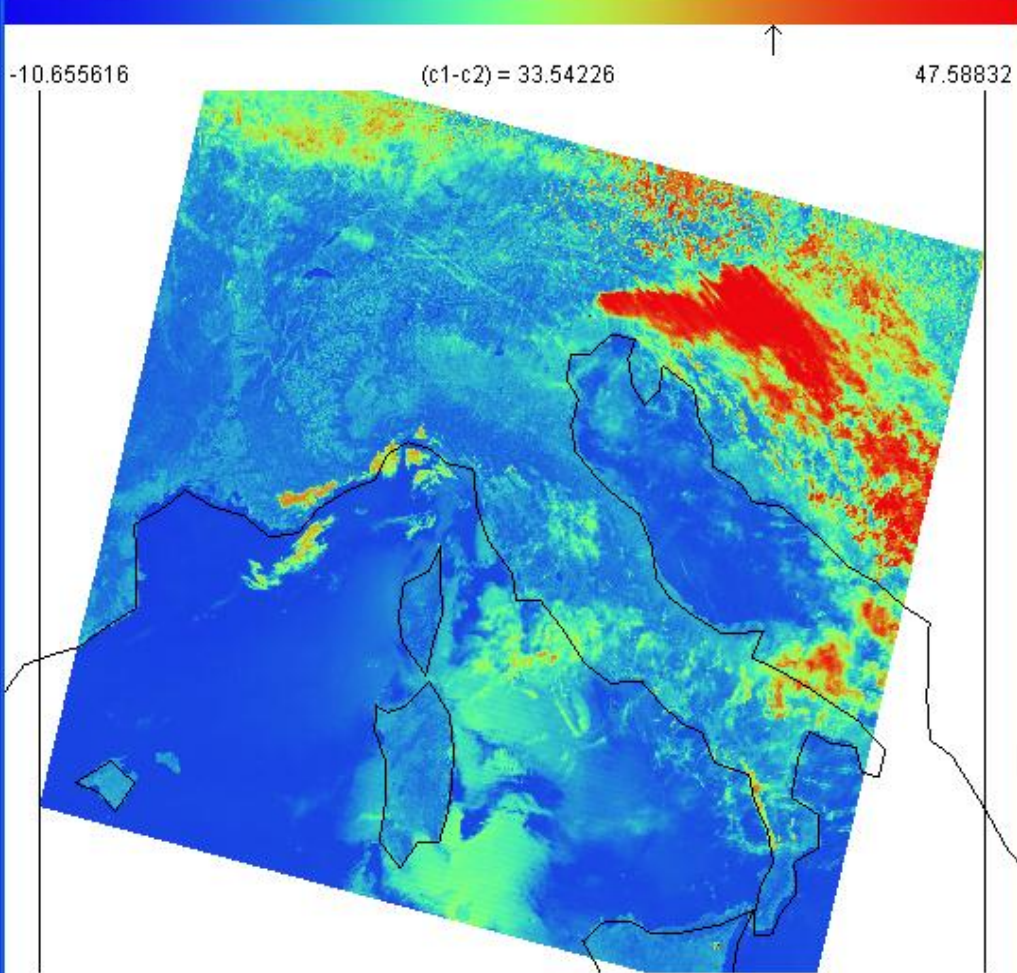
Earth →





Tools Settings

Tools Settings

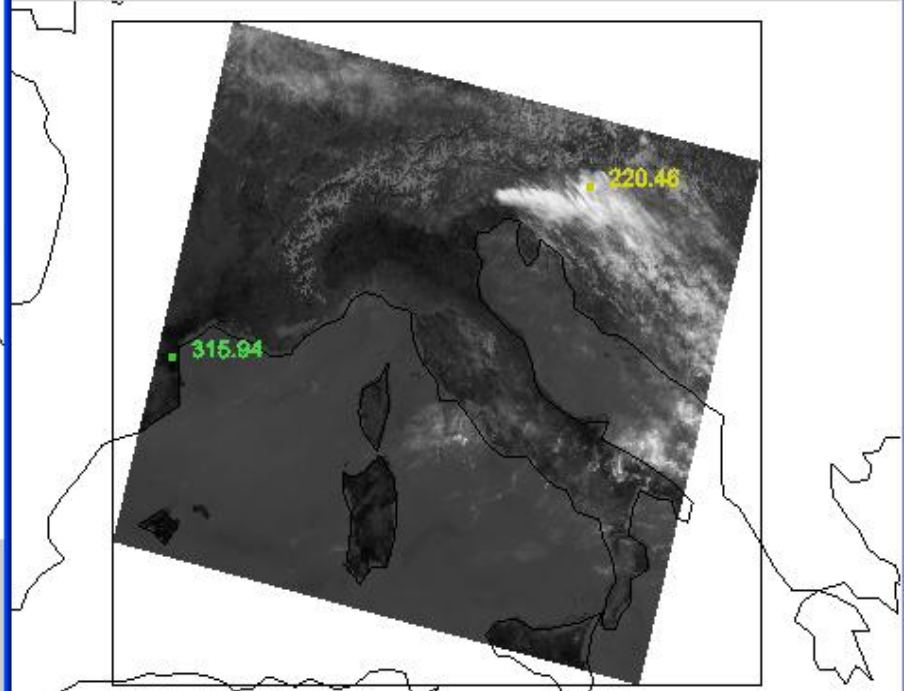


Band: 31 wavelength 11.00 μm

c1:20, c2:31
BT4 - BT11

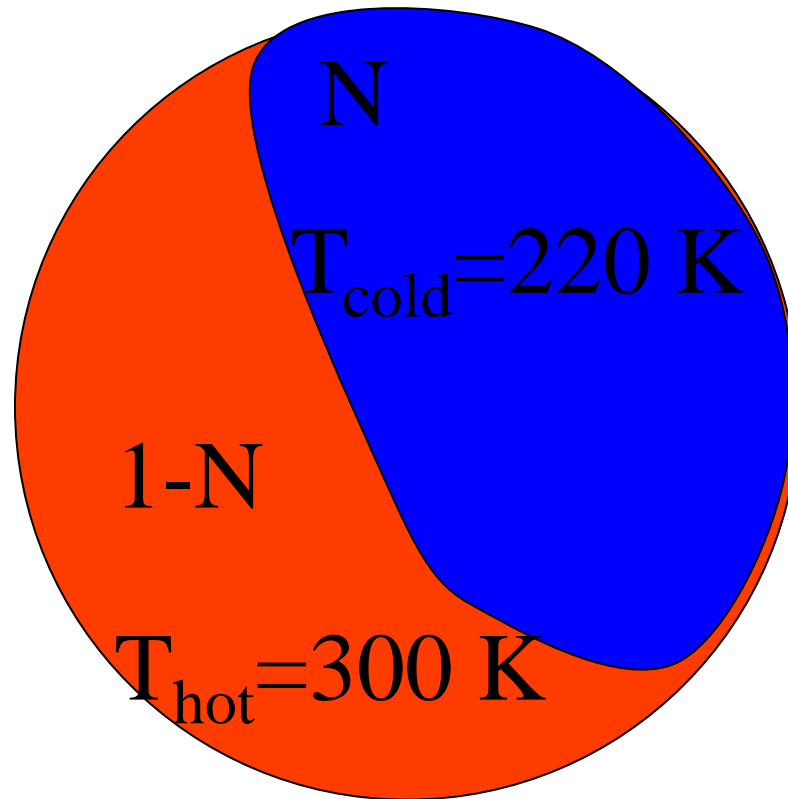
XAxis YAxis

Box Curve



Instrument: MODIS Lat = 49.230 Lon = 3.858

Non-Homogeneous FOV



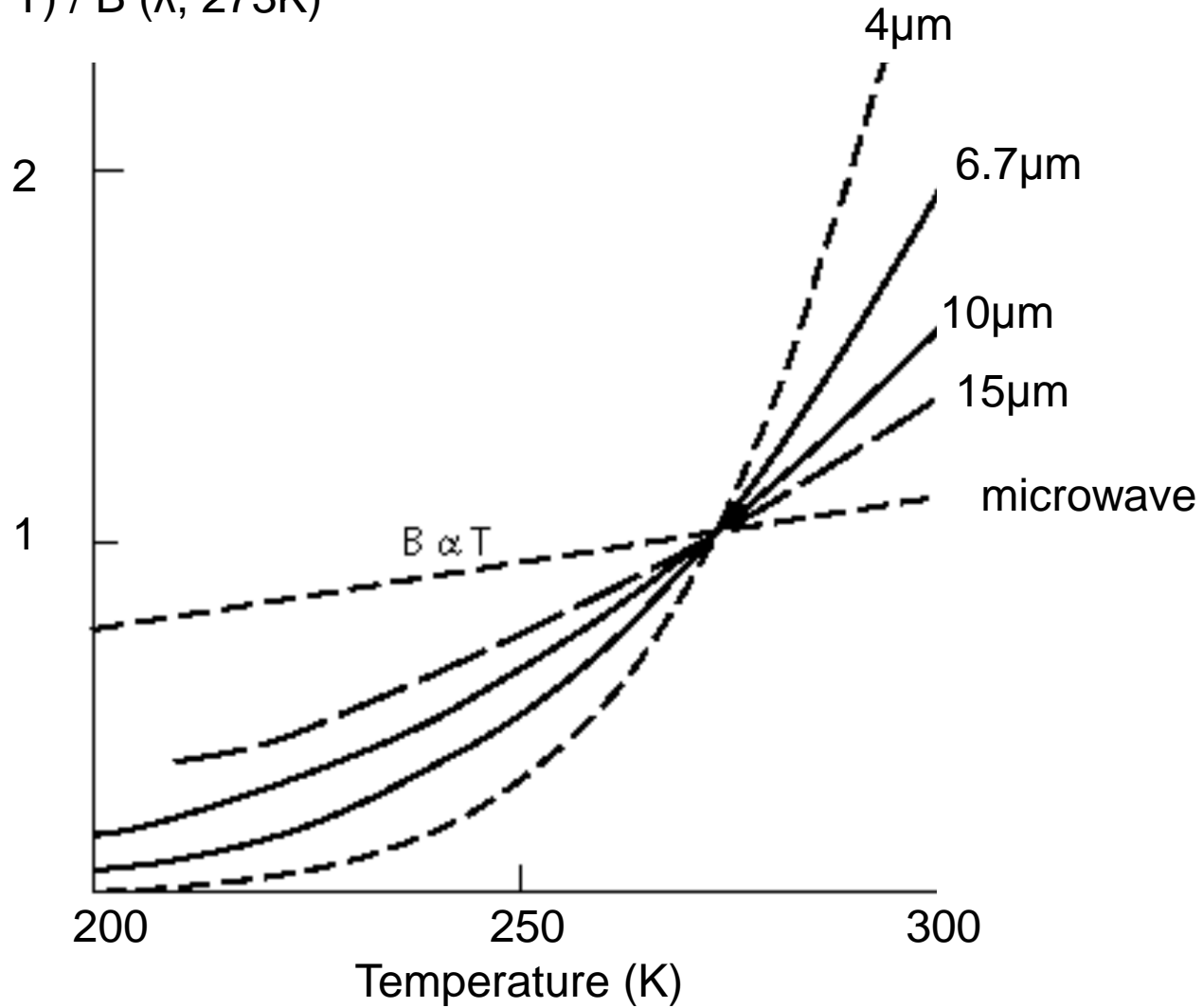
$$B = N * B(T_{\text{cold}}) + (1-N) * B(T_{\text{hot}})$$

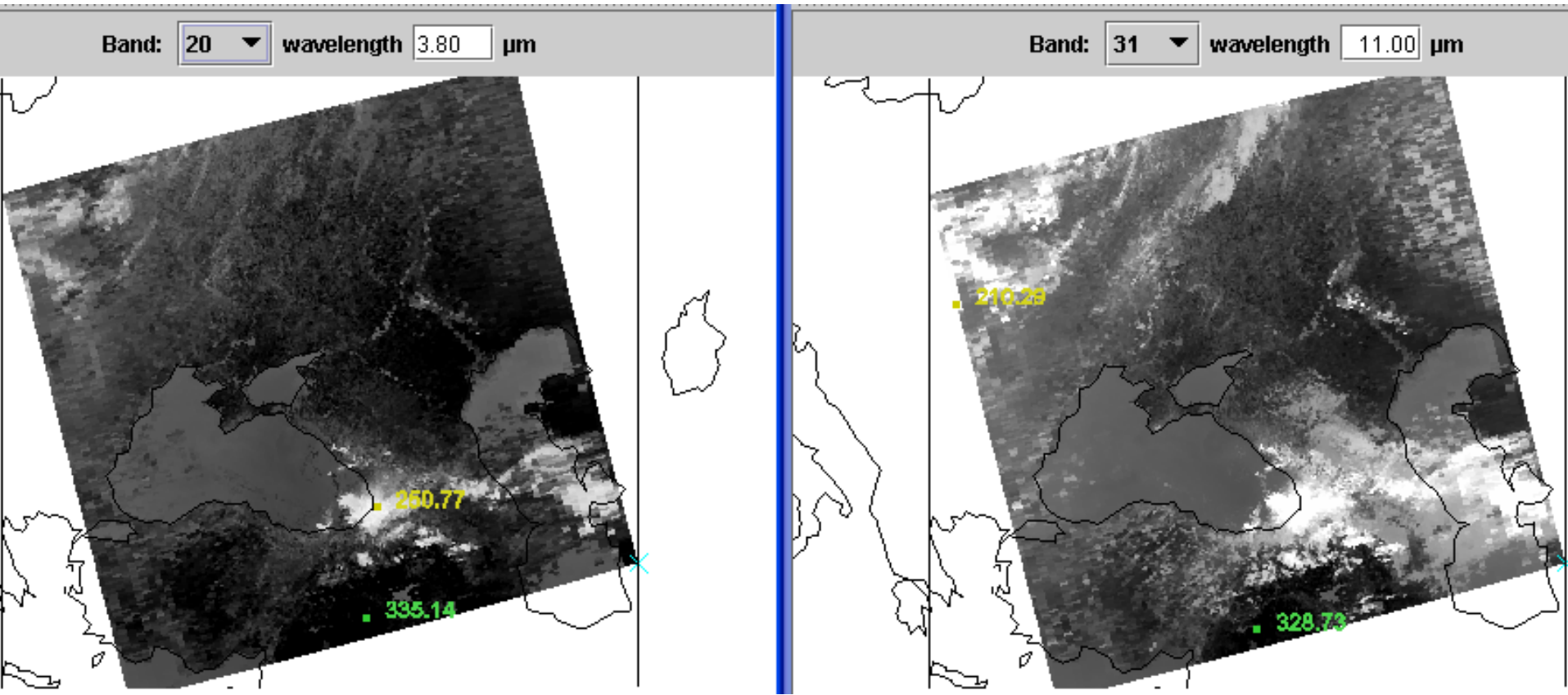
$$BT = N * T_{\text{cold}} + (1-N) * T_{\text{hot}}$$

The equation above is crossed out with a large red circle and a diagonal slash, indicating it is incorrect.

Temperature Sensitivity of $B(\lambda, T)$ for typical earth temperatures

$B(\lambda, T) / B(\lambda, 273K)$





Cloud edges and broken clouds appear different in 11 and 4 um images.

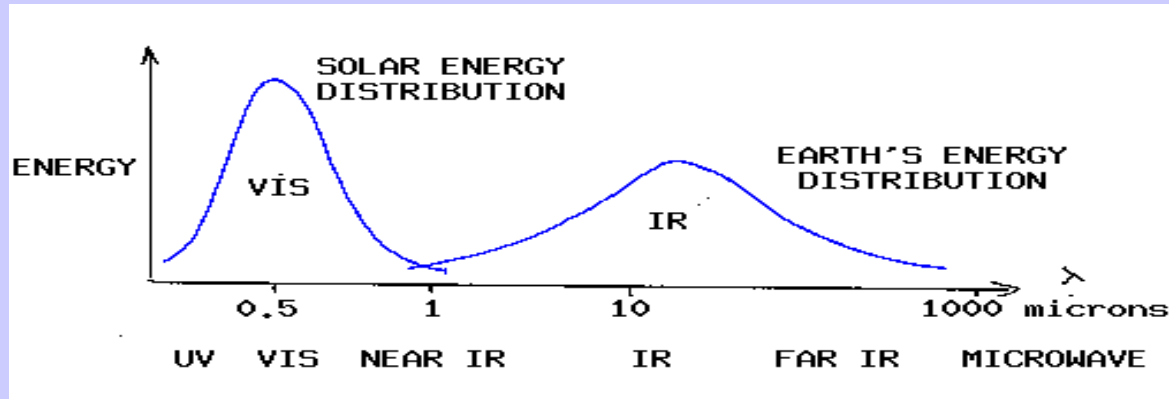
$$T(11)**4=(1-N)*Tclr**4+N*Tcld**4\sim(1-N)*300**4+N*200**4$$

$$T(4)**12=(1-N)*Tclr**12+N*Tcld**12\sim(1-N)*300**12+N*200**12$$

Cold part of pixel has more influence for B(11) than B(4)

Solar and Earth Radiation

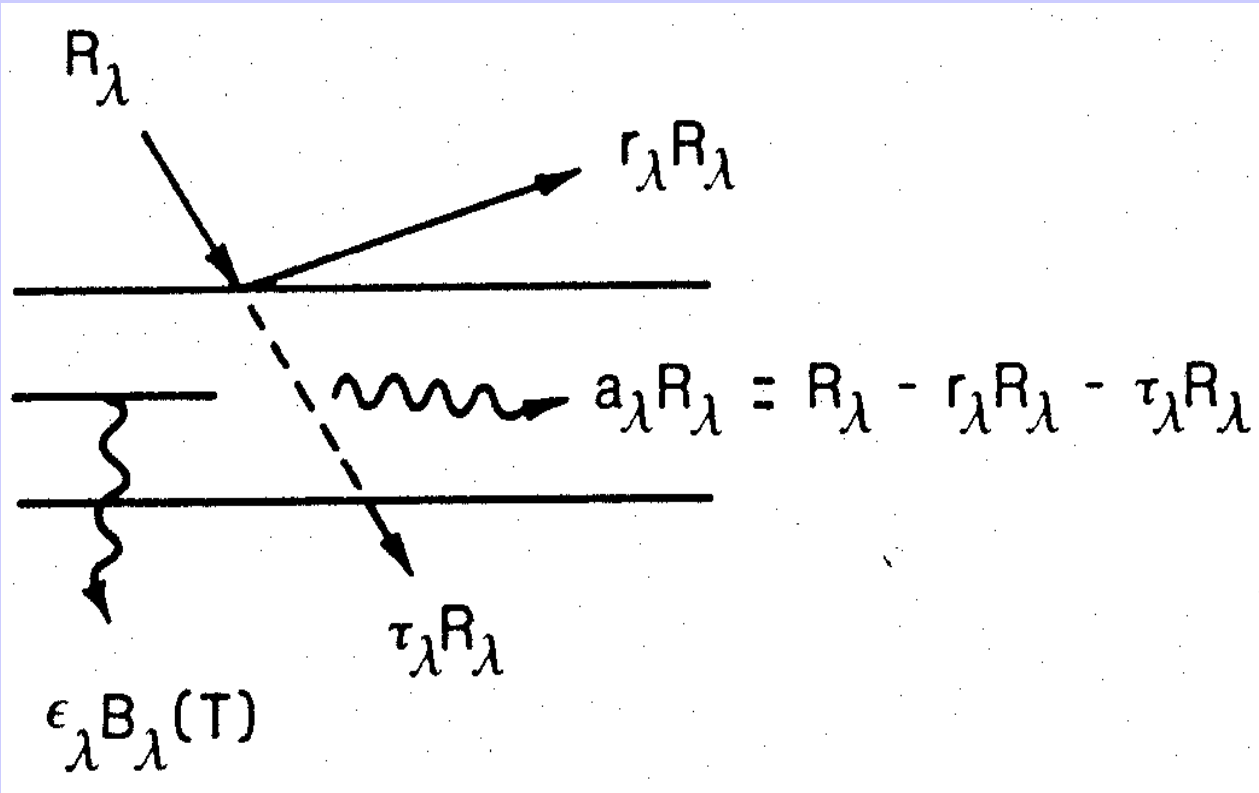
Solar (visible) and Earth emitted (infrared) energy



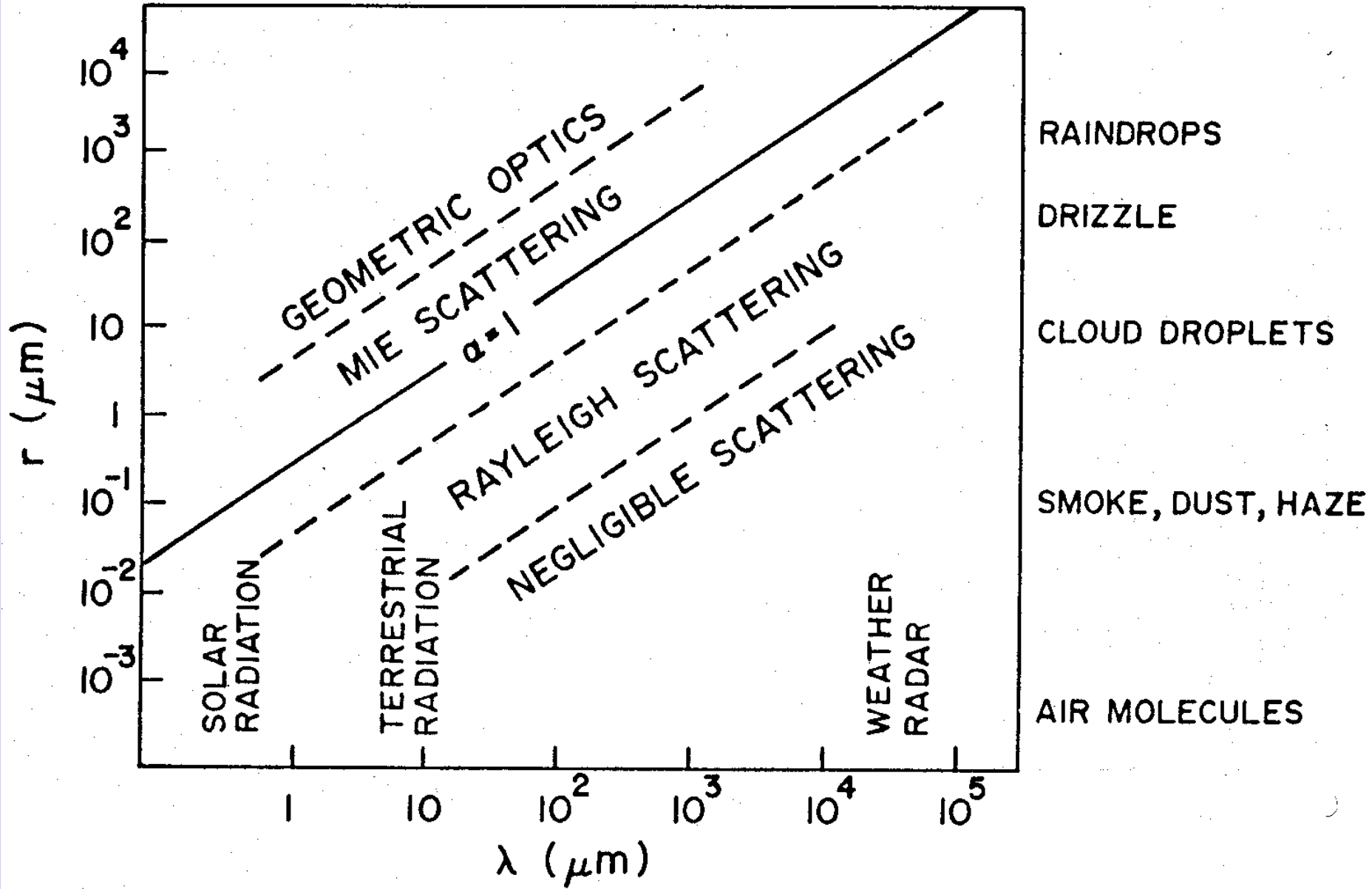
Incoming solar radiation (mostly visible) drives the earth-atmosphere (which emits infrared).

Over the annual cycle, the incoming solar energy that makes it to the earth surface (about 50 %) is balanced by the outgoing thermal infrared energy emitted through the atmosphere.

The atmosphere transmits, absorbs (by H₂O, O₂, O₃, dust) reflects (by clouds), and scatters (by aerosols) incoming visible; the earth surface absorbs and reflects the transmitted visible. Atmospheric H₂O, CO₂, and O₃ selectively transmit or absorb the outgoing infrared radiation. The outgoing microwave is primarily affected by H₂O and O₂.

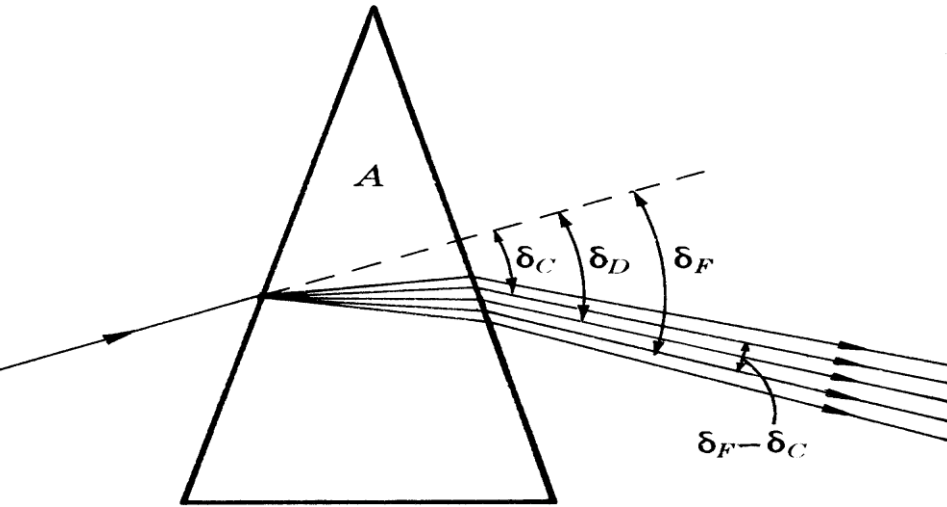


‘ENERGY
CONSERVATION’

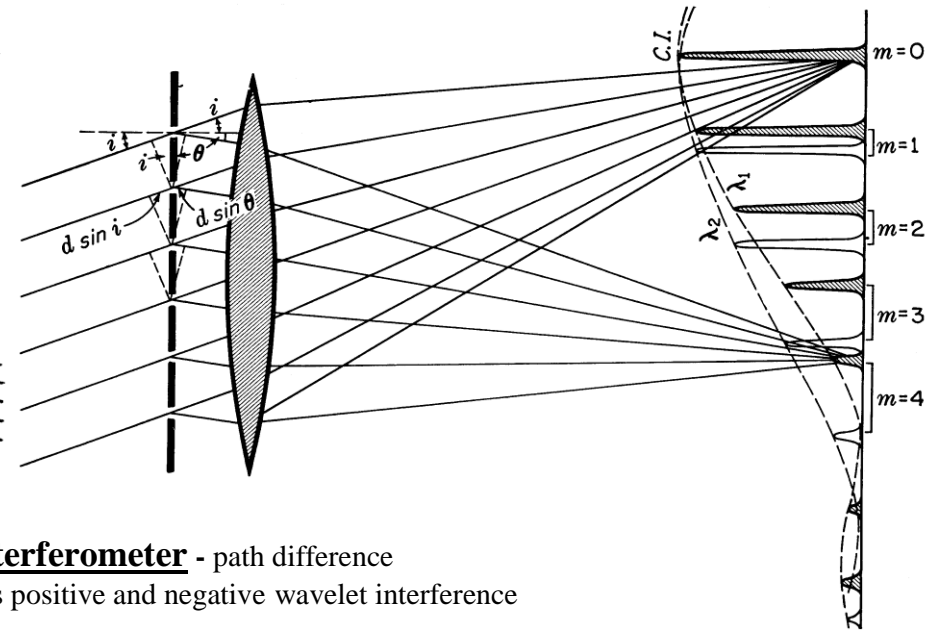


Spectral Separation Visible, NIR, & IR

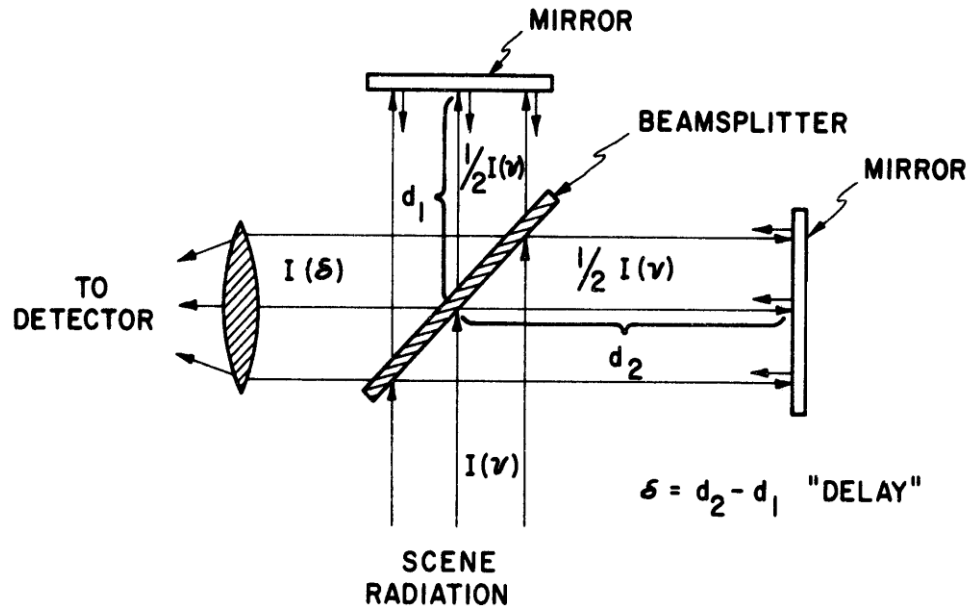
Spectral Separation with a Prism: longer wavelengths deflected less



Spectral Separation with a Grating: path difference from slits produces positive and negative wavelet interference on screen



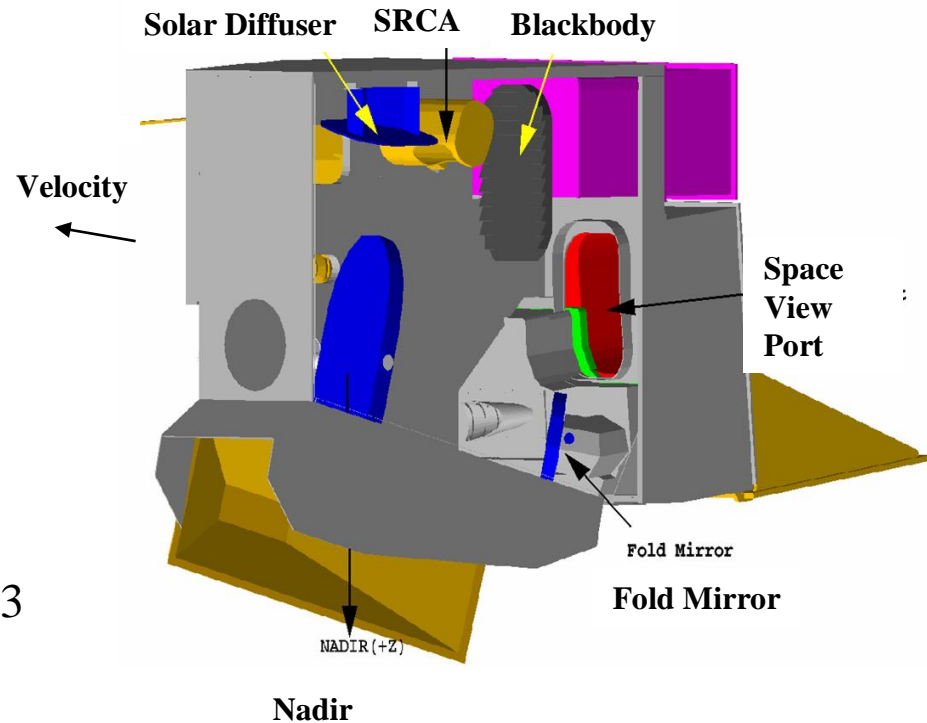
Spectral Separation with an Interferometer - path difference (or delay) from two mirrors produces positive and negative wavelet interference



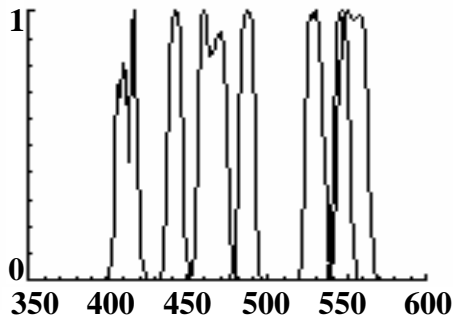
Visible & NIR

MODIS Instrument Overview

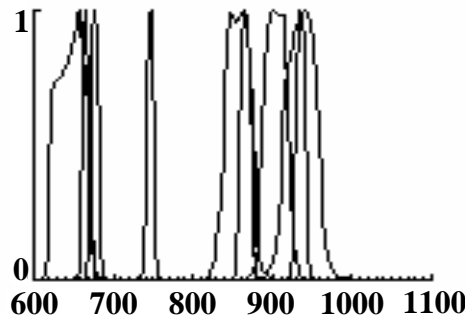
- 36 spectral bands (490 detectors) cover wavelength range from 0.4 to 14.5 μm
- Spatial resolution at nadir: 250m (2 bands), 500m (5 bands) and 1000m
- 4 FPAs: VIS, NIR, SMIR, LWIR
- On-Board Calibrators: SD/SDSM, SRCA, and BB (plus space view)
- 12 bit (0-4095) dynamic range
- 2-sided Paddle Wheel Scan Mirror scans 2330 km swath in 1.47 sec
- Day data rate = 10.6 Mbps; night data rate = 3.3 Mbps (100% duty cycle, 50% day and 50% night)



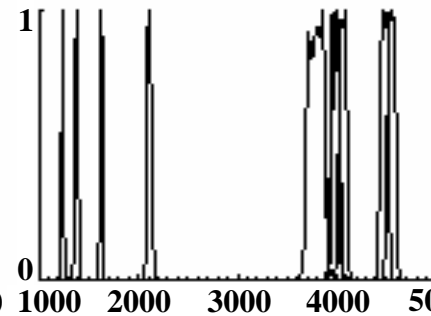
VIS



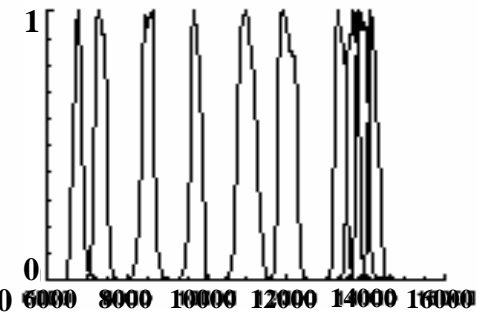
NIR



S/MWIR



LWIR



Visible Infrared Imaging Radiometer Suite Raytheon SAS El Segundo, Ca



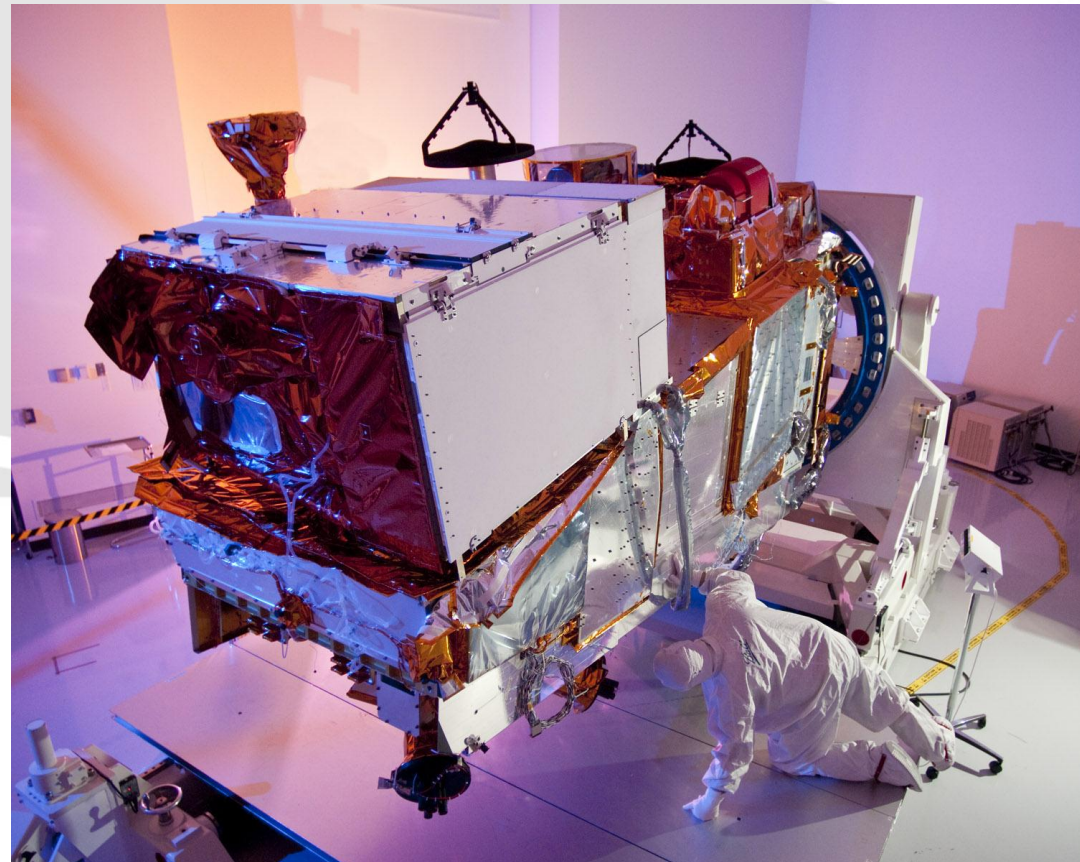
Description

- **Purpose:** Global observations of land, ocean, & atmosphere parameters at high temporal resolution (~ daily)
- **Predecessor Instruments:** AVHRR, OLS, MODIS, SeaWiFS
- **Approach:** Multi-spectral scanning radiometer (22 bands between 0.4 μm and 12 μm) 12-bit quantization
- **Swath width:** 3000 km

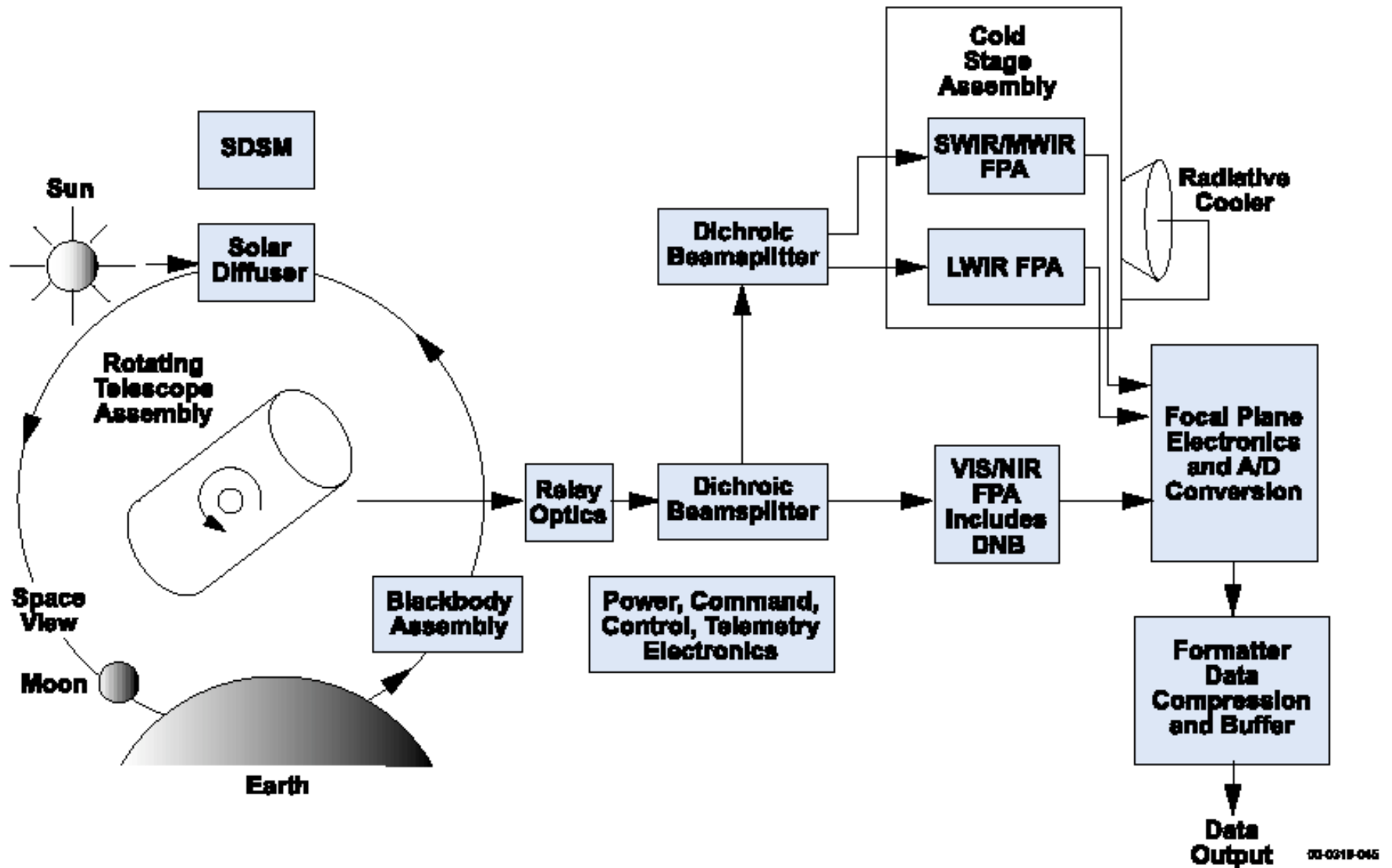
Spatial Resolution

- 16 bands at 750m
- 5 bands at 325m
- DNB

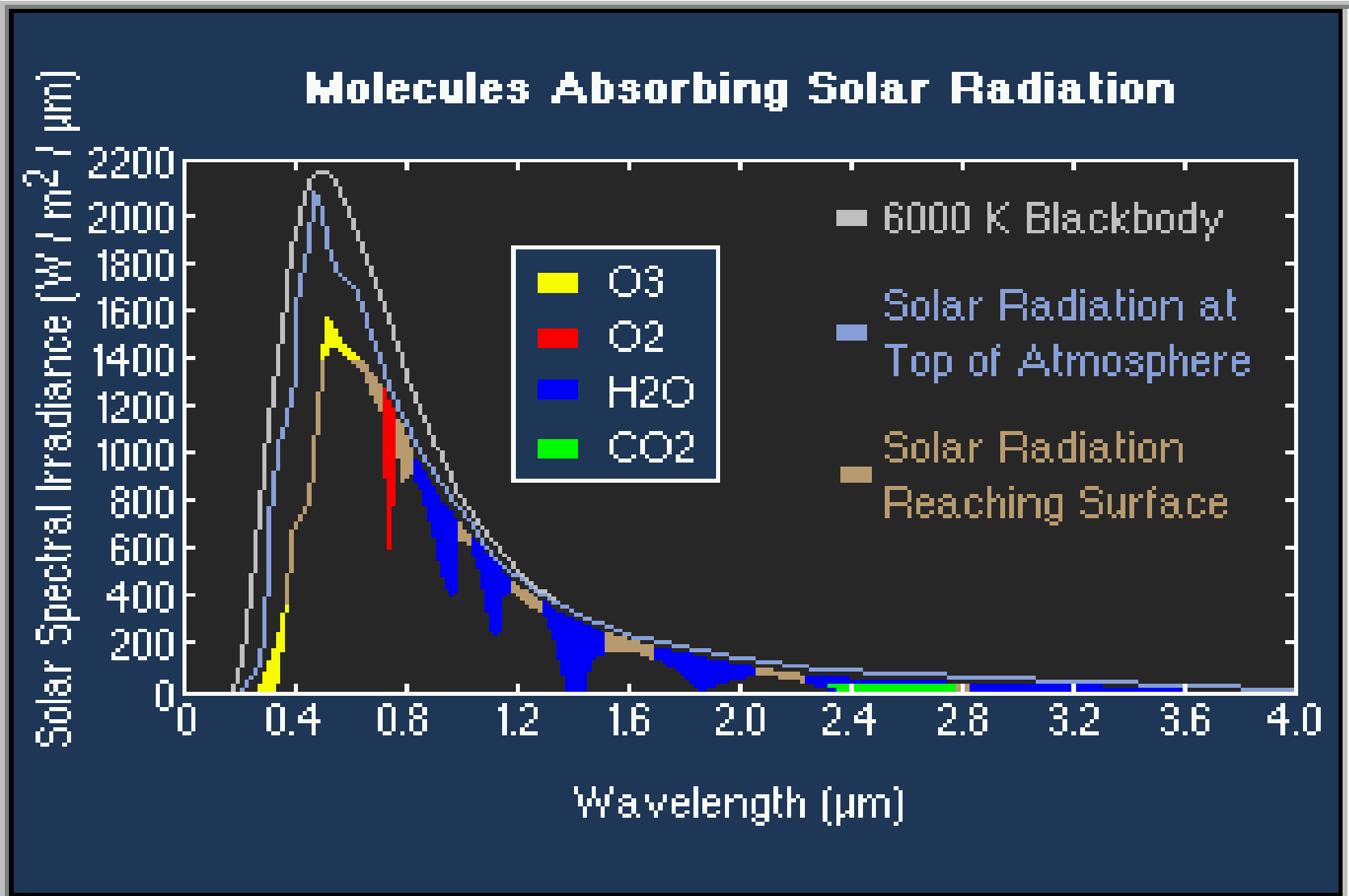
VIIRS on NPP



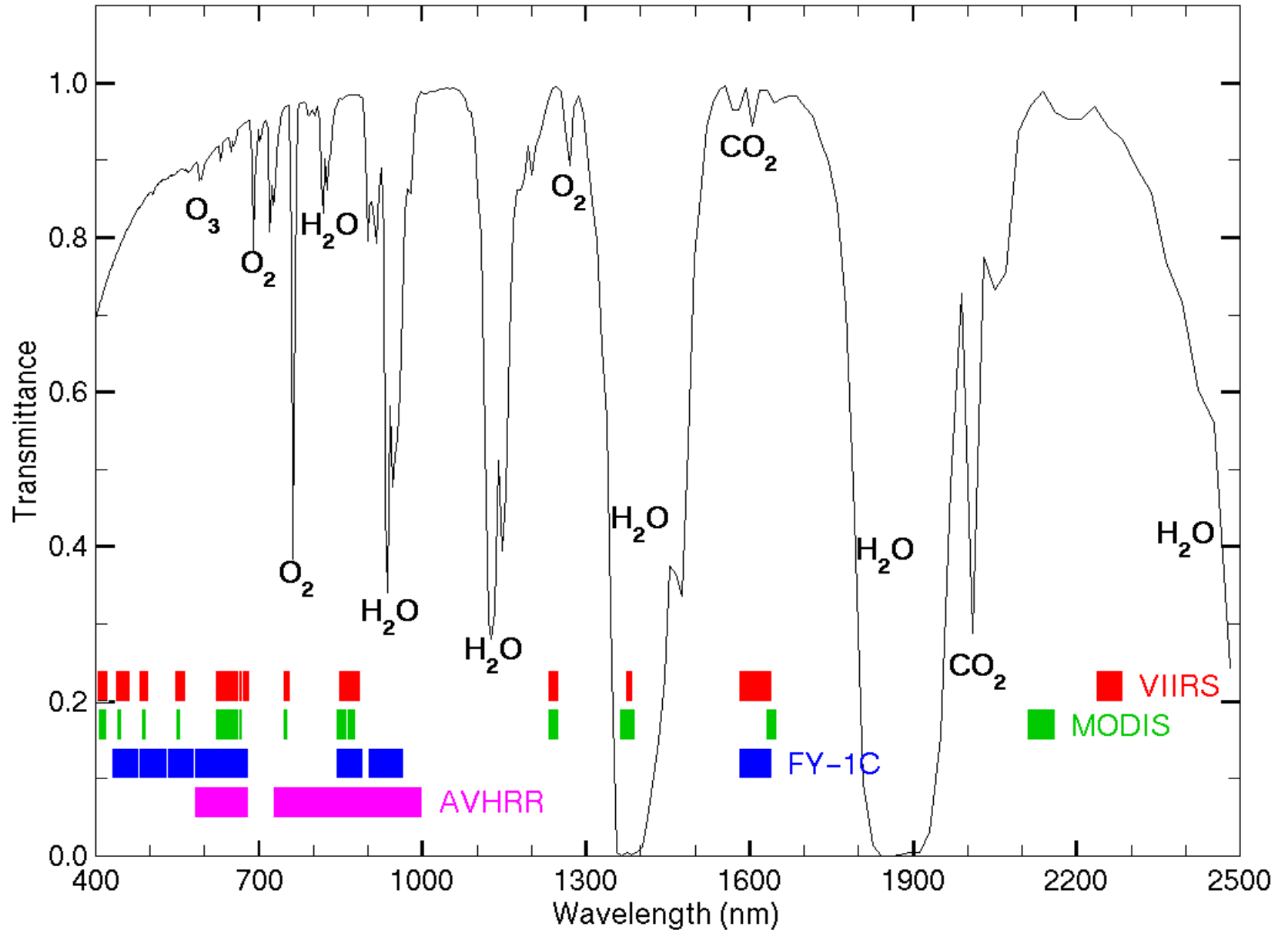
VIIRS Sensor From Photons In To Bits Out

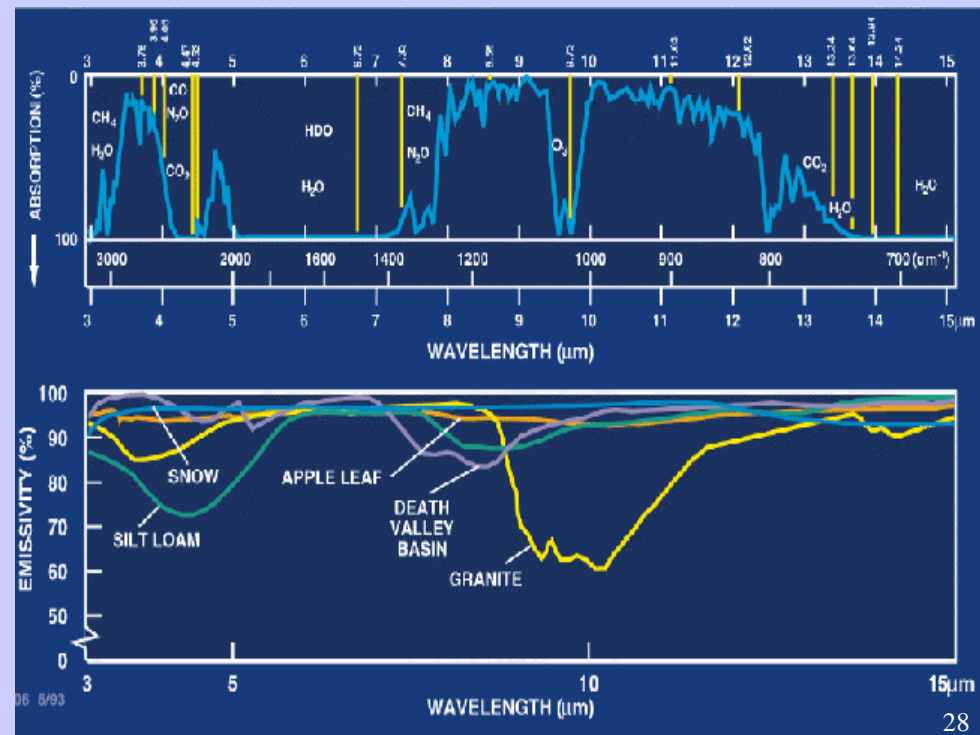
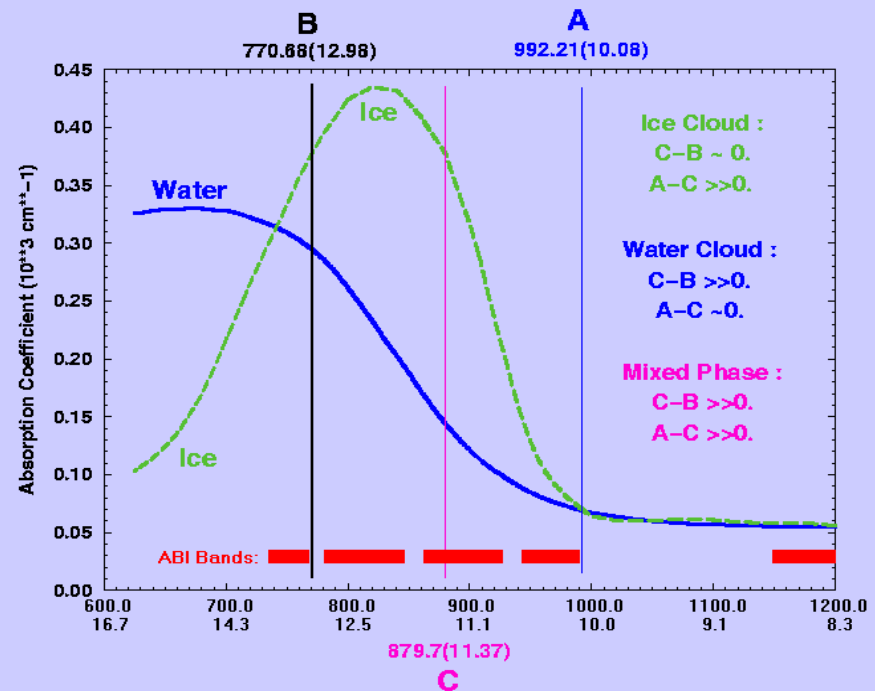
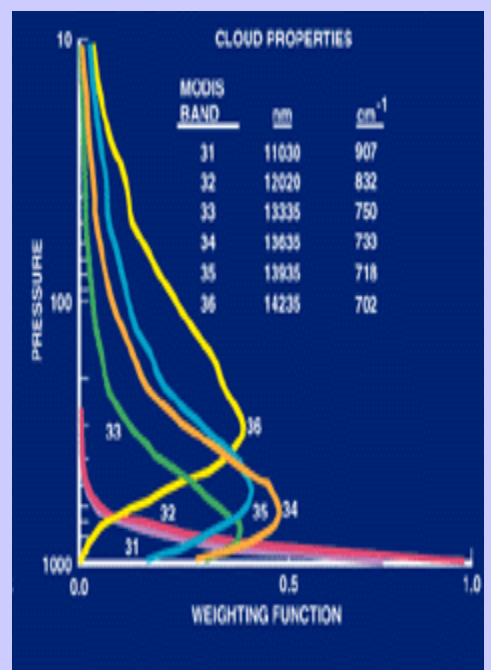
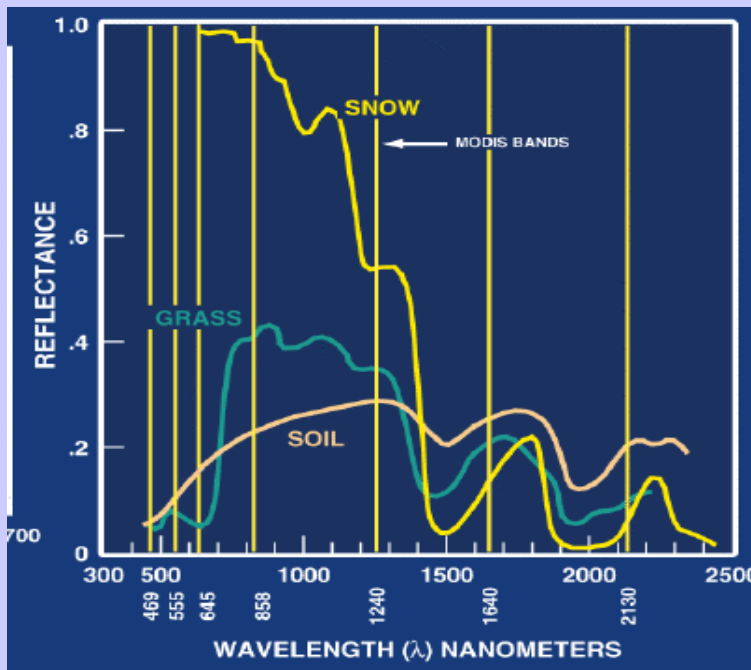
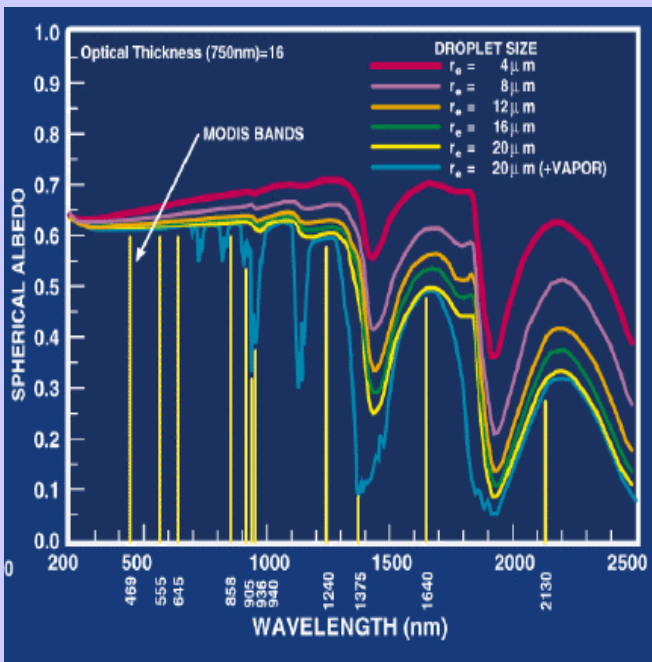


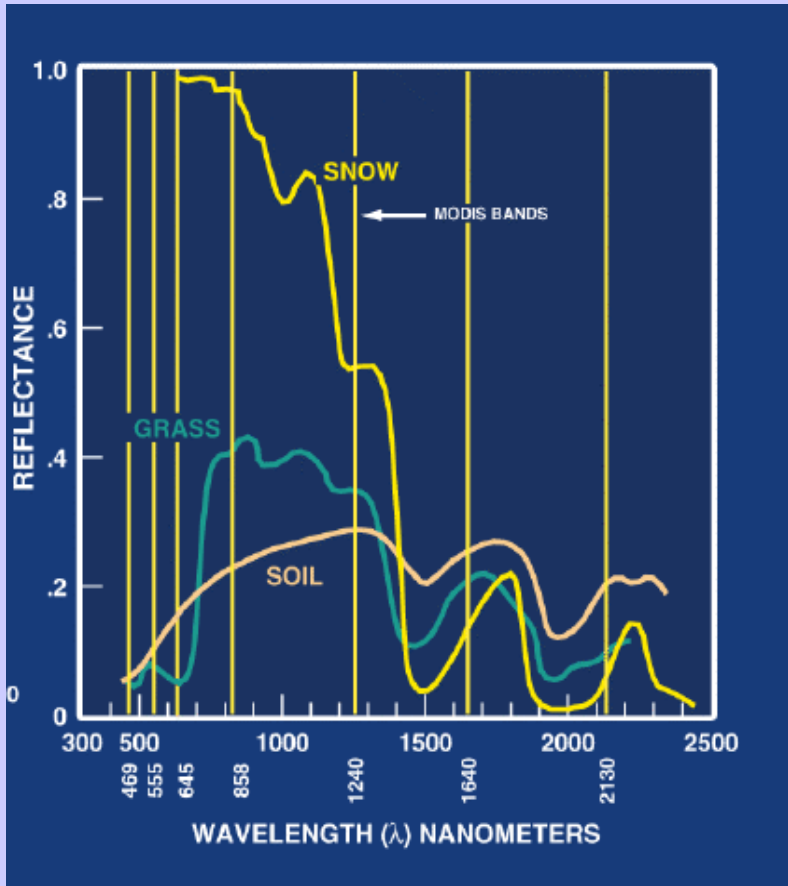
Solar Spectrum



VIIRS, MODIS, FY-1C, AVHRR





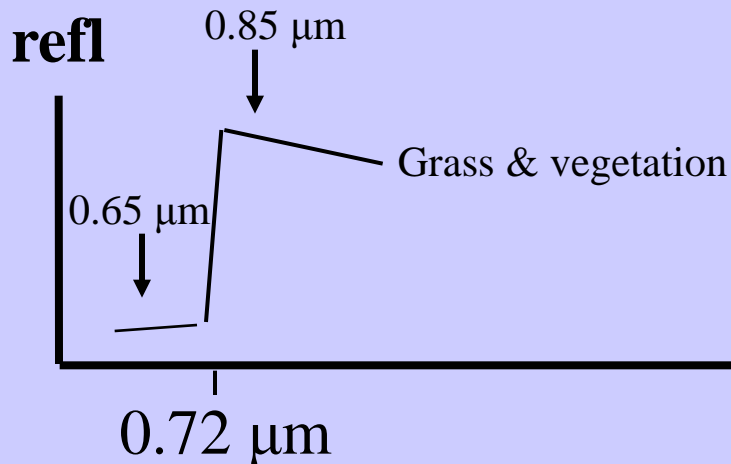


Investigating with Multi-spectral Combinations

Given the spectral response of a surface or atmospheric feature

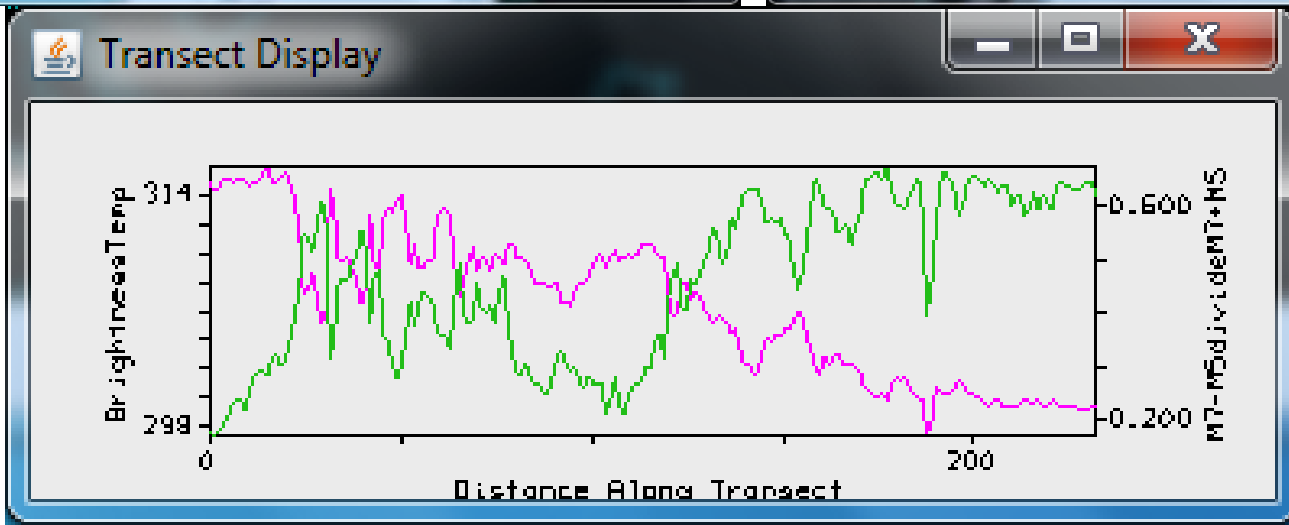
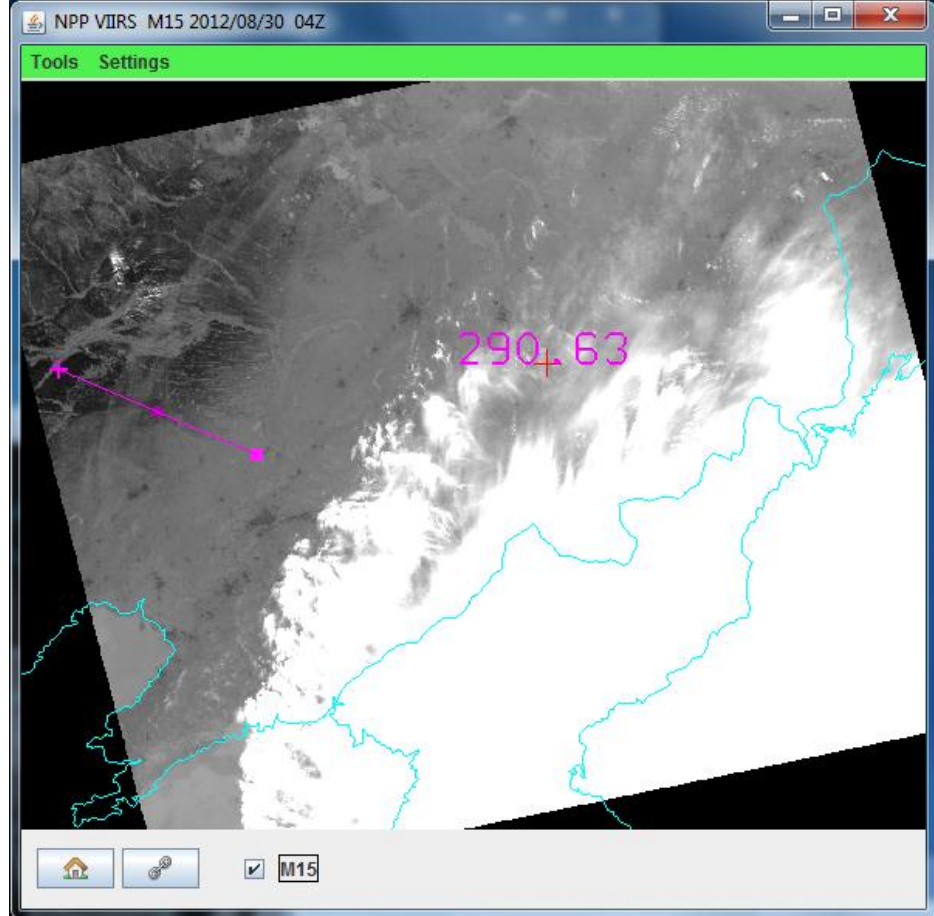
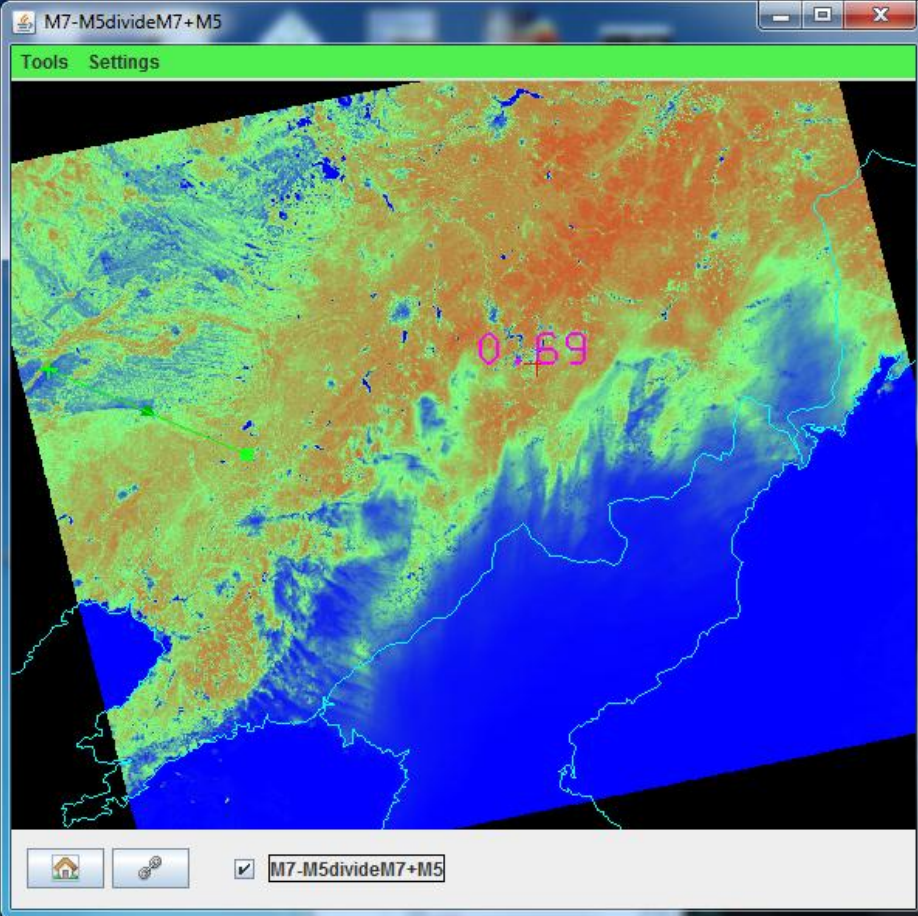
Select a part of the spectrum where the reflectance or absorption changes with wavelength

e.g. reflection from grass



If 0.65 μm and 0.85 μm channels see the same reflectance than surface viewed is not grass;

if 0.85 μm sees considerably higher reflectance than 0.65 μm then surface might be grass



John, Becky,
Lisha, Denis

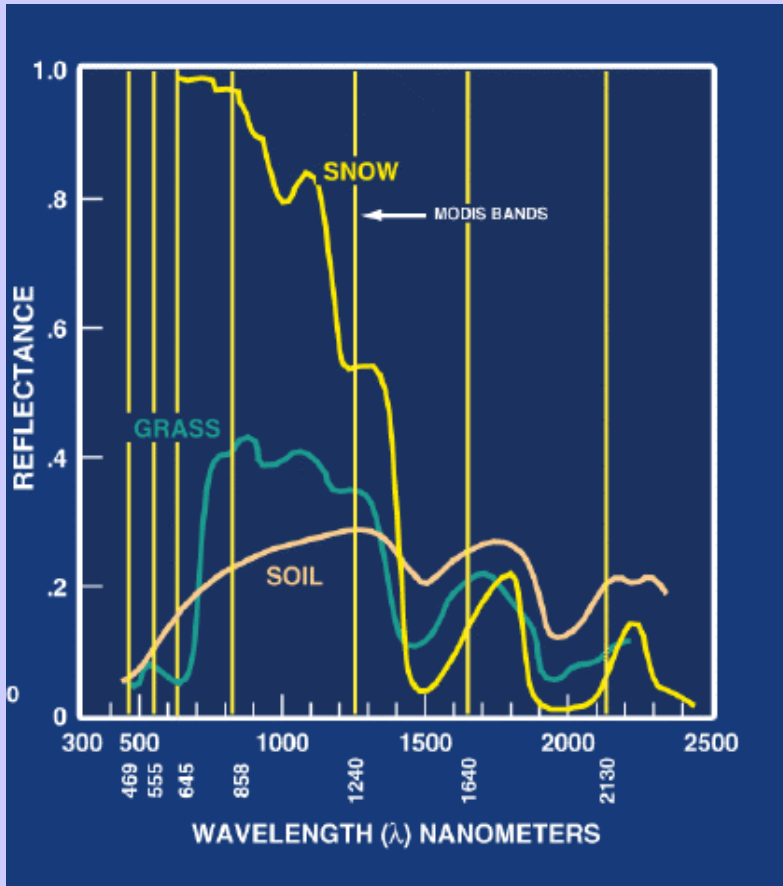
Investigating with Multi-spectral Combinations

Given the spectral response of a surface or atmospheric feature

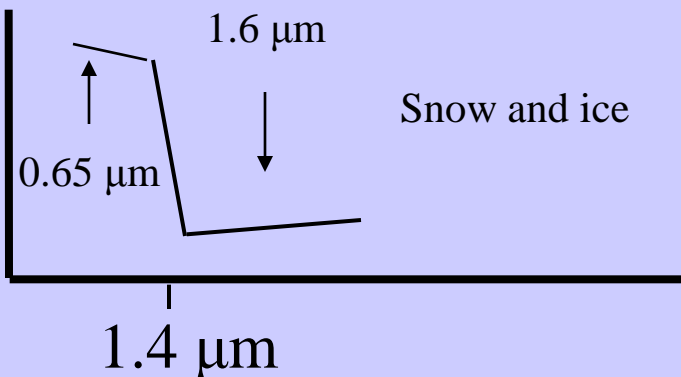
Select a part of the spectrum where the reflectance or absorption changes with wavelength

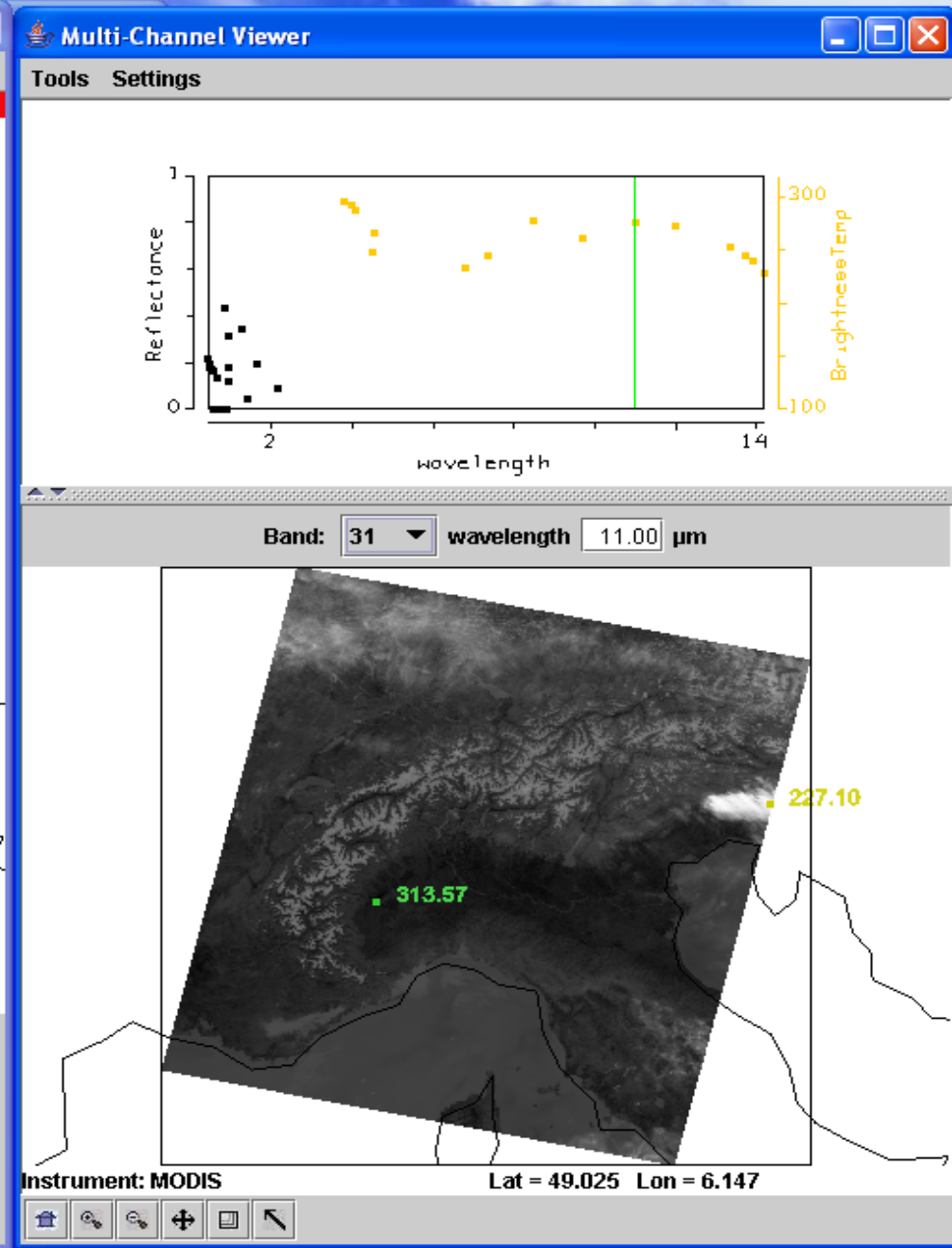
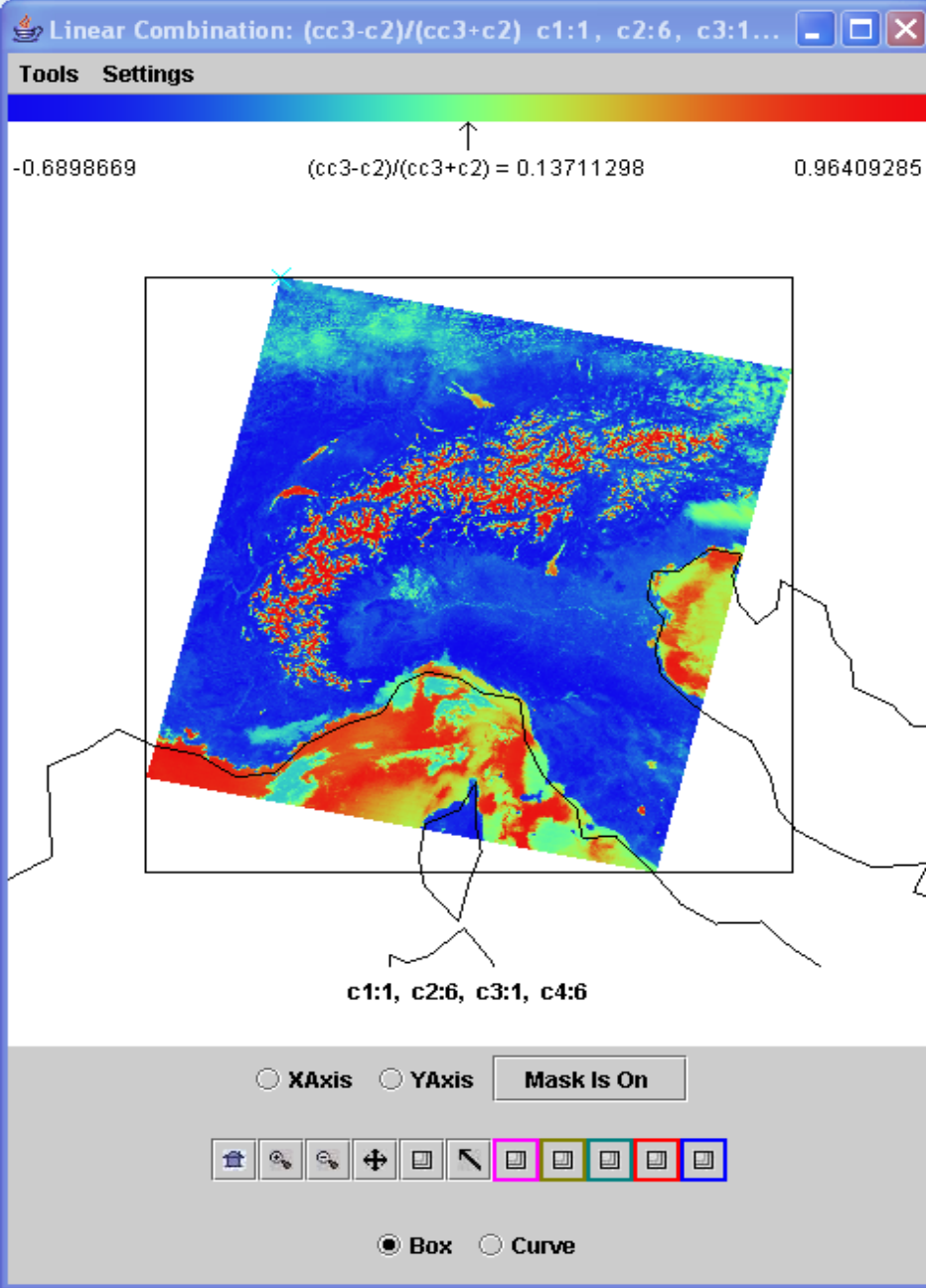
e.g. reflection from snow/ice

If $0.65\ \mu\text{m}$ and $1.6\ \mu\text{m}$ channels see the same reflectance than surface viewed is not snow;
if $1.6\ \mu\text{m}$ sees considerably lower reflectance than $0.65\ \mu\text{m}$ then surface might be snow



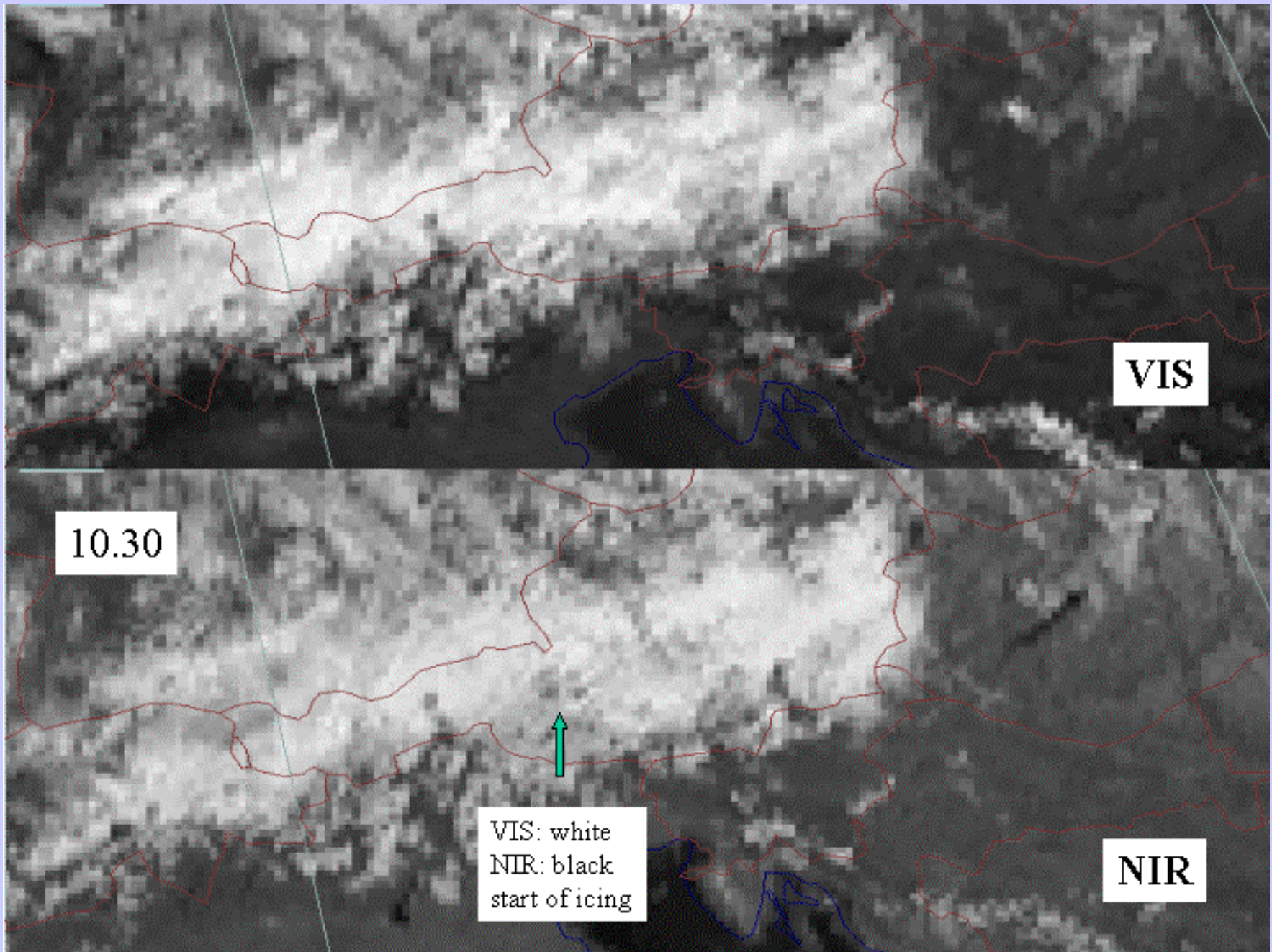
refl





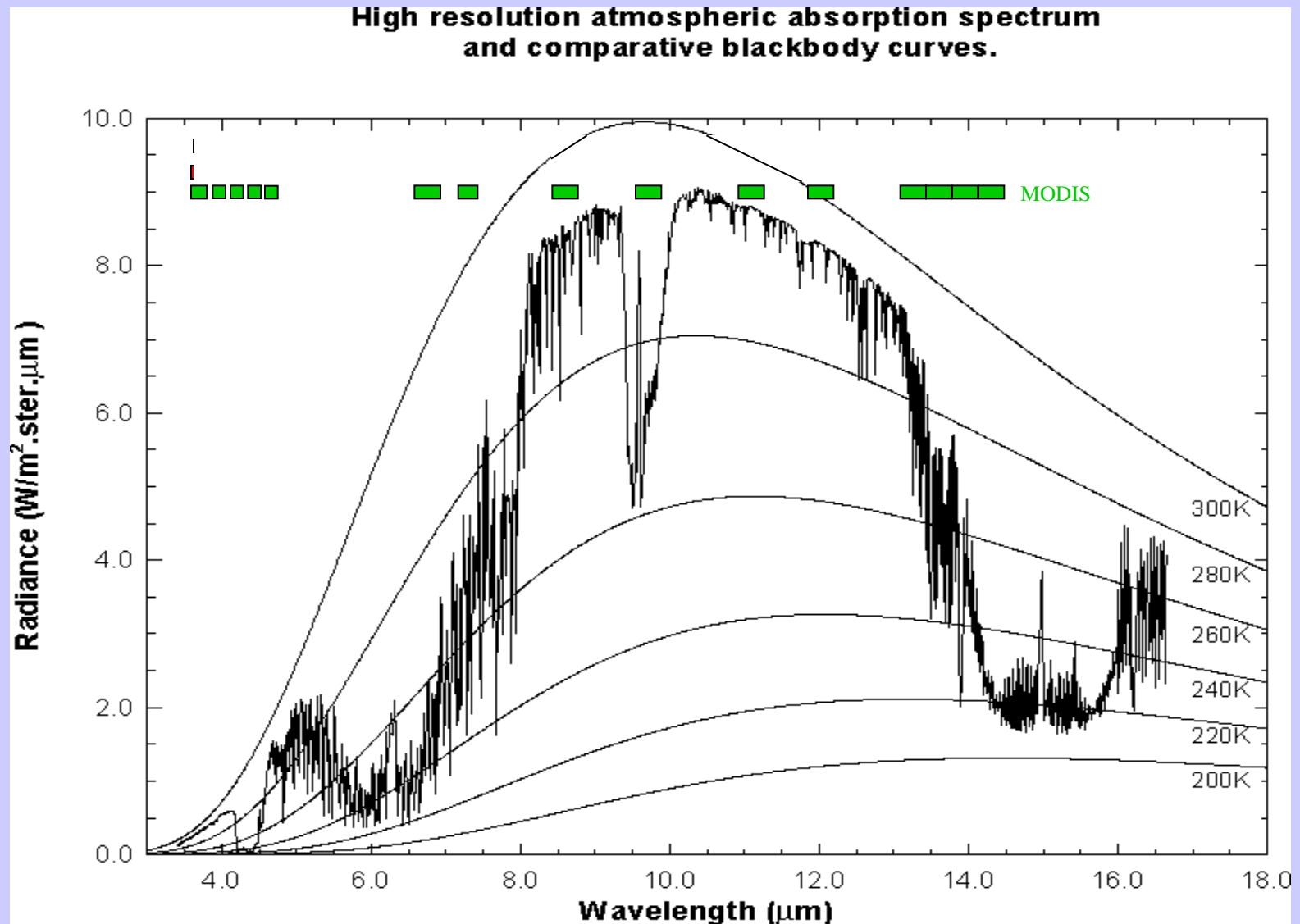
$NDSI = [r_{0.6} - r_{1.6}] / [r_{0.6} + r_{1.6}]$ is near one in snow in Alps

Meteosat-8 sees icing in clouds (Lutz et al)

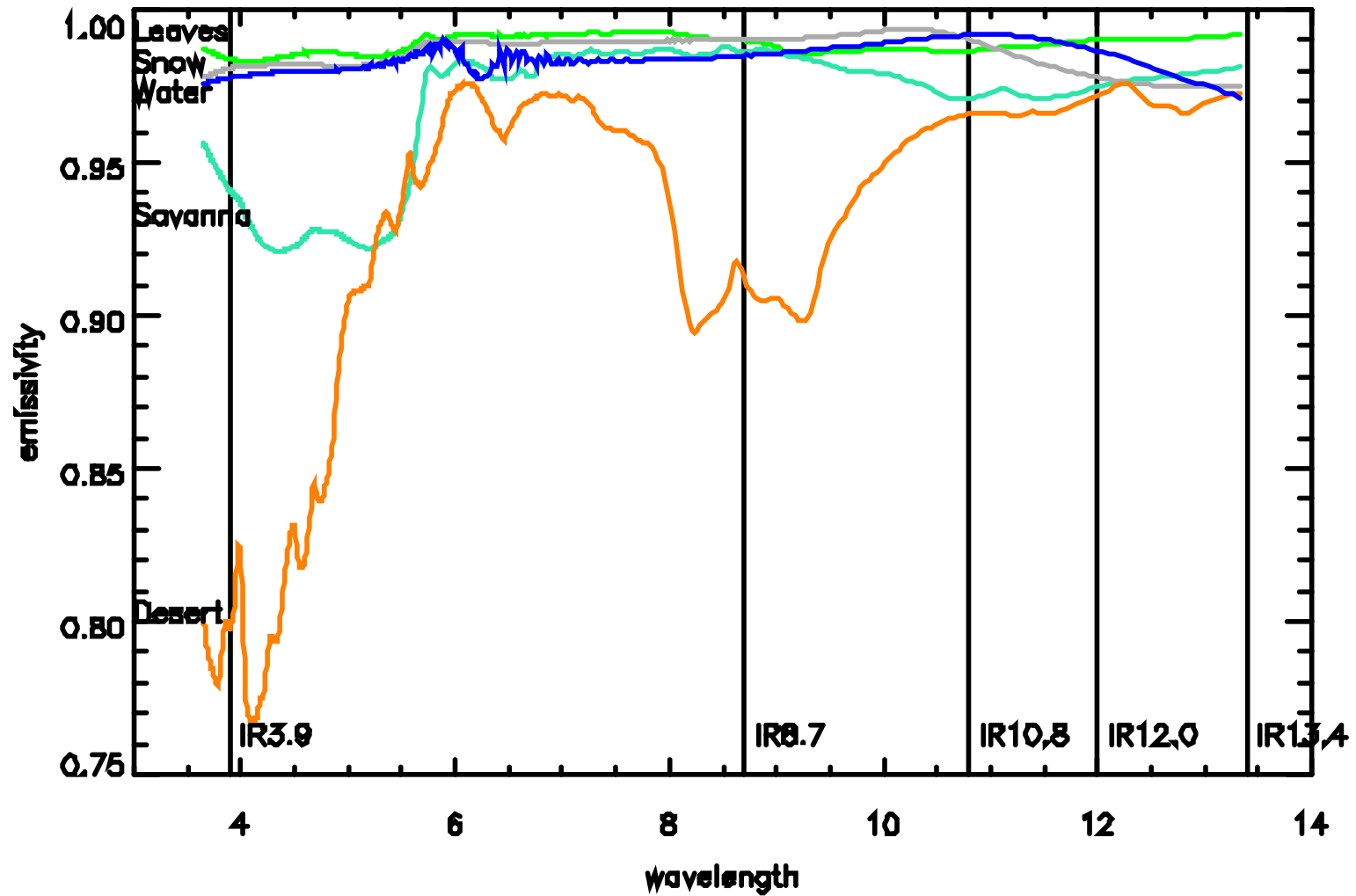


IR

MODIS IR Spectral Bands

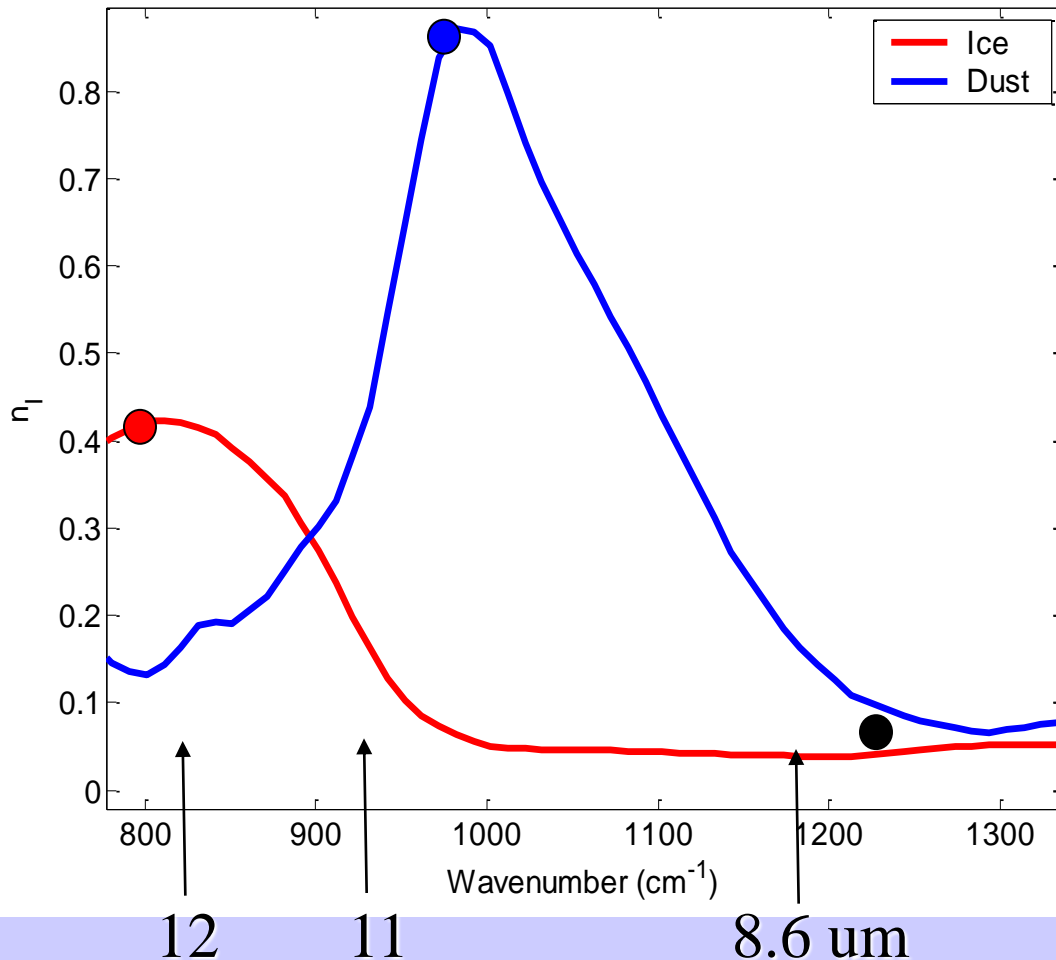


Surface Emissivity



Dust and Cirrus Signals

Imaginary Index of Refraction of Ice and Dust



- Both ice and silicate absorption small in 1200 cm⁻¹ window

- In the 800-1000 cm⁻¹ atmospheric window:

Silicate index *increases*

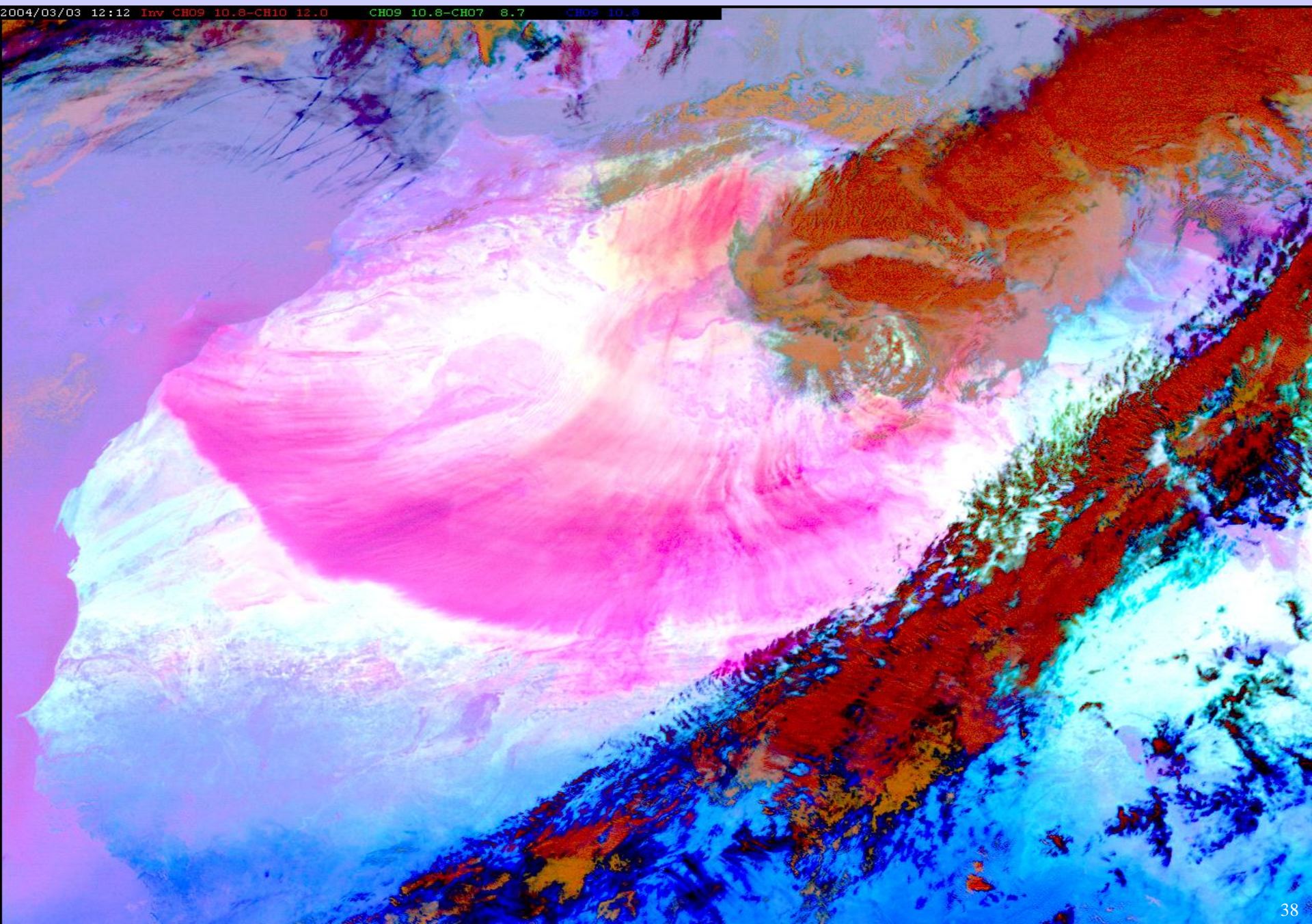
Ice index *decreases*

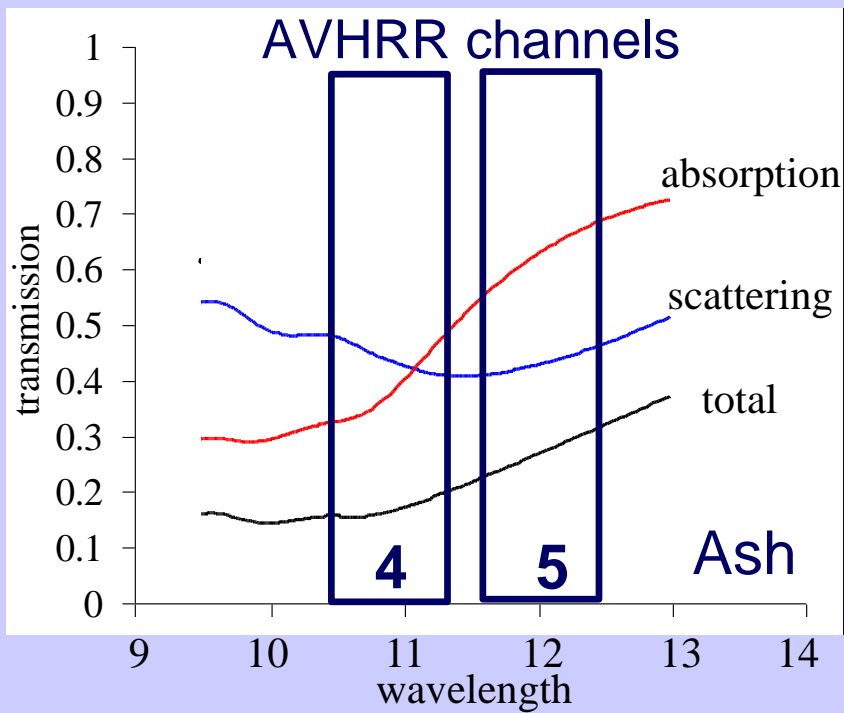
with wavenumber

Volz, F.E. : Infrared optical constant of ammonium sulphate, Sahara Dust, volcanic pumice and flash, *Appl Optics* **12** 564-658 (1973)

SEVIRI sees dust storm over Africa

2004/03/03 12:12 Inv CH09 10.8-CH10 12.0 CH09 10.8-CH07 8.7 CH09 10.8



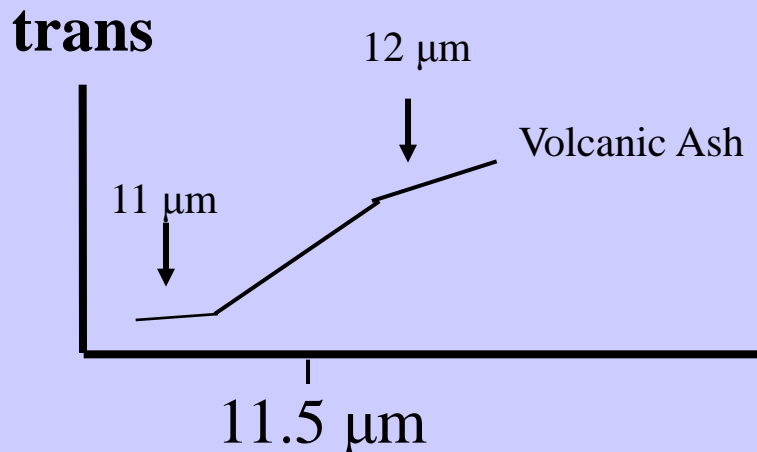


Investigating with Multi-spectral Combinations

Given the spectral response of a surface or atmospheric feature

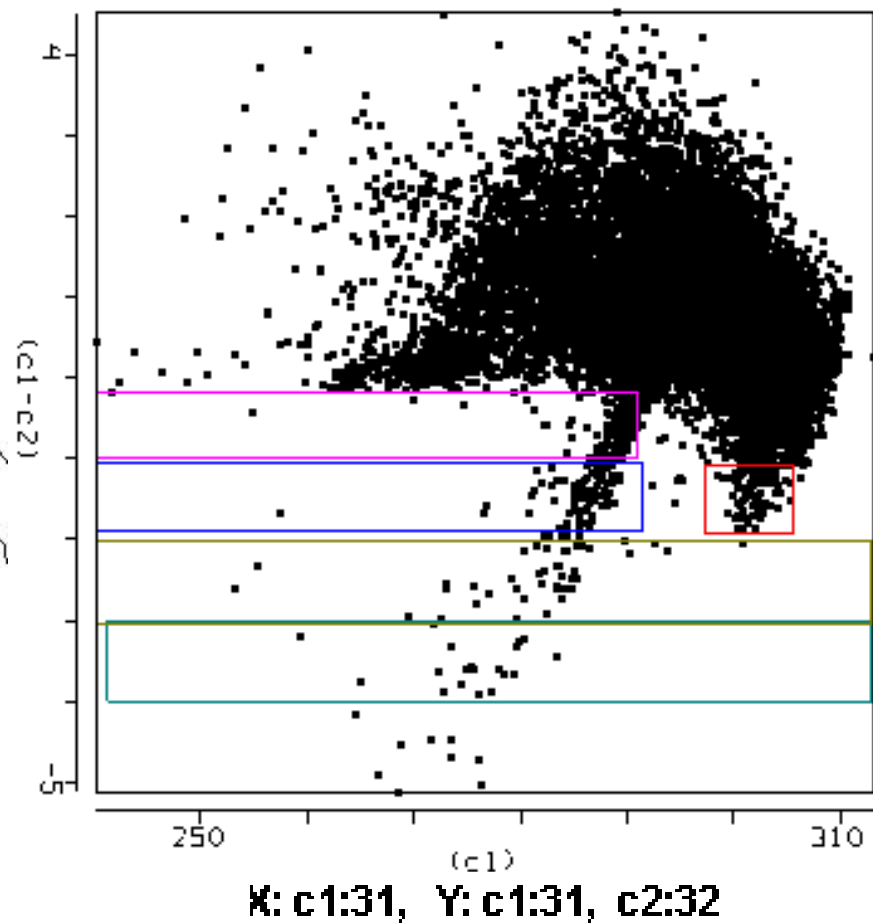
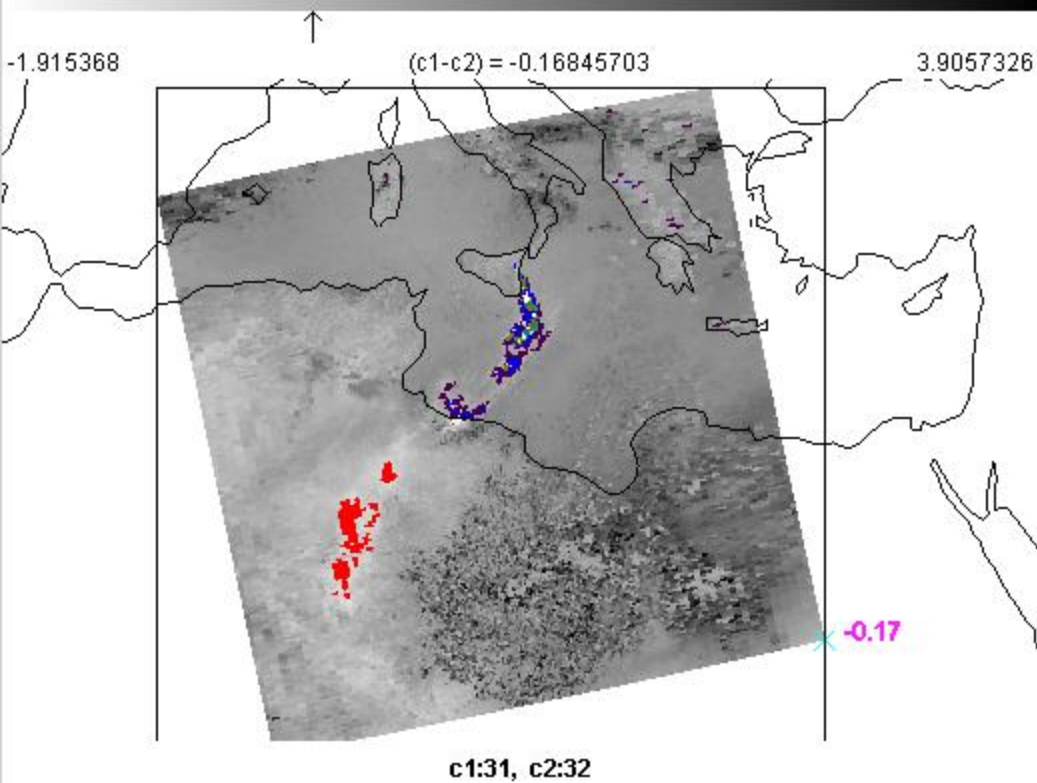
Select a part of the spectrum where the reflectance or absorption changes with wavelength

e.g. transmission through ash



If 11 μm sees the same or higher BT than 12 μm the atmosphere viewed does not contain volcanic ash;
if 12 μm sees considerably higher BT than 11 μm then the atmosphere probably contains volcanic ash

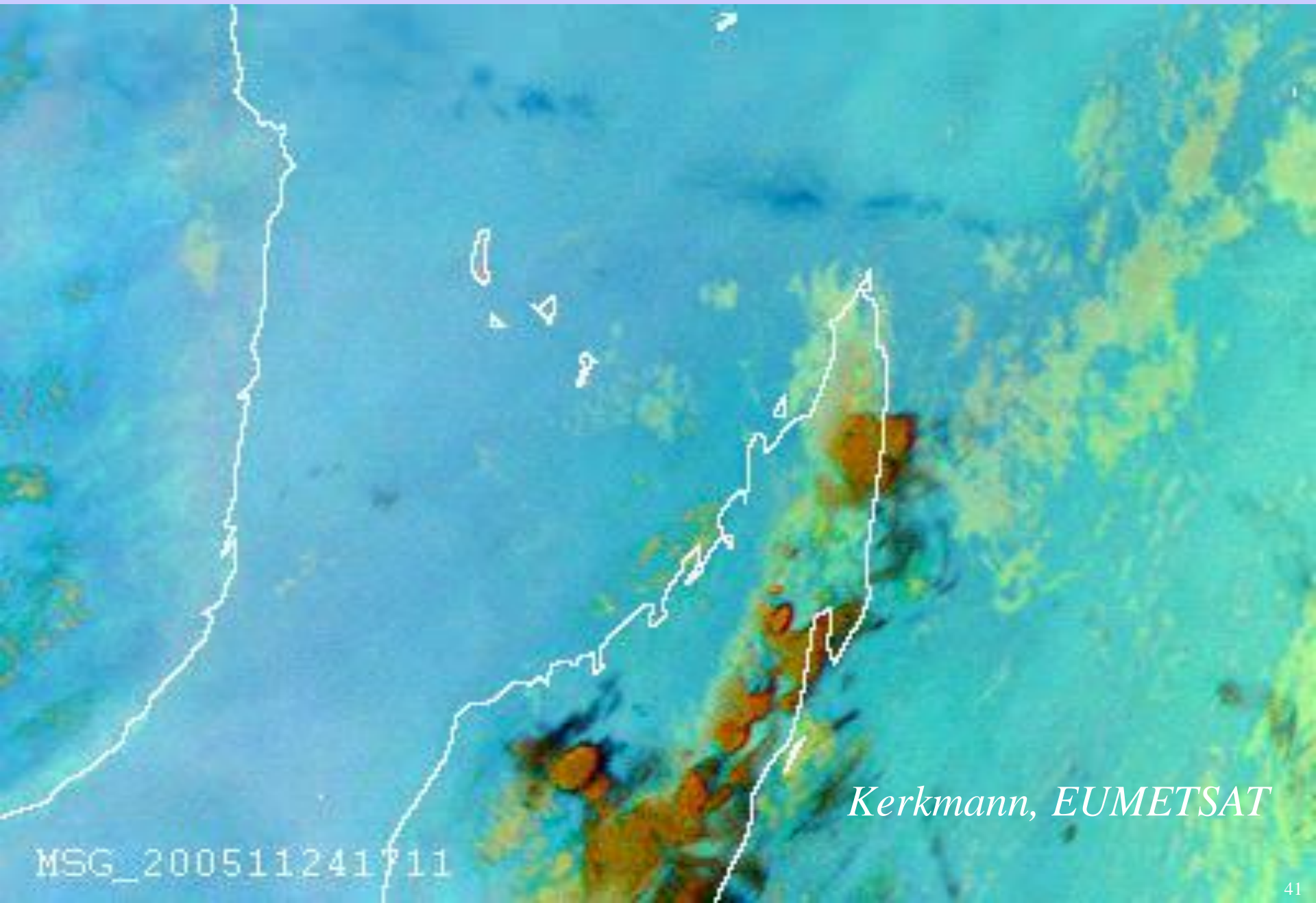
Frank Honey, CSIRO 1980s



Volcanic Ash is characterised by low brightness temperatures (i.e. High in the atmosphere) and negative differences in band 31-32.

The emissivity of desert at 12 μm is higher than at 11 μm , and hence $\text{BT}(12 \mu\text{m}) > \text{BT}(11 \mu\text{m})$ thus negative values. The red pixels are very arid regions of the desert and are not ash clouds.

SEVIRI sees volcanic ash & SO2 and downwind inhibition of convection



Kerkmann, EUMETSAT

MSG_200511241711

Radiative Transfer Equation

When reflection from the earth surface is also considered, the RTE for infrared radiation can be written

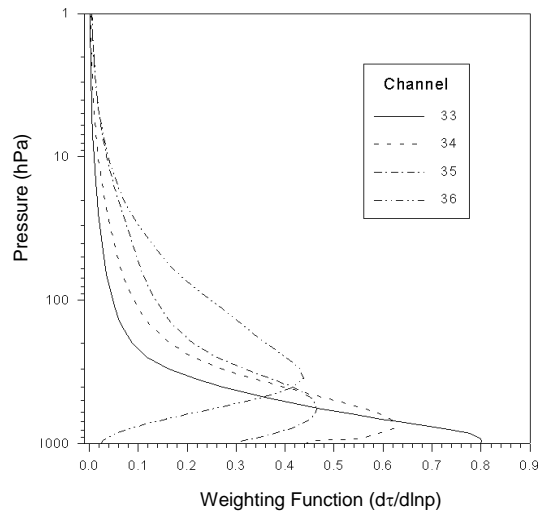
$$I_{\lambda} = \varepsilon_{\lambda}^{\text{sfc}} B_{\lambda}(T_s) \tau_{\lambda}(p_s) + \int_{p_s}^0 B_{\lambda}(T(p)) F_{\lambda}(p) [d\tau_{\lambda}(p) / dp] dp$$

where

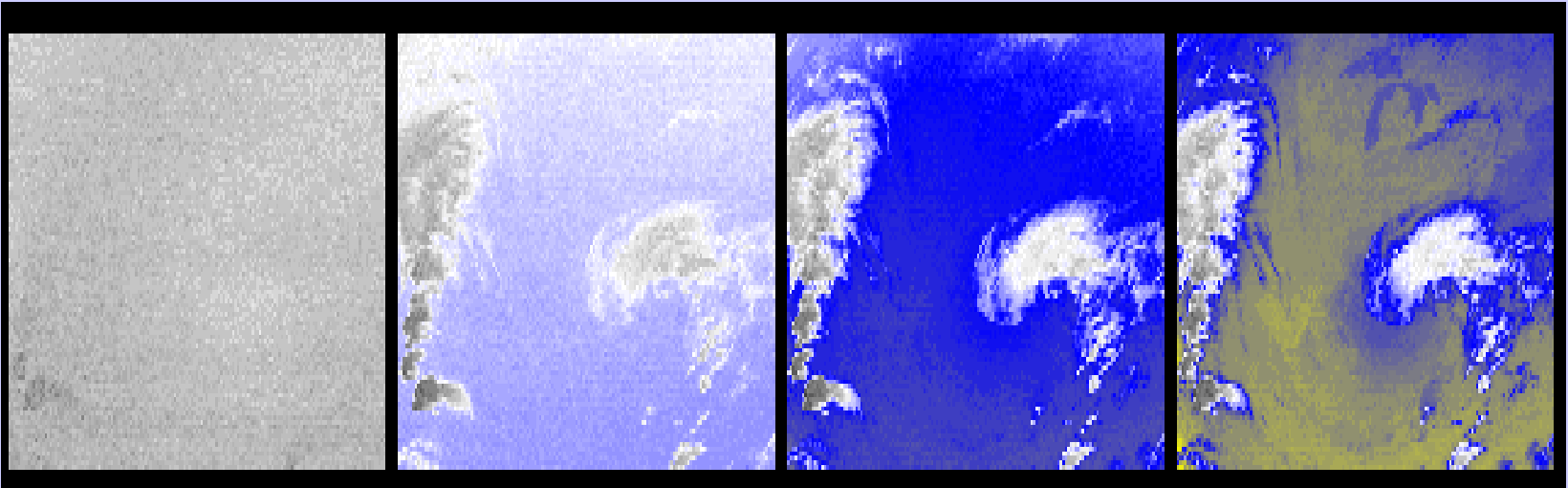
$$F_{\lambda}(p) = \{ 1 + (1 - \varepsilon_{\lambda}) [\tau_{\lambda}(p_s) / \tau_{\lambda}(p)]^2 \}$$

The first term is the spectral radiance emitted by the surface and attenuated by the atmosphere, often called the boundary term and the second term is the spectral radiance emitted to space by the atmosphere directly or by reflection from the earth surface.

The atmospheric contribution is the weighted sum of the Planck radiance contribution from each layer, where the weighting function is $[d\tau_{\lambda}(p) / dp]$. This weighting function is an indication of where in the atmosphere the majority of the radiation for a given spectral band comes from.



CO2 channels see different layers in the atmosphere

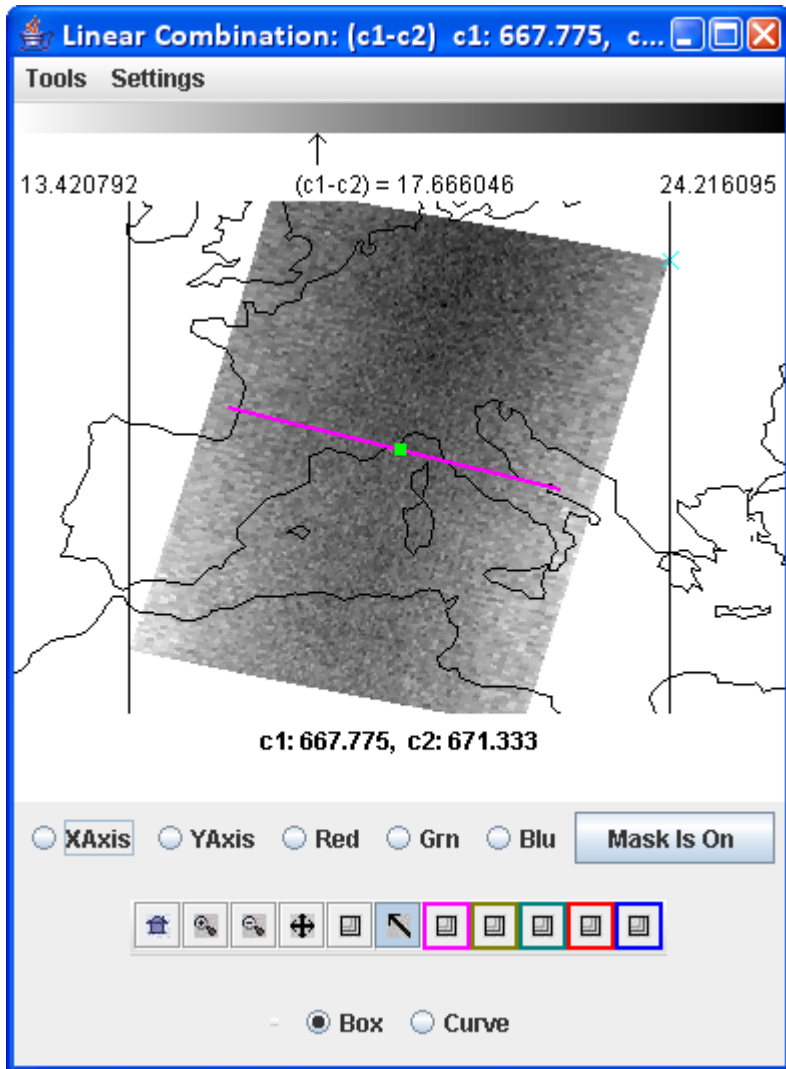


14.2 um

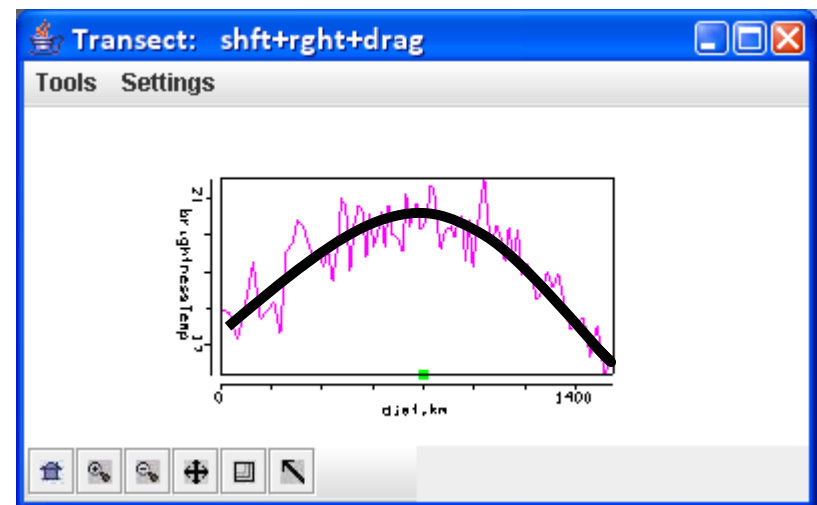
13.9 um

13.6 um

13.3 um

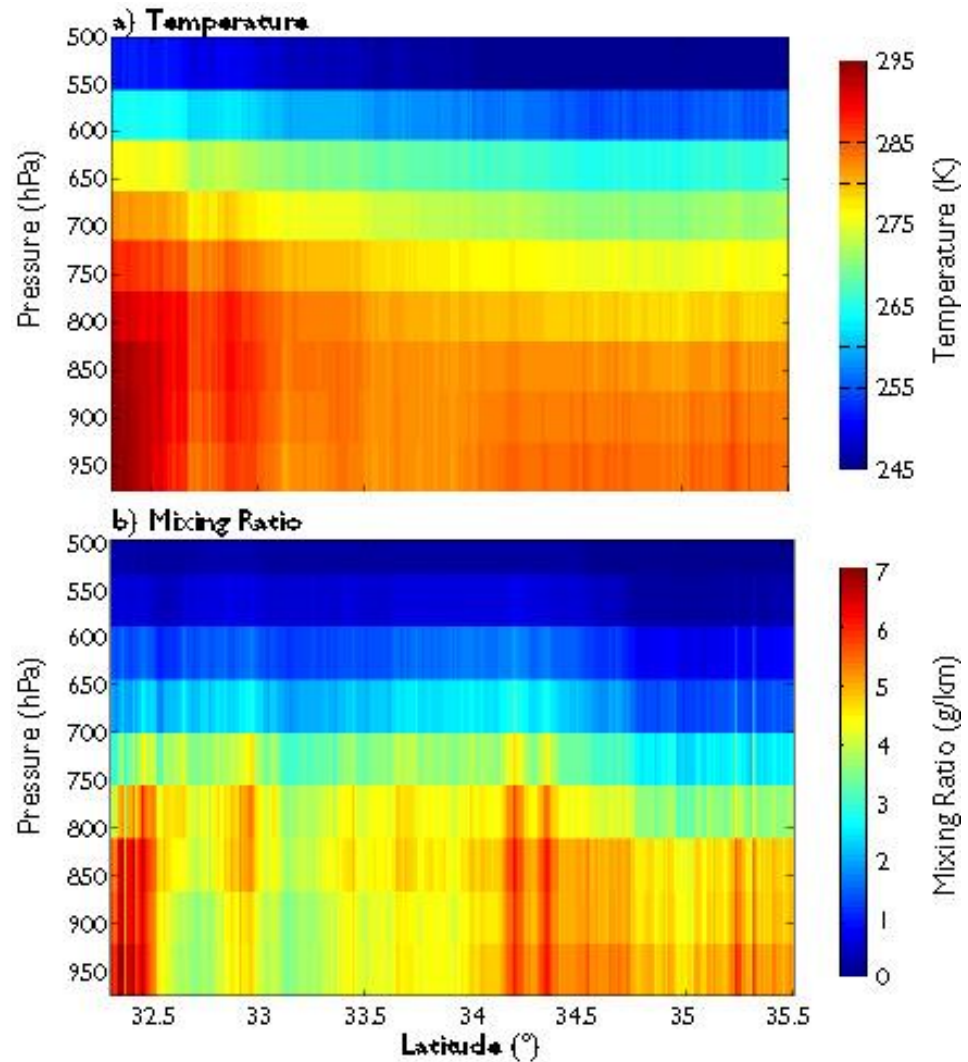
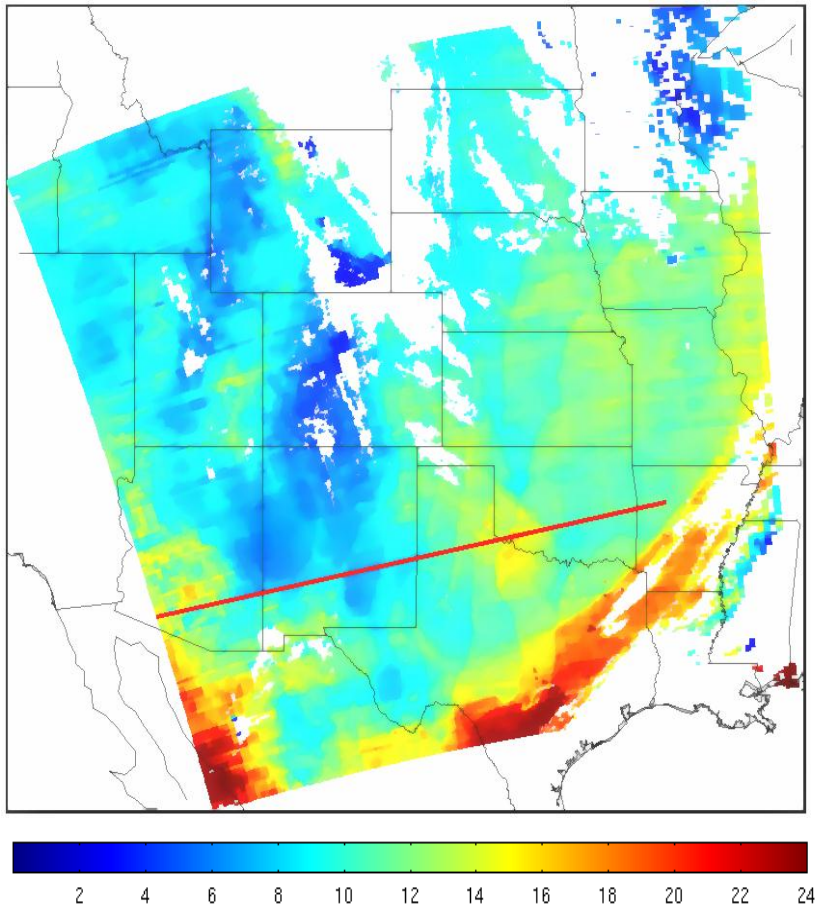


Perpedicular at nadir



Limb darkening

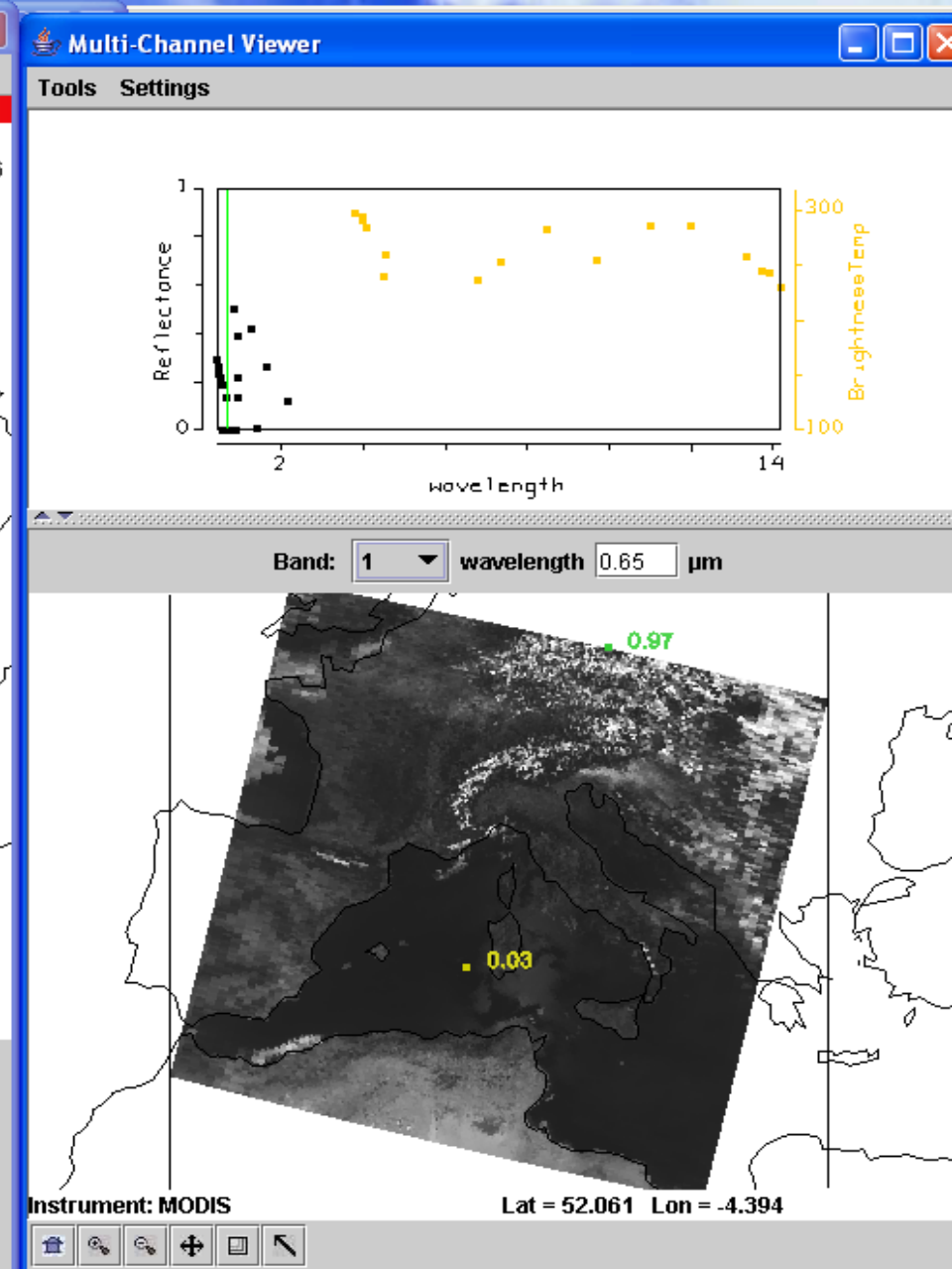
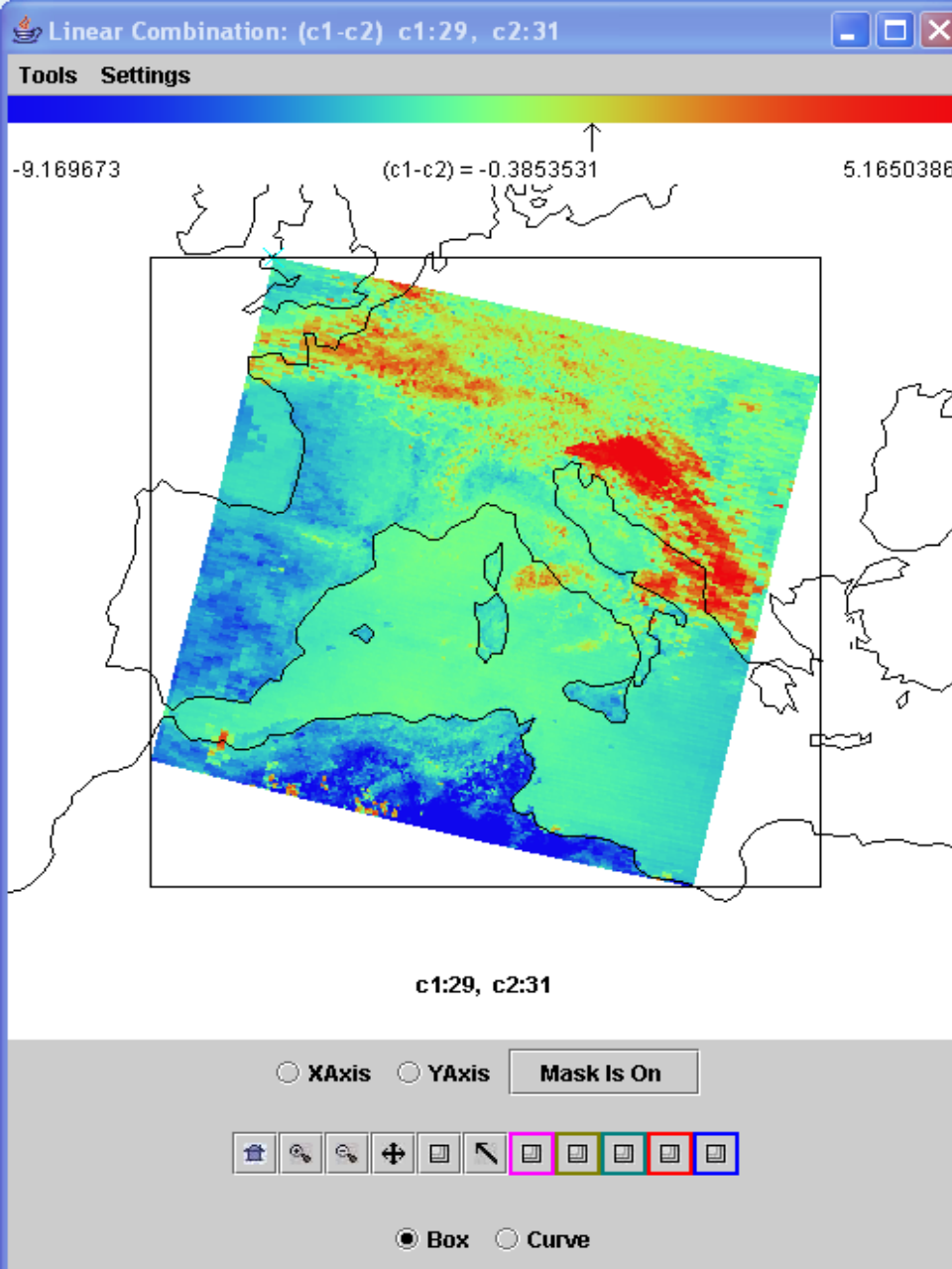
MODIS TPW



Clear sky layers of temperature and moisture on 2 June 2001

Cloud Mask Tests

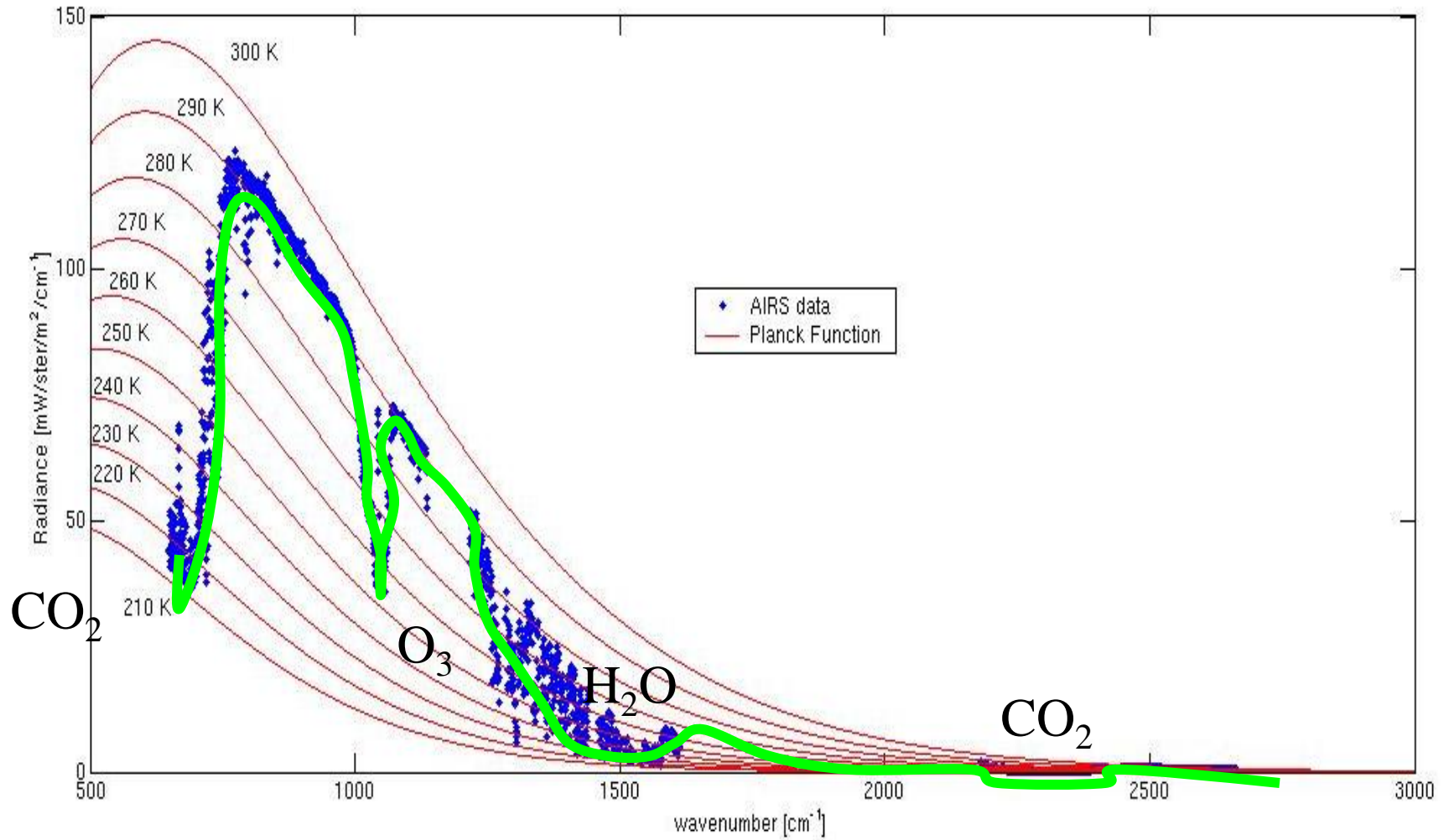
- BT11 clouds over ocean
- BT13.9 high clouds
- BT6.7 high clouds
- BT3.9-BT11 broken or scattered clouds
- BT11-BT12 high clouds in tropics
- BT8.6-BT11 ice clouds
- BT6.7-BT11 or BT13.9-BT11 clouds in polar regions
- BT11+aPW(BT11-BT12) clouds over ocean
- r0.65 clouds over land
- r0.85 clouds over ocean
- r1.38 thin cirrus
- r1.6 clouds over snow, ice cloud
- r0.85/r0.65 or NDVI clouds over vegetation
- σ (BT11) clouds over ocean



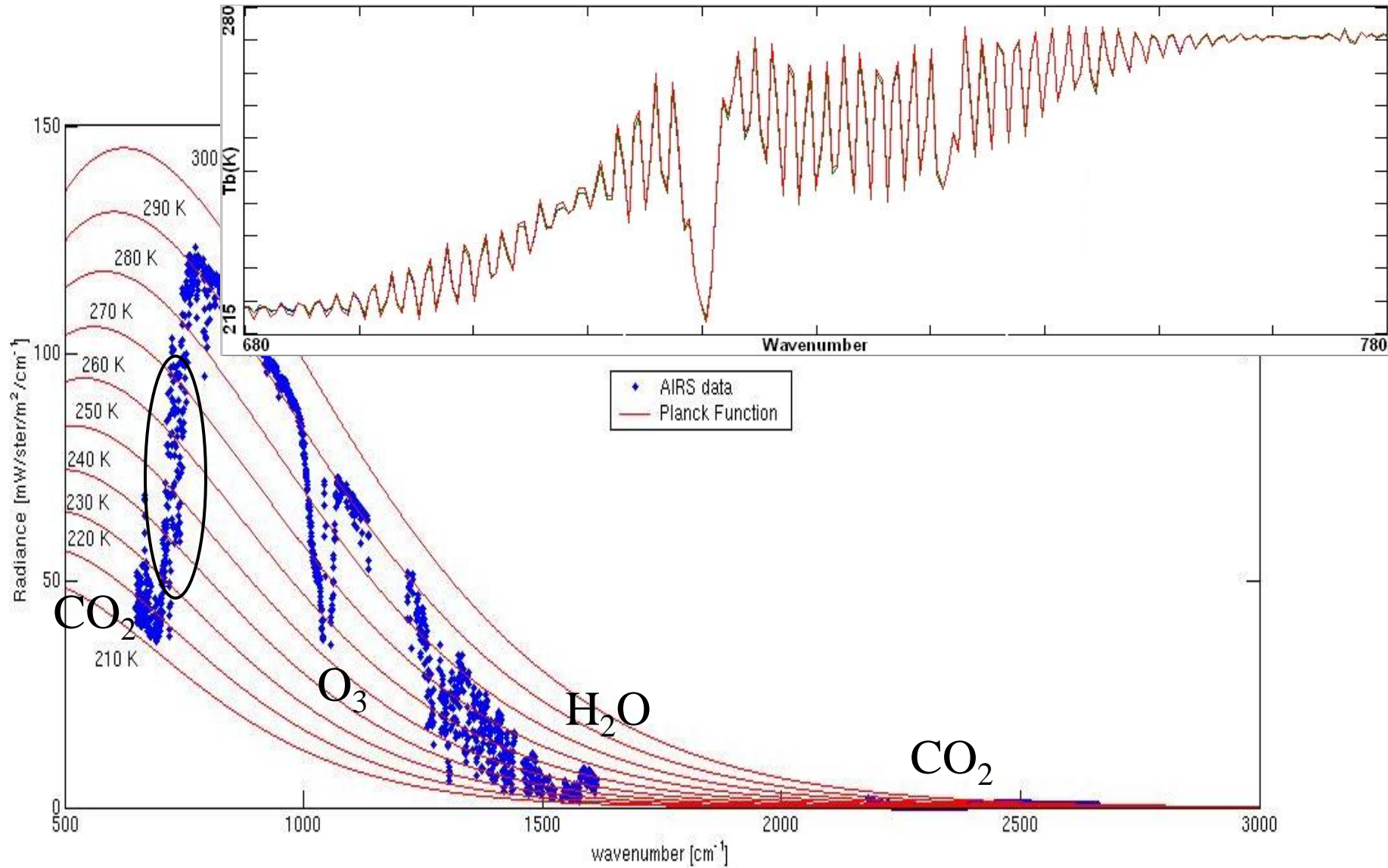
Ice clouds are revealed with $BT_{8.6} - BT_{11} > 0$ & water clouds and fog show in $r_{0.65}$

High Spectral Resolution IR

Vibrational Lines



Rotational Lines



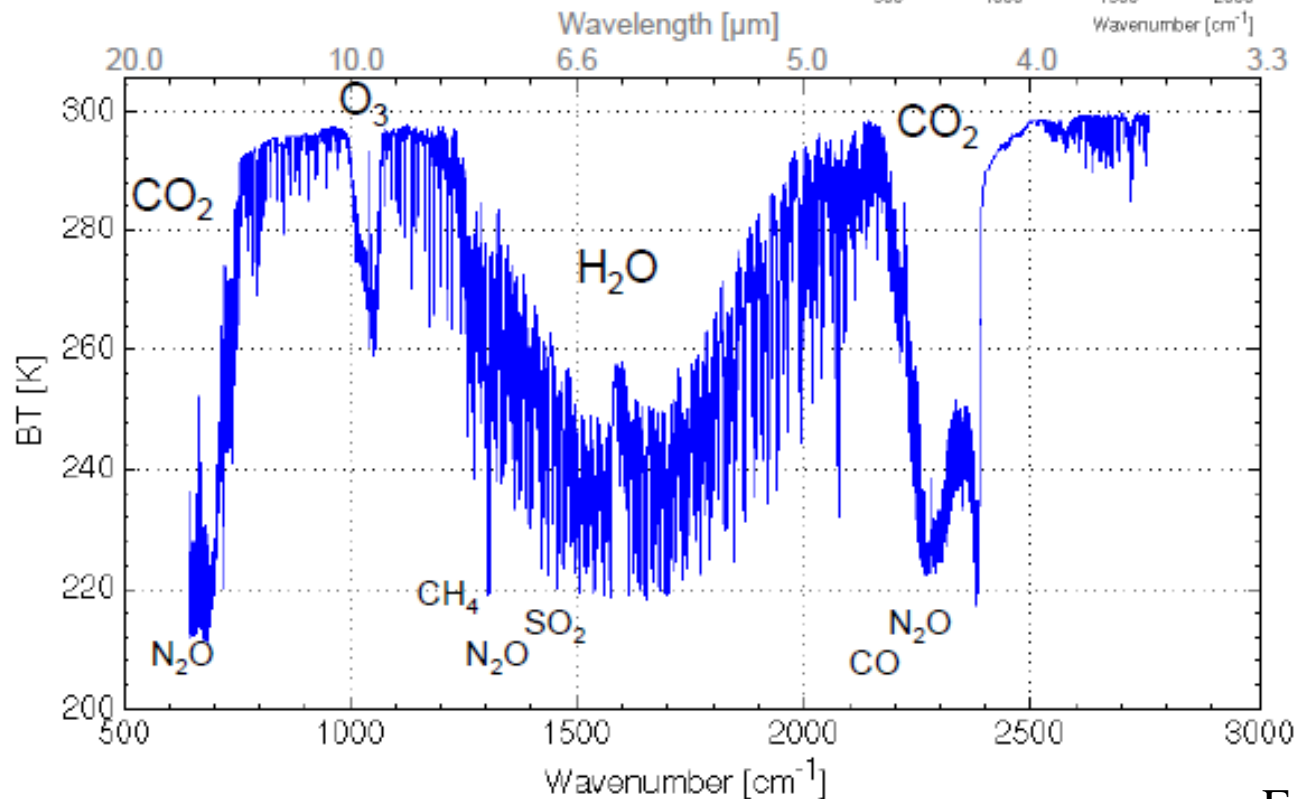
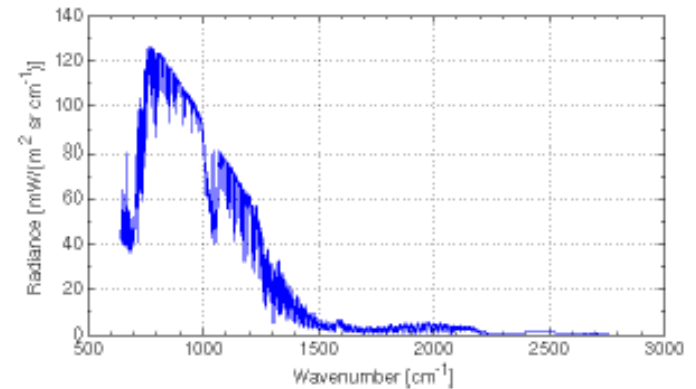
Infrared Radiance and Brightness Temperature Spectrum

Planck Function

$$B_\nu(T) = \frac{2hc^2\nu^3}{\exp\left(\frac{h\nu}{kT}\right) - 1}$$

Upwelling IR radiation

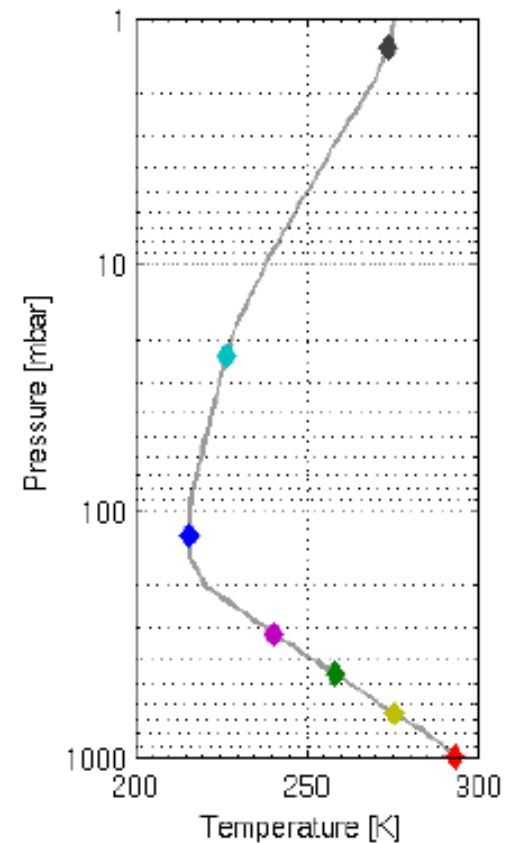
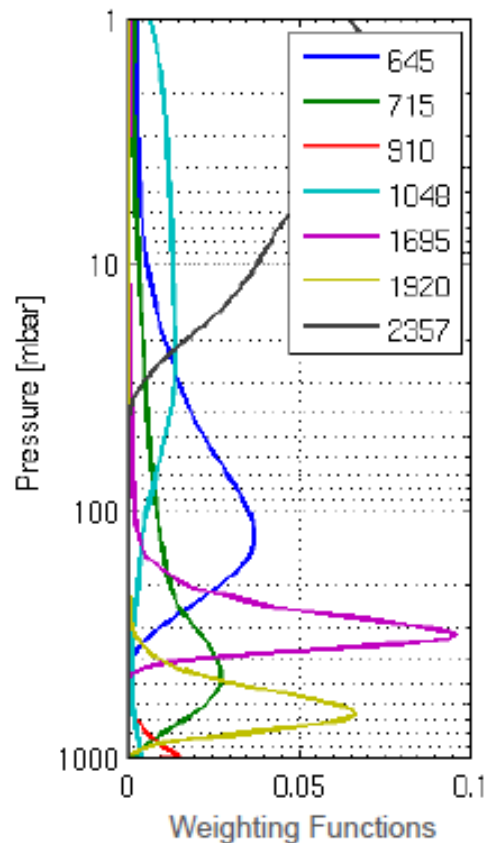
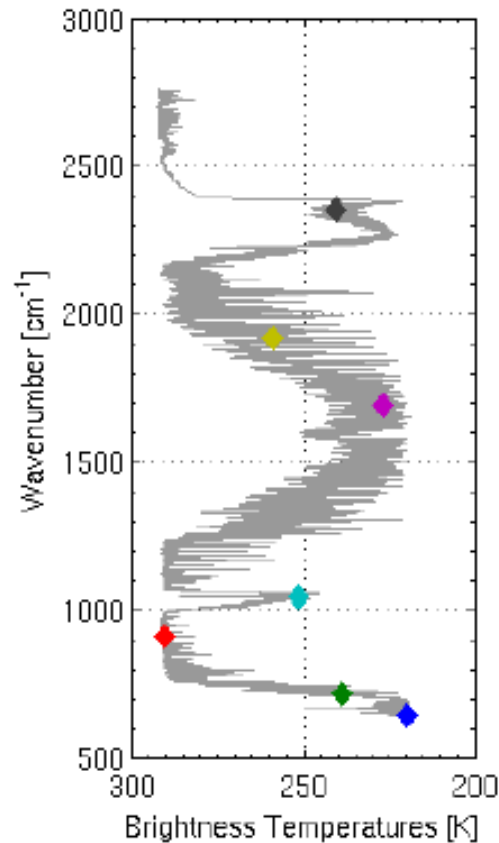
$$R_\nu = \int_{z_0}^{\infty} B_\nu(T(z)) \frac{d\tau_\nu(z)}{dz} dz$$



Atmospheric Temperature Profile Retrieval

$$R_v = \int_{ps}^0 B_v(T(p)) W_v(p) dp$$

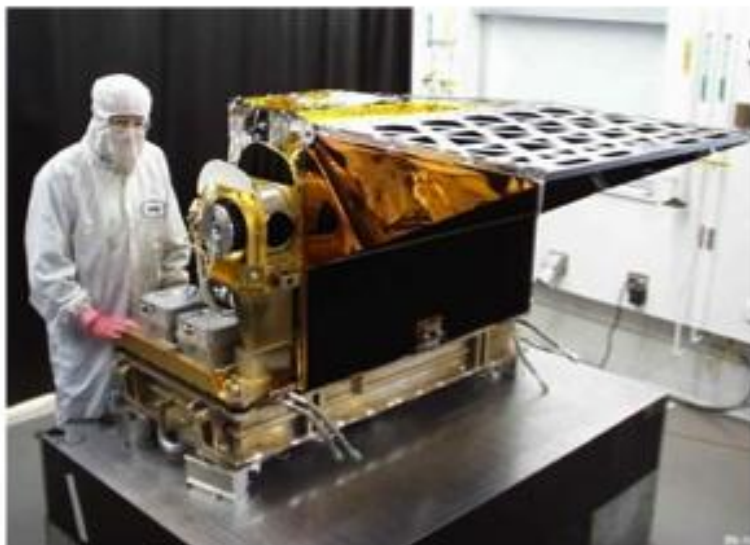
$$W_v(p) = \frac{\partial \tau_v(p)}{\partial \ln p}$$



High-spectral measurements



Profiles at high-vertical resolution



AIRS

Atmospheric InfraRed Sounder

Grating spectrometer

166 kg, 256 W

13.5 km FOV at nadir, contiguous

Launched on Aqua in 2002

IASI

Infrared Atmospheric Sounding Interferometer

Michelson interferometer

236 kg, 210 W

2x2 12 km FOVs at nadir, non-contiguous

Launched on Metop-A in 2006



CrIS

Cross-track Infrared Sounder

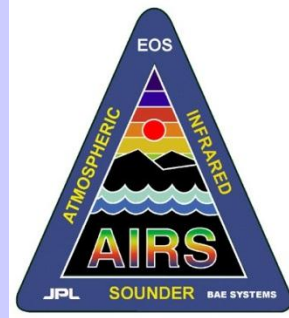
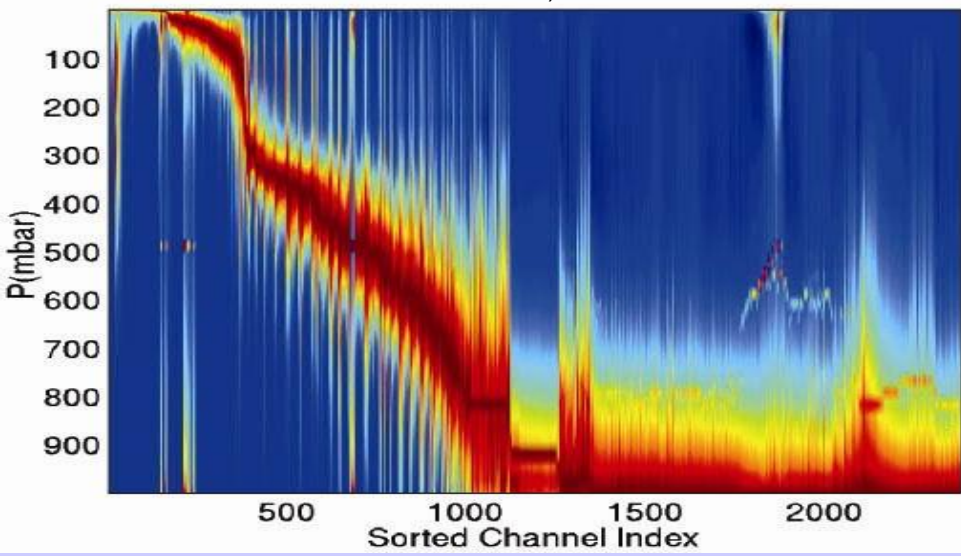
Michelson interferometer

146 kg, 110 W

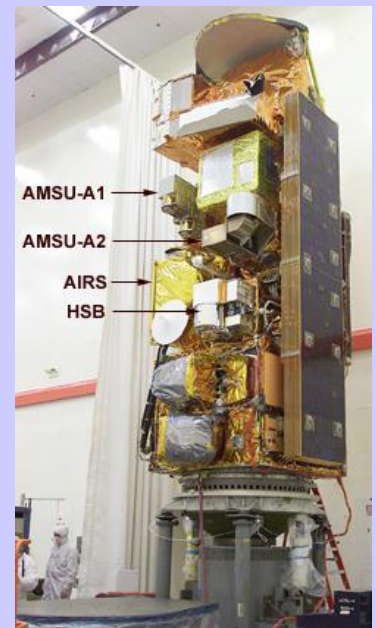
3x3 14 km FOVs at nadir, contiguous

To be launched on NPP

temperature weighting functions sorted by pressure of their peak (blue = 0)



AIRS On Aqua

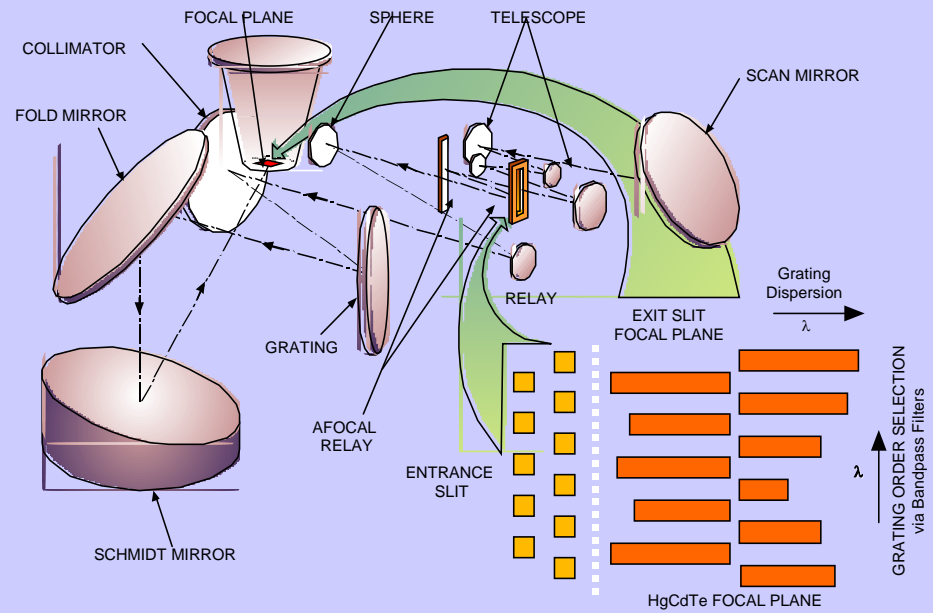


Instrument

- Hyperspectral radiometer with **resolution of 0.5 – 2 cm⁻¹**
- Extremely well calibrated pre-launch
- **Spectral range: 650 – 2700 cm⁻¹**
- Associated microwave instruments (AMSU, HSB)

Design

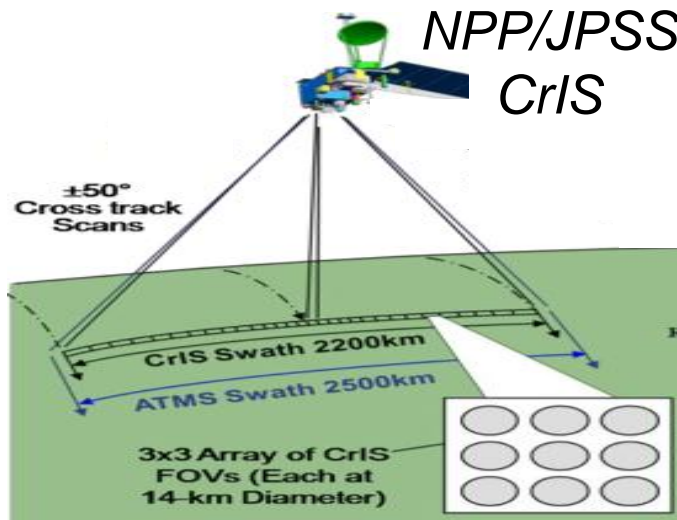
- Grating Spectrometer passively cooled to 160K, stabilized to 30 mK
- **PV and PC HgCdTe focal plane cooled to 60K** with redundant active pulse tube cryogenic coolers
- **Focal plane has ~5000 detectors**, 2378 channels. PV detectors (all below 13 microns) are doubly redundant. Two channels per resolution element ($n/D_n = 1200$)
- 310 K Blackbody and space view provides radiometric calibration
- Paralyene coating on calibration mirror and upwelling radiation provides spectral calibration
- **NEDT (per resolution element) ranges from 0.05K to 0.5K**



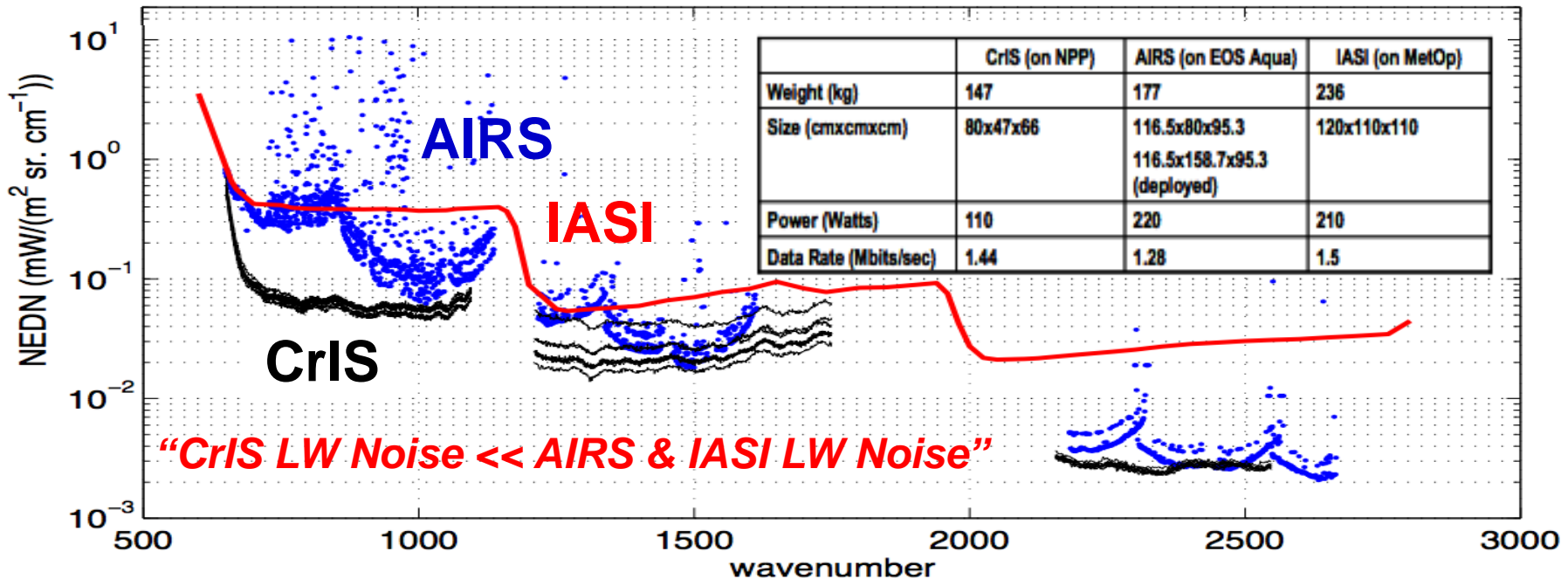
Spectral filters at each entrance slit and over each FPA array isolate color band (grating order) of interest

Cross-Track Infrared Sounder (CrIS)

NPOESS Preparatory Satellite – Launch: October 2011

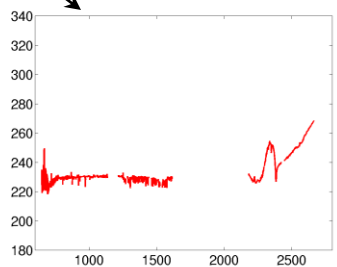
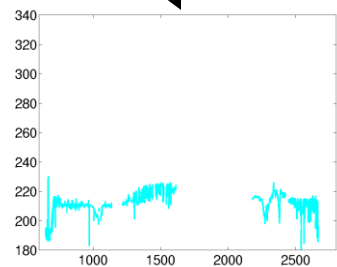
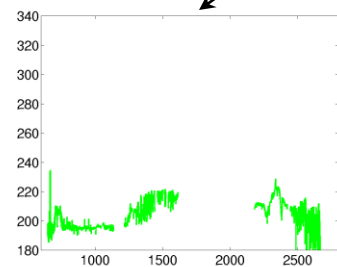
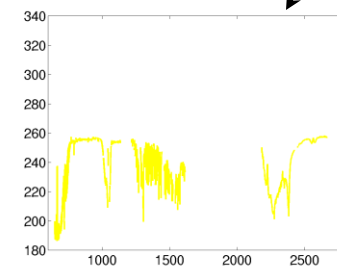
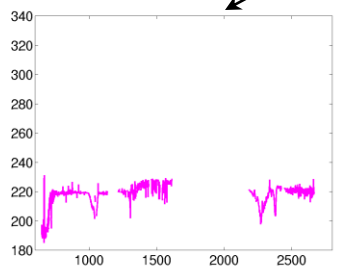
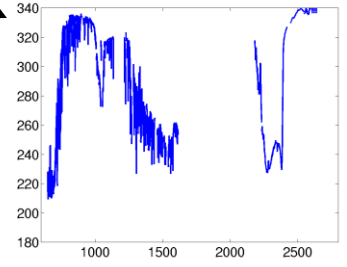
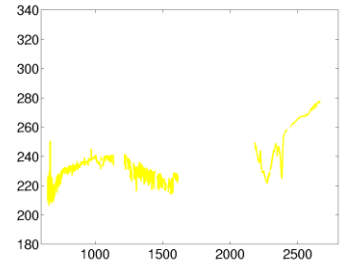
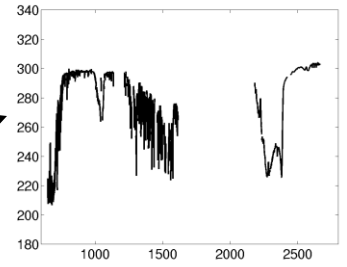
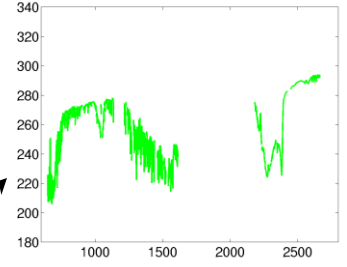
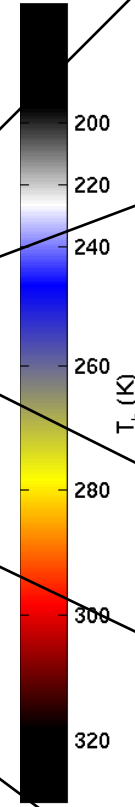
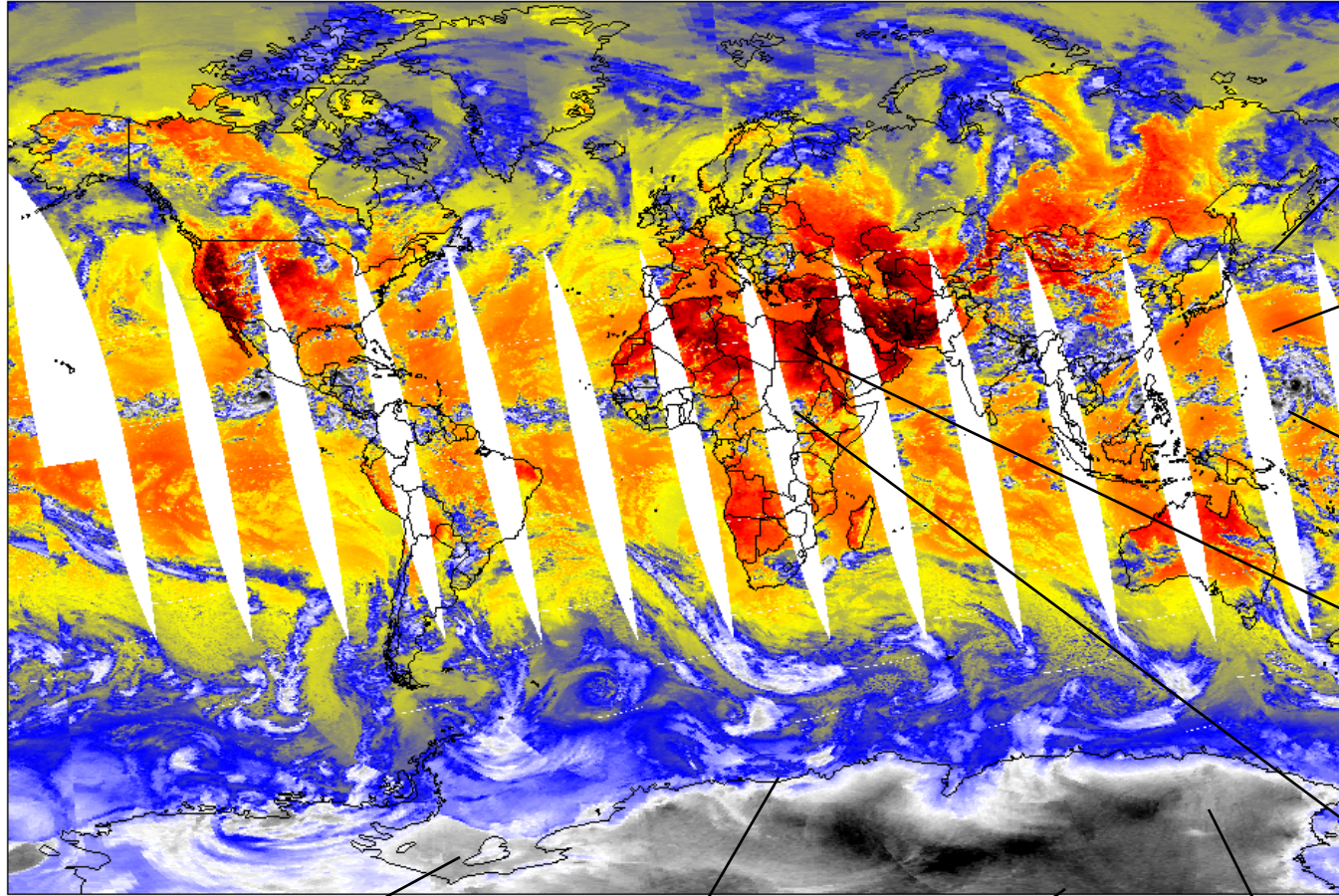


- Michelson Interferometer: 0.625, 1.25, 2.5 cm^{-1} (resolving power of 1000)
- Spectral range: 660-2600 cm^{-1}
- 3 x 3 HgCdTe focal plane passively cooled (4-stages) to 85K
- Focal plane 27 detectors, **1305 spectral channels**
- 310 K Blackbody and space view provides radiometric calibration
- NEDT ranges from 0.05 K to 0.5 K

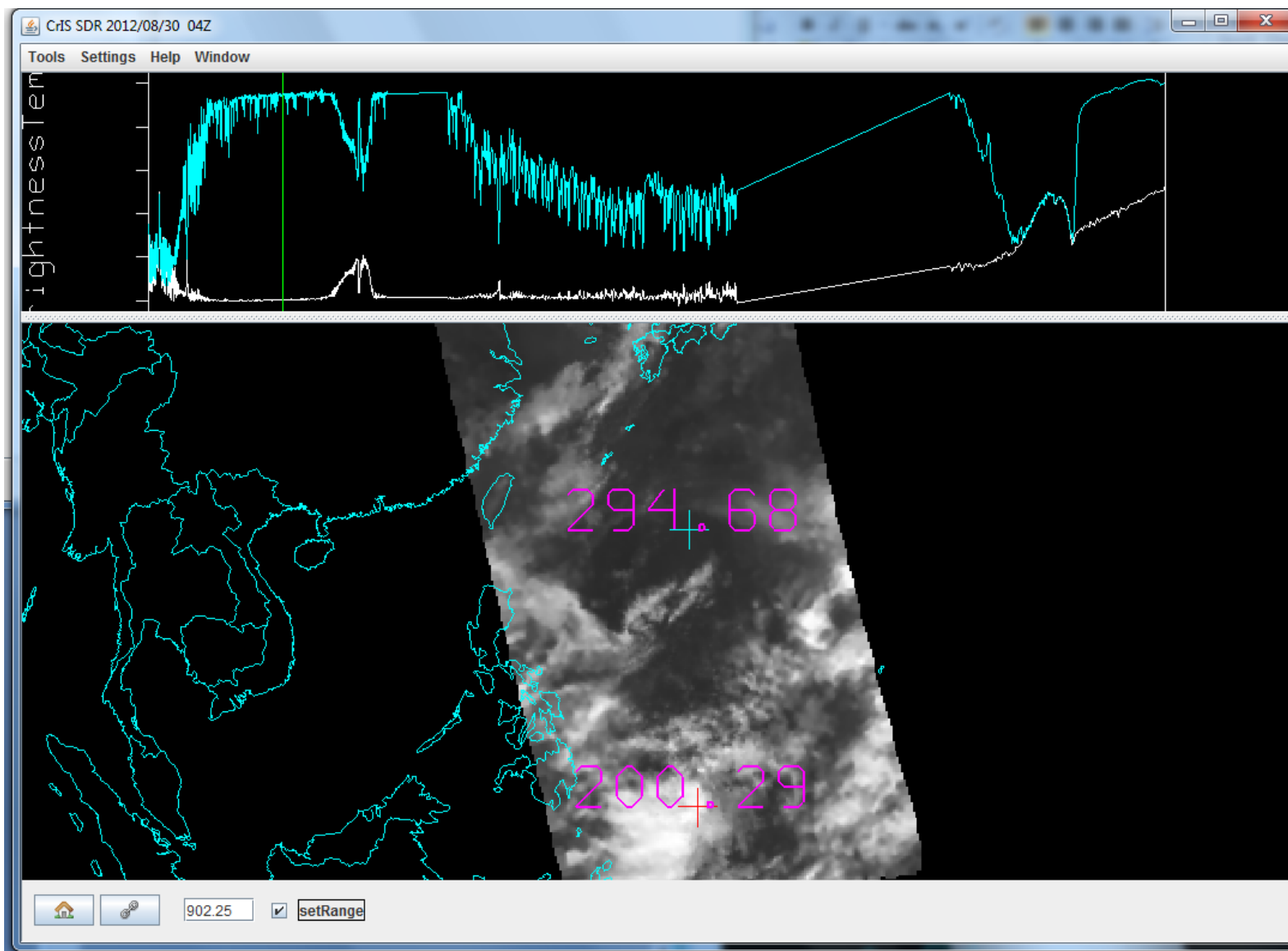


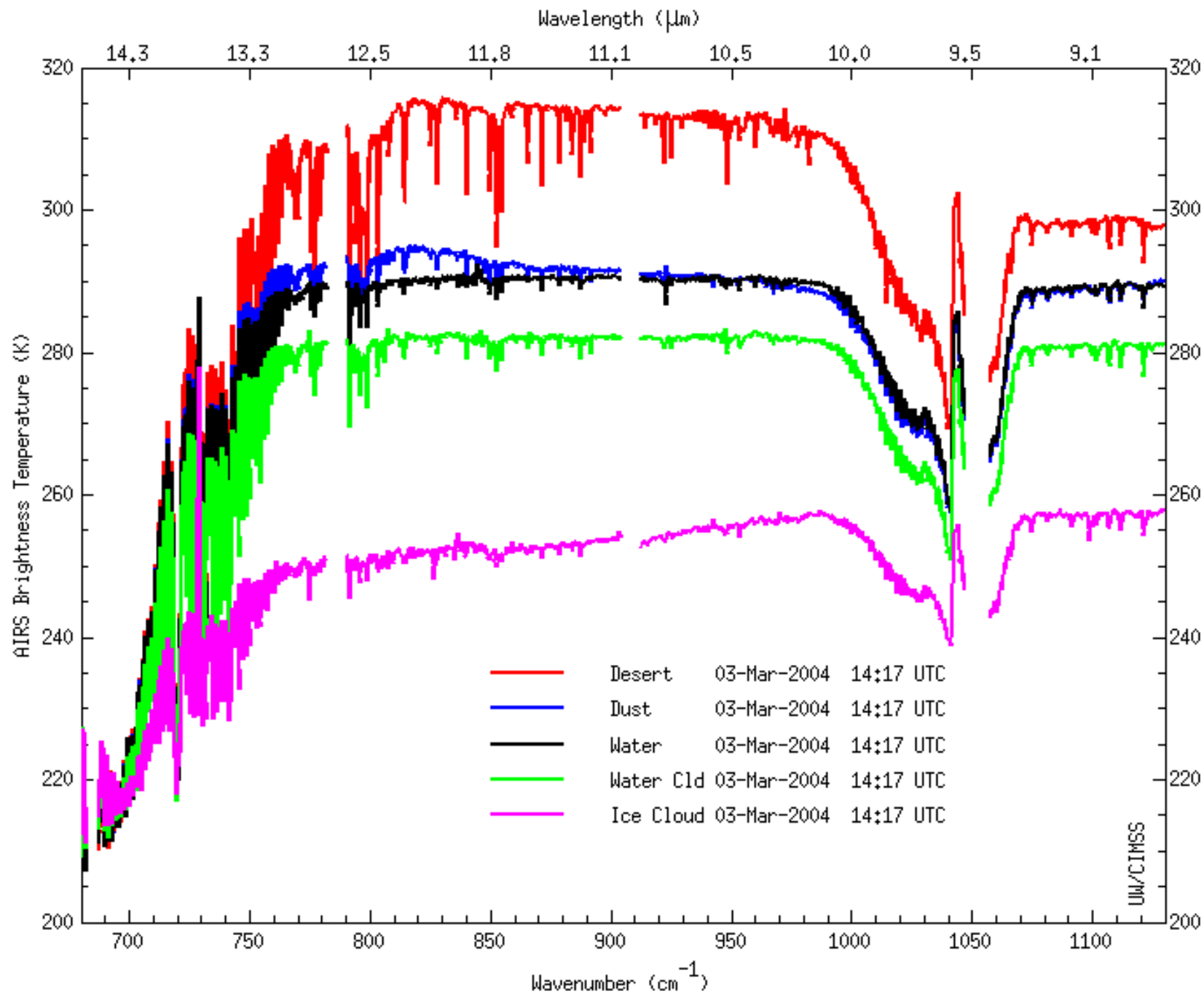
AIRS Spectra from around the Globe

20-July-2002 Ascending LW_Window

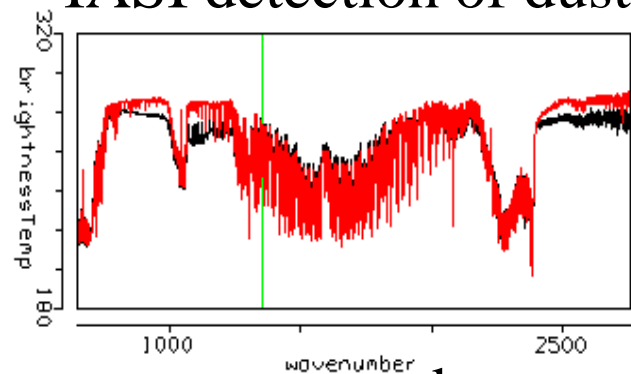


Gregg, Bill, Pei



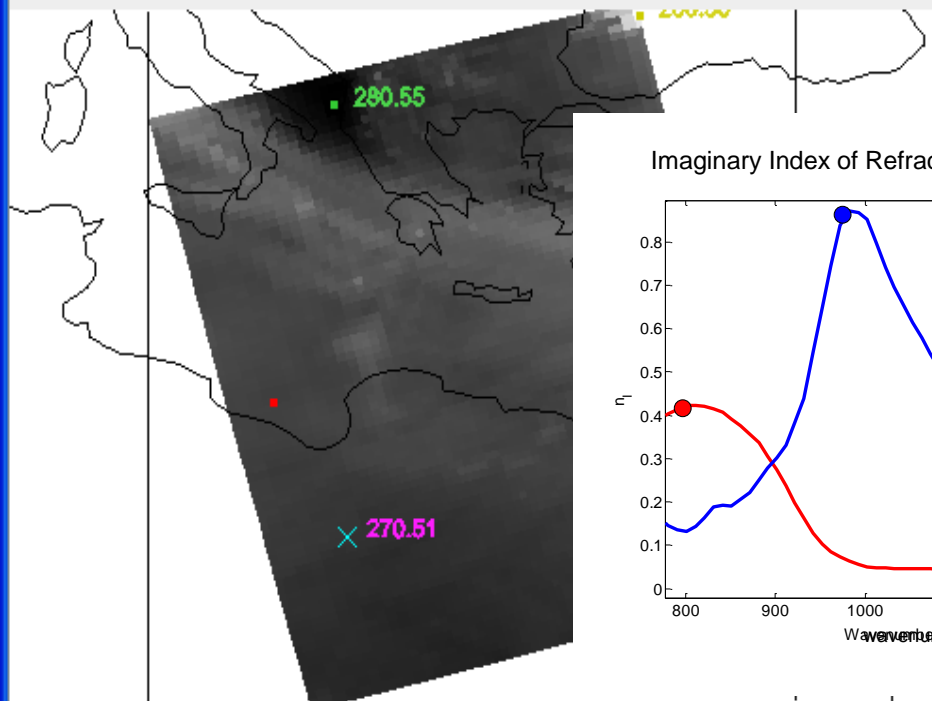


IASI detection of dust



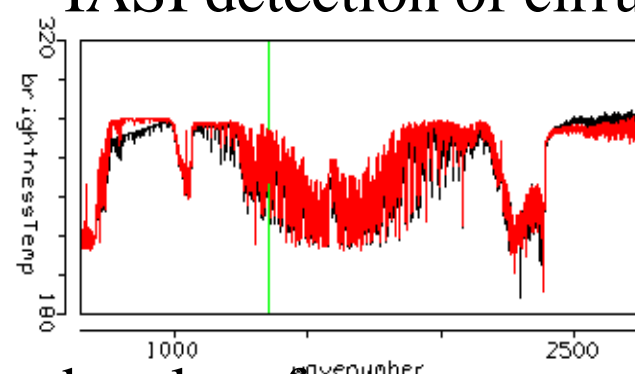
red spectrum is from nearby clear fov

wavenumber 1349.75 cm⁻¹

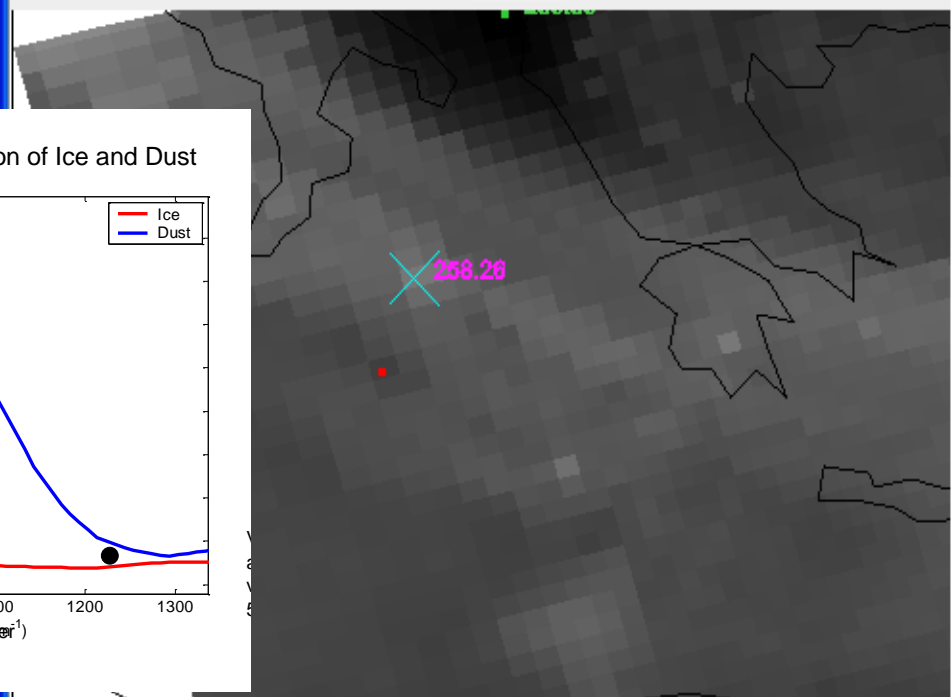


Instrument: "" Lat = 27.557 Lon = 20.077

IASI detection of cirrus

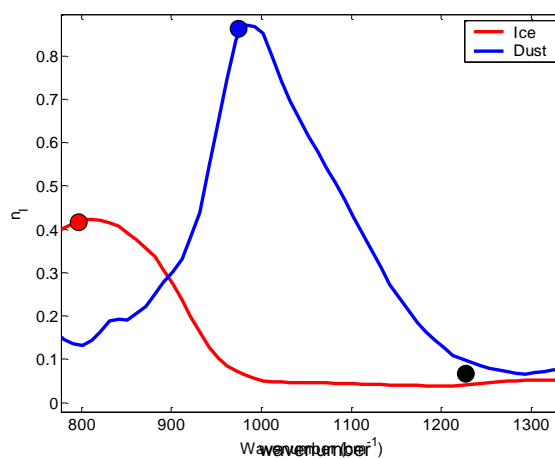


wavenumber 1349.75 cm⁻¹



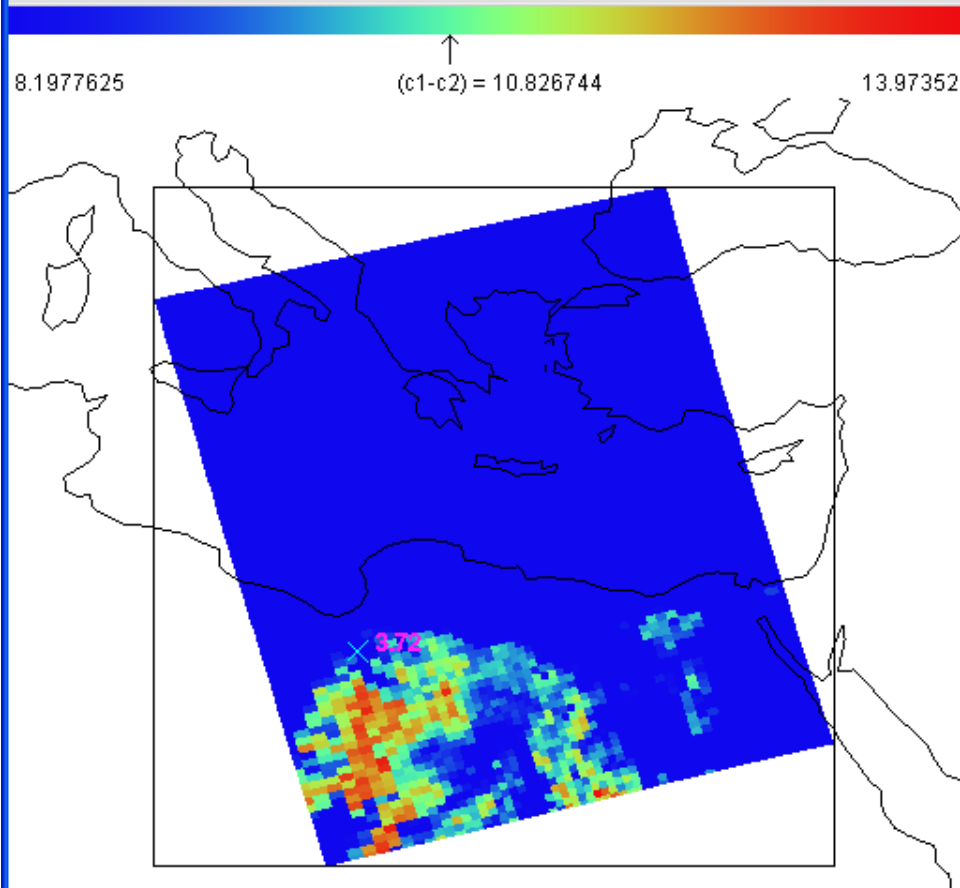
Instrument: "" Lat = 36.595 Lon = 17.650

Imaginary Index of Refraction of Ice and Dust



Tools Settings

Tools Settings Import



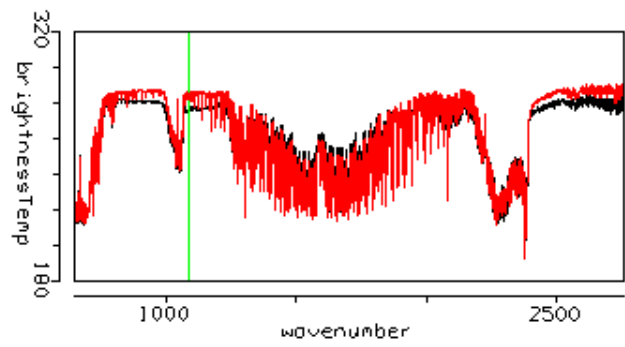
IASI detects barren regions

c1: 981.000, c2:1086.000

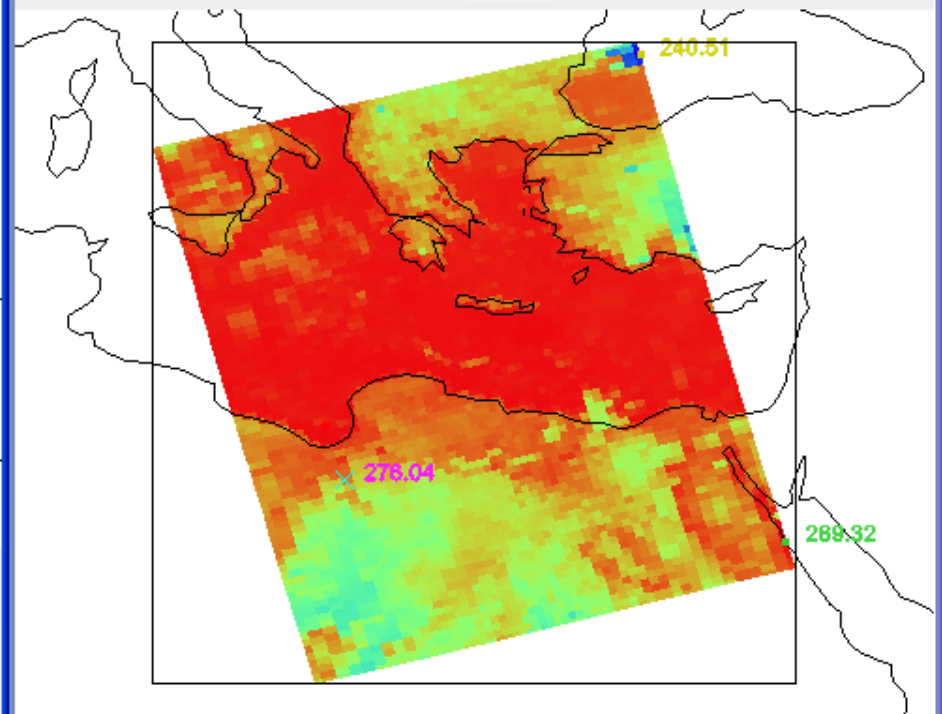
XAxis YAxis Red Grn Blu



Box Curve



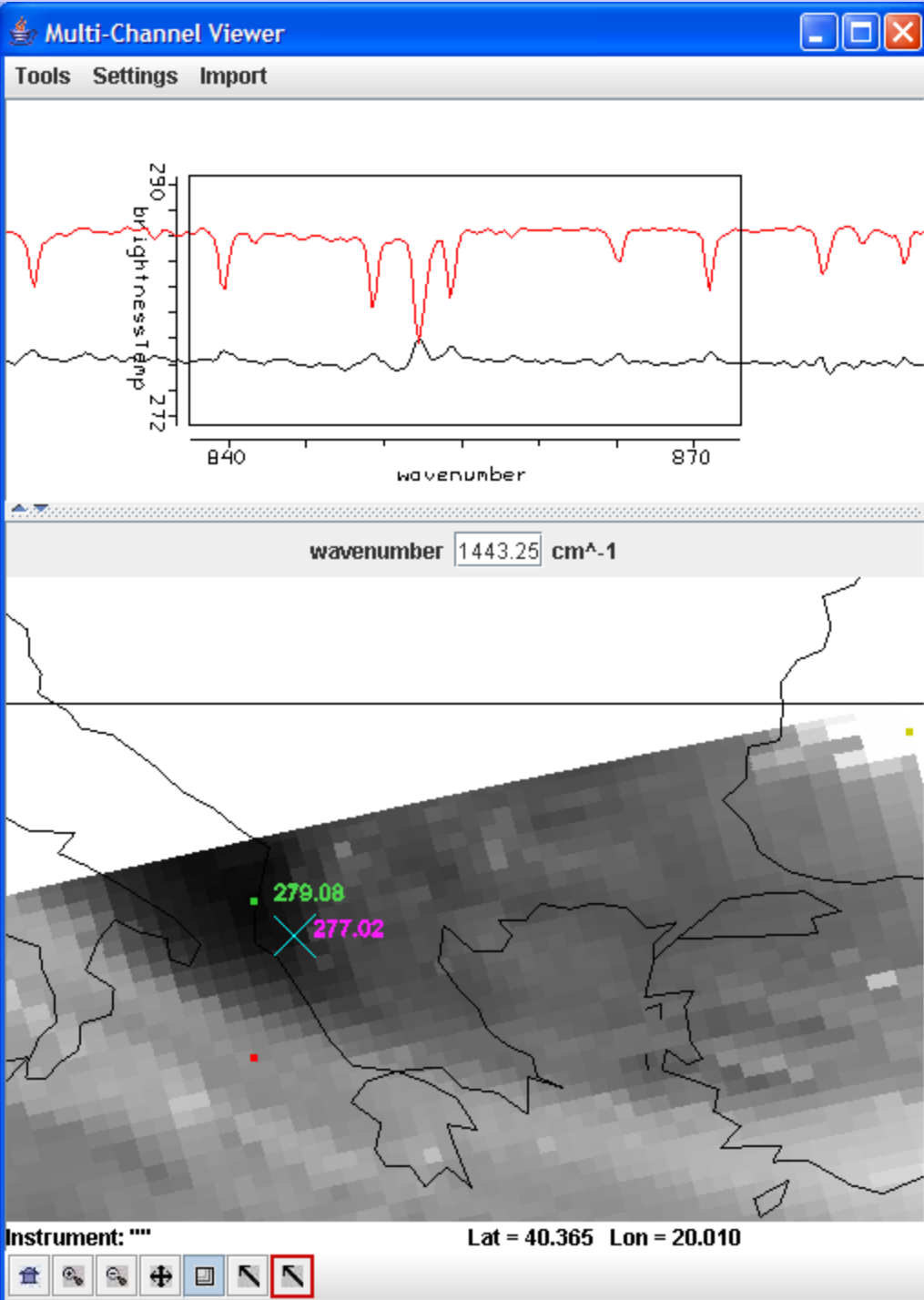
wavenumber 1086.00 cm⁻¹



Instrument: ""

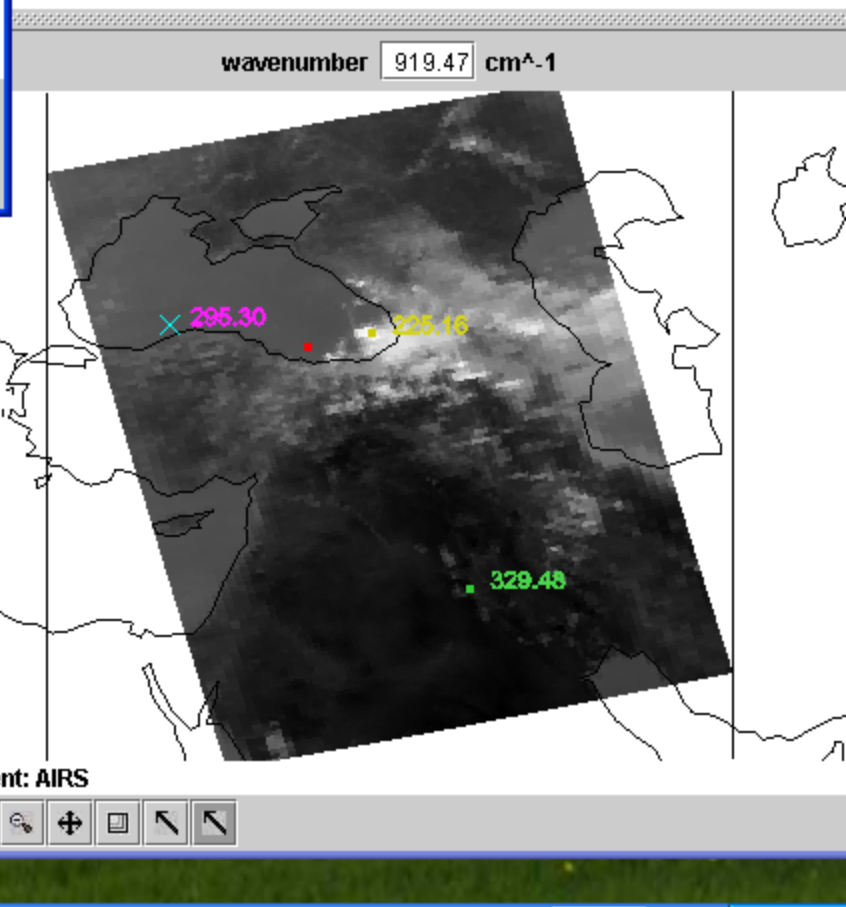
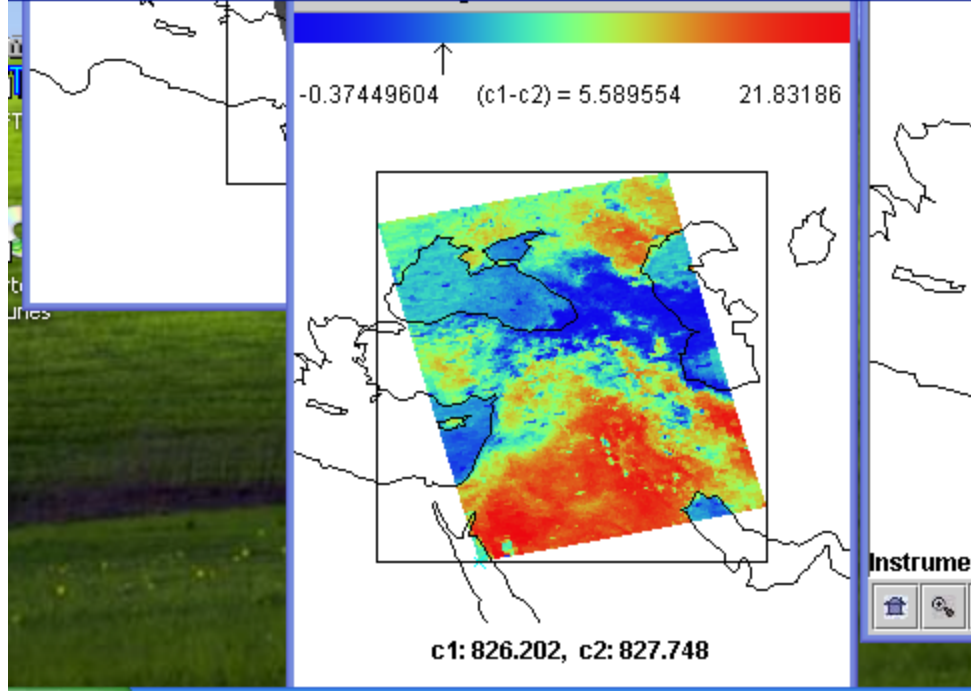
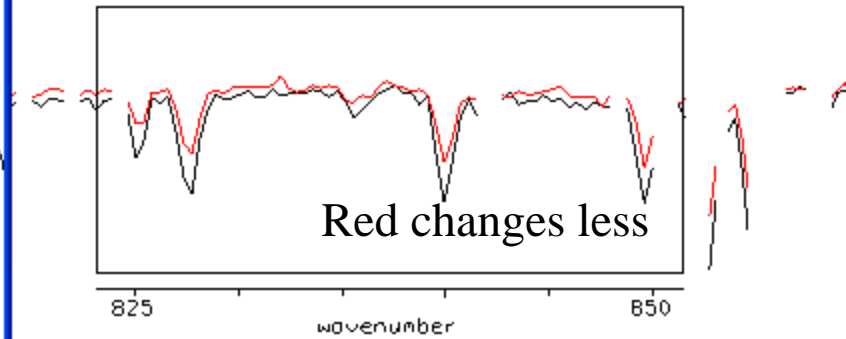
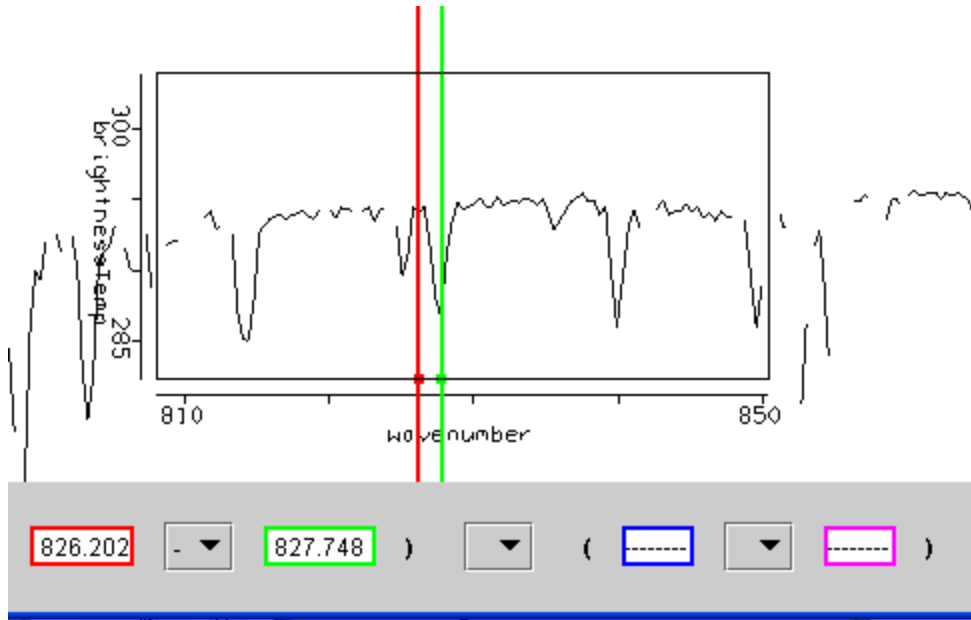
Lat = 31.015 Lon = 19.149

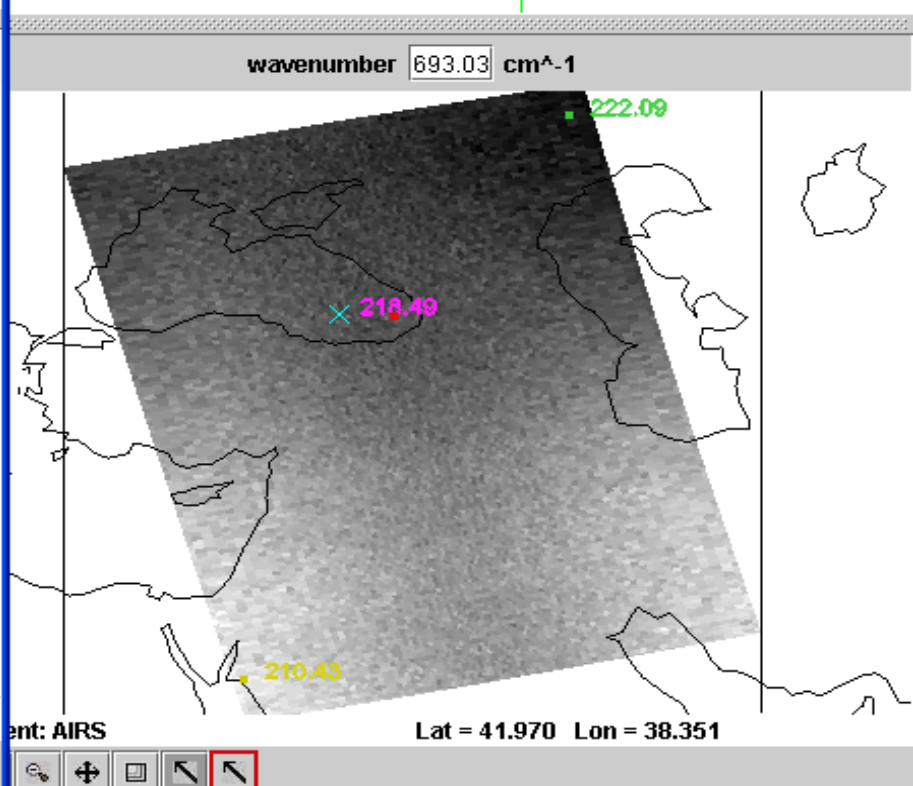
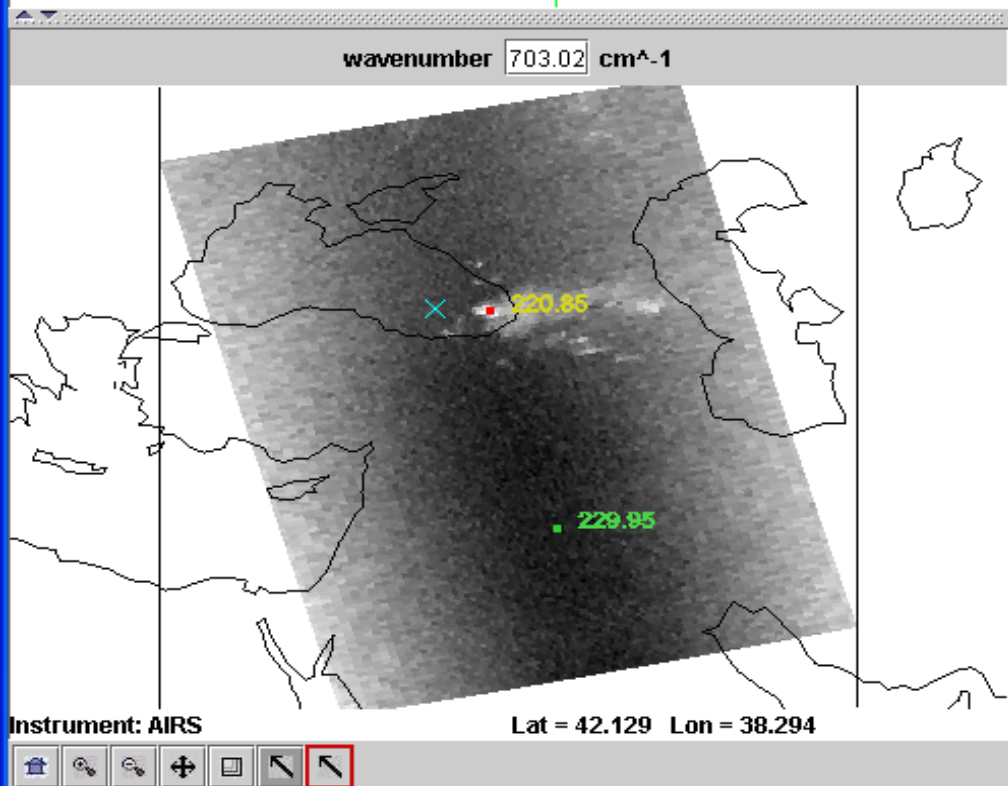
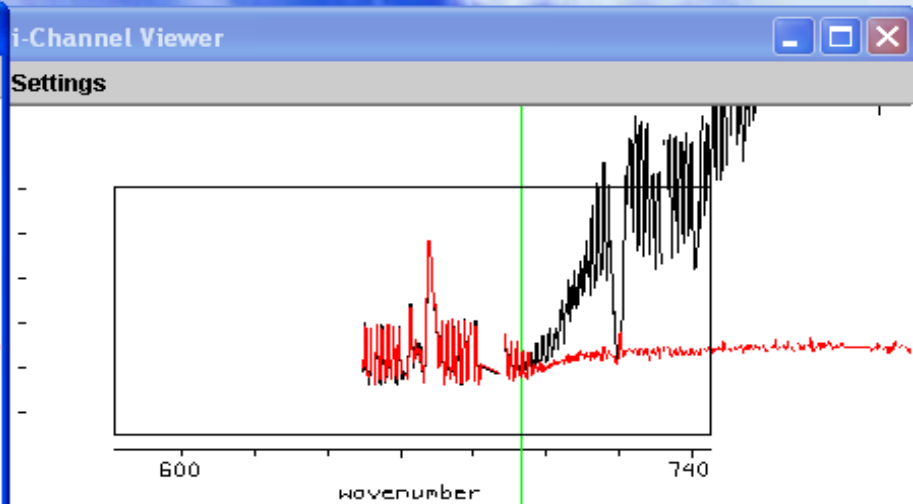
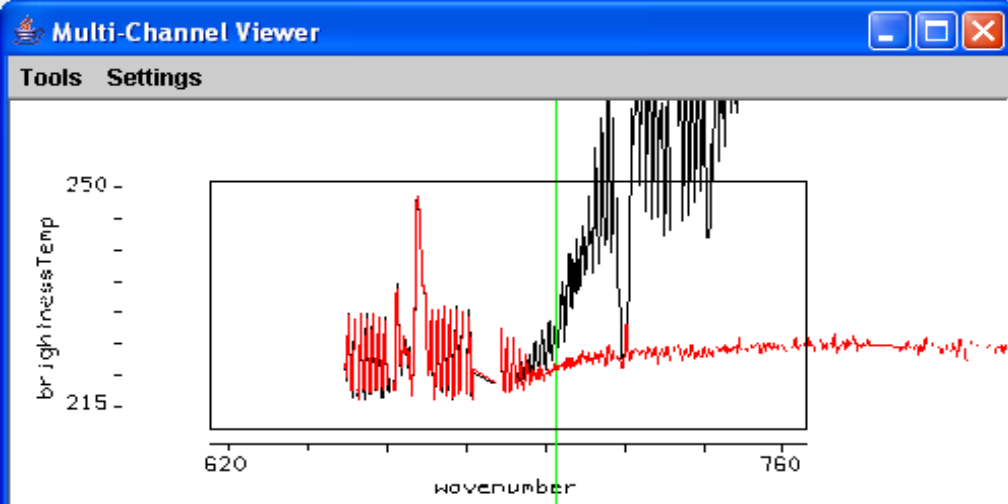




IASI sees
low level inversion
over land

Offline-Online in LW IRW showing low level moisture





Cld and clr spectra in CO₂ absorption separate when weighting functions sink to cloud level

MW

ATMS Design Challenge

AMSU-A1



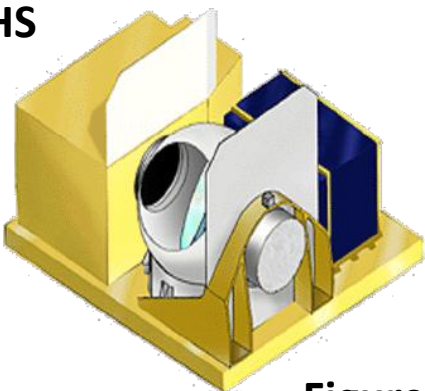
- 73x30x61 cm
- 67 W
- 54 kg
- 3-yr life

AMSU-A2



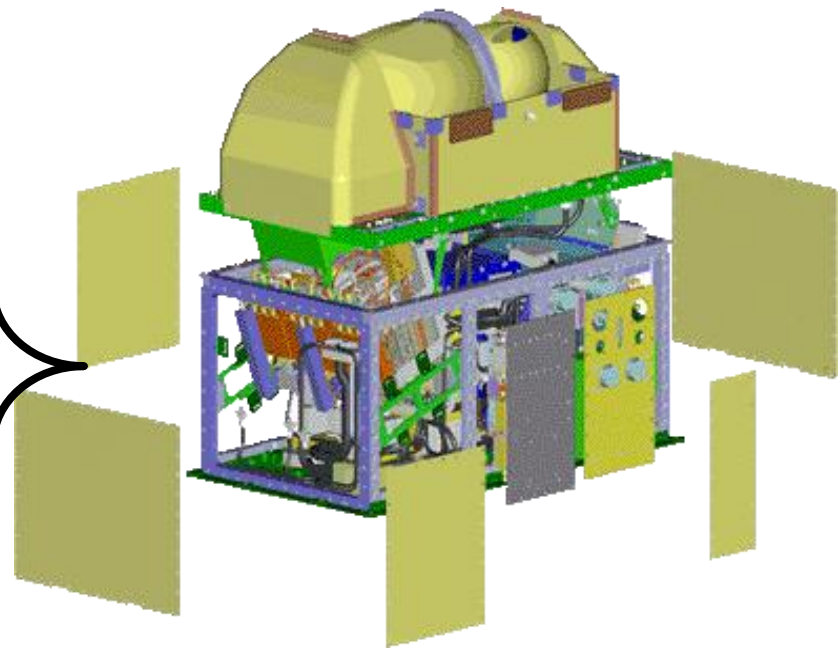
- 75x70x64 cm
- 24 W
- 50 kg
- 3-yr life

MHS



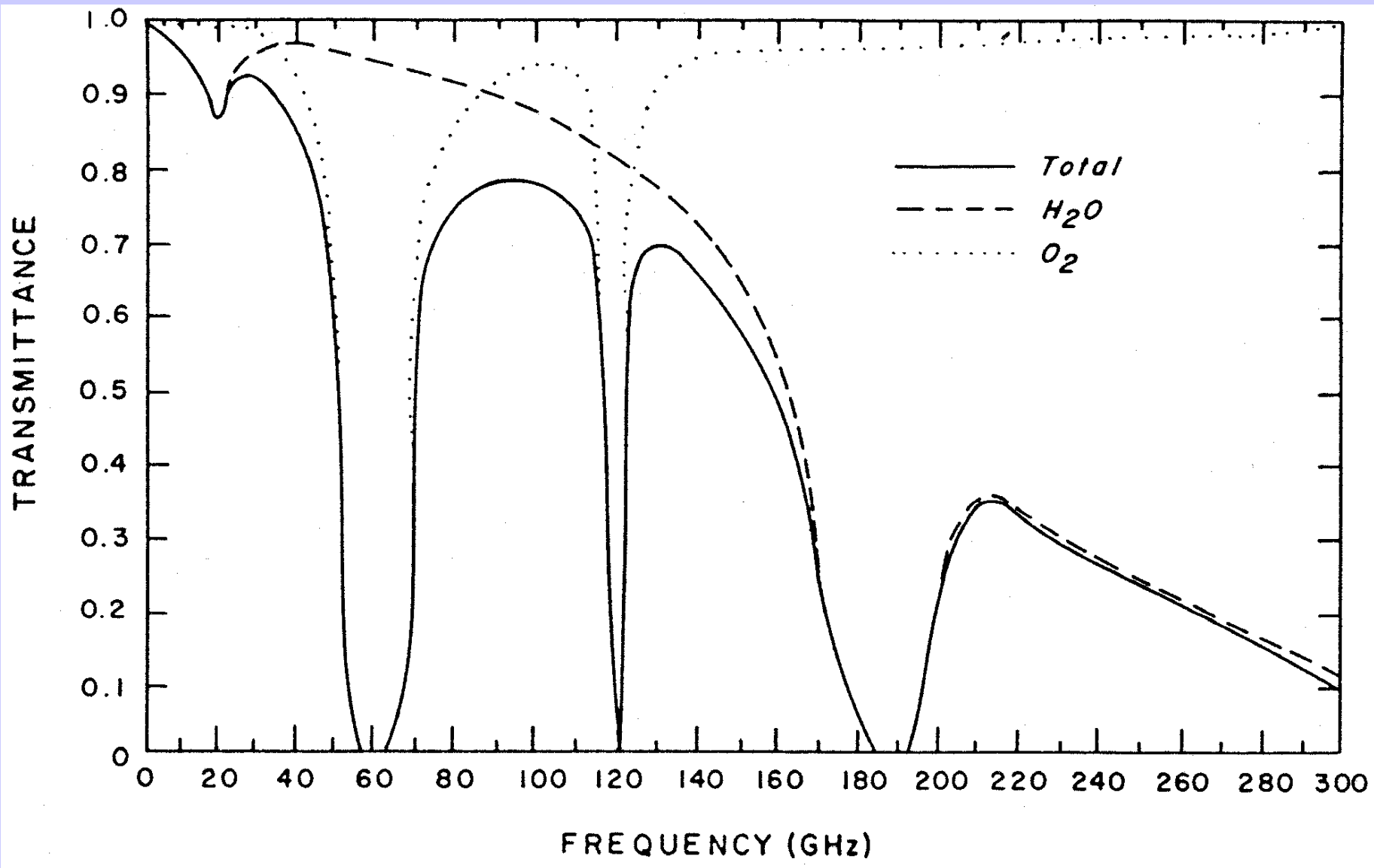
- 75x56x69 cm
- 61 W
- 50 kg
- 4-yr life

Reduce the volume by 3x



- 70x40x60 cm
- 110 W
- 85 kg
- 8 year life

Figure courtesy NGES, Azusa, CA



Radiation is governed by Planck's Law

$$B(\lambda, T) = \frac{c_1}{\lambda^5} \left[e^{-c_2/\lambda T} - 1 \right]^{-1}$$

In microwave region $c_2/\lambda T \ll 1$ so that

$$e^{-c_2/\lambda T} = 1 - c_2/\lambda T + \text{second order}$$

And classical Rayleigh Jeans radiation equation emerges

$$B_\lambda(T) \approx \left[\frac{c_1}{c_2} \right] \left[\frac{T}{\lambda^4} \right]$$

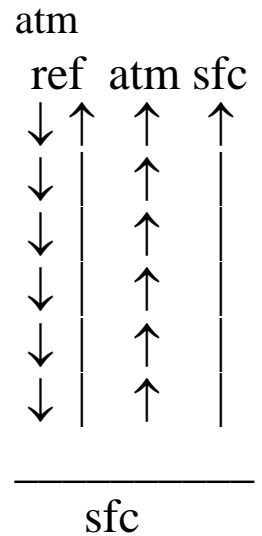
Radiance is linear function of brightness temperature.

Microwave Form of RTE

$$I_{\lambda}^{\text{sfc}} = \varepsilon_{\lambda} B_{\lambda}(T_s) \tau_{\lambda}(p_s) + (1-\varepsilon_{\lambda}) \tau_{\lambda}(p_s) \int_0^{p_s} B_{\lambda}(T(p)) \frac{\partial \tau'_{\lambda}(p)}{\partial \ln p} d \ln p$$

$$I_{\lambda} = \varepsilon_{\lambda} B_{\lambda}(T_s) \tau_{\lambda}(p_s) + (1-\varepsilon_{\lambda}) \tau_{\lambda}(p_s) \int_0^{p_s} B_{\lambda}(T(p)) \frac{\partial \tau'_{\lambda}(p)}{\partial \ln p} d \ln p$$

$$+ \int_{p_s}^0 B_{\lambda}(T(p)) \frac{\partial \tau_{\lambda}(p)}{\partial \ln p} d \ln p$$



In the microwave region $c_2/\lambda T \ll 1$, so the Planck radiance is linearly proportional to the temperature

$$B_{\lambda}(T) \approx [c_1 / c_2] [T / \lambda^4]$$

So

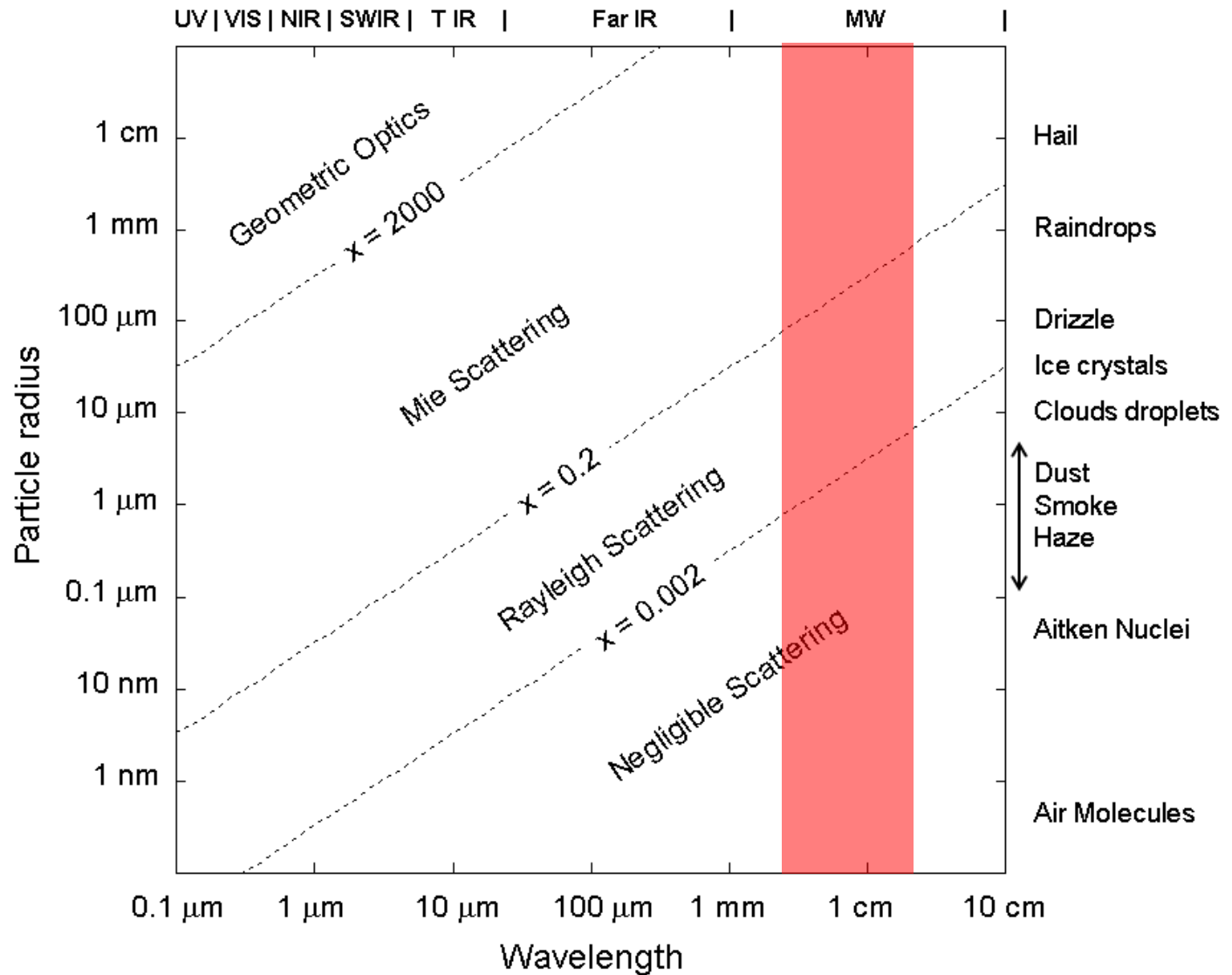
$$T_{b\lambda} = \varepsilon_{\lambda} T_s(p_s) \tau_{\lambda}(p_s) + \int_{p_s}^0 T(p) F_{\lambda}(p) \frac{\partial \tau_{\lambda}(p)}{\partial \ln p} d \ln p$$

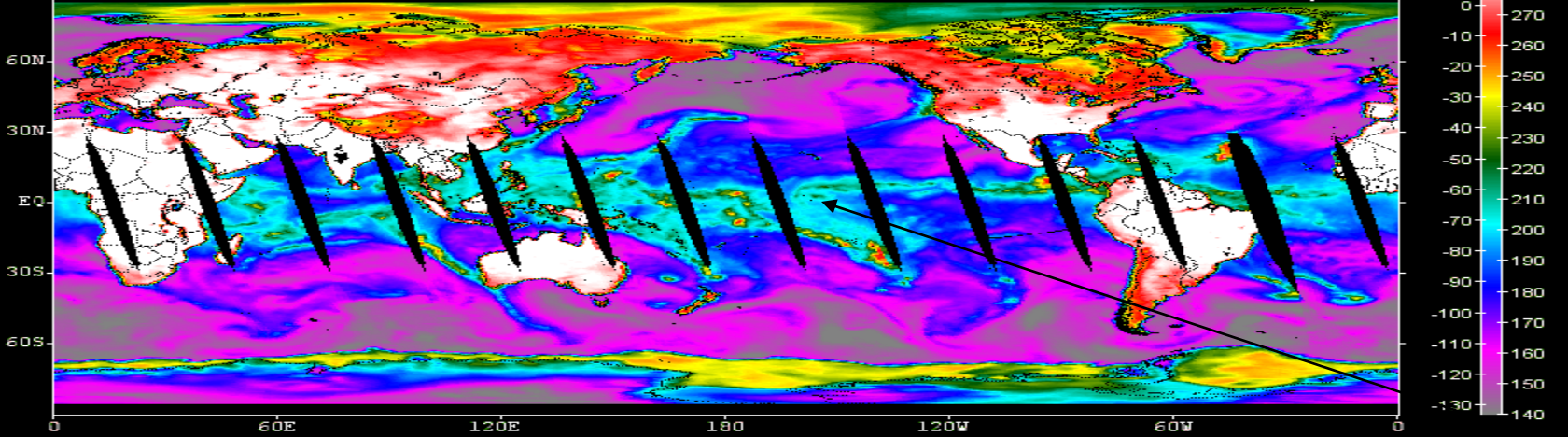
where

$$F_{\lambda}(p) = \left\{ 1 + (1 - \varepsilon_{\lambda}) \left[\frac{\tau_{\lambda}(p_s)}{\tau_{\lambda}(p)} \right]^2 \right\} .$$

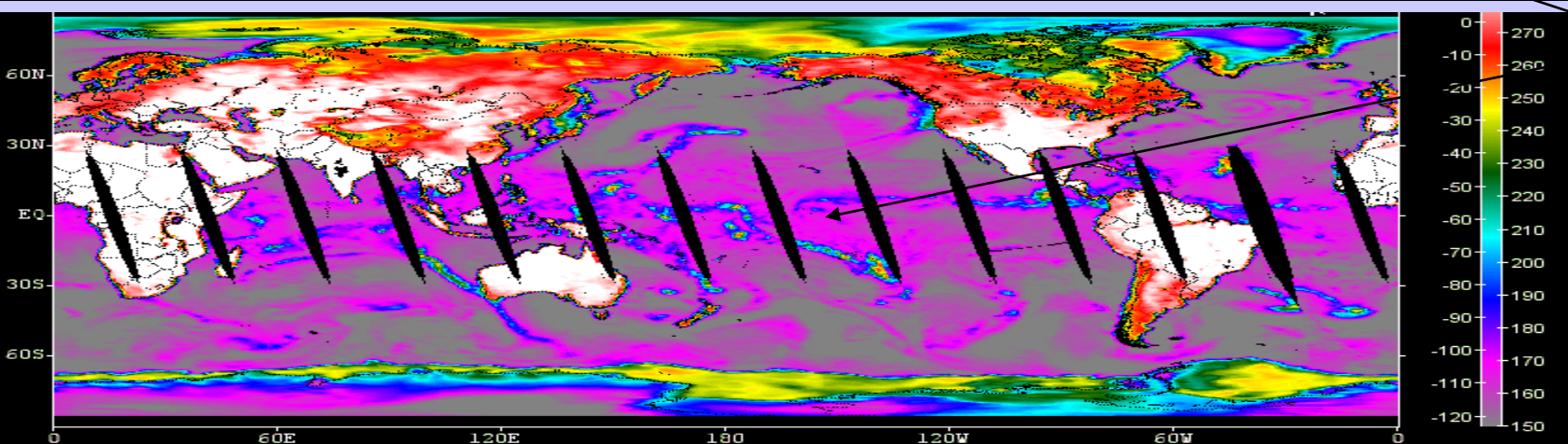
Scattering of MW radiation

□ Scattering regimes

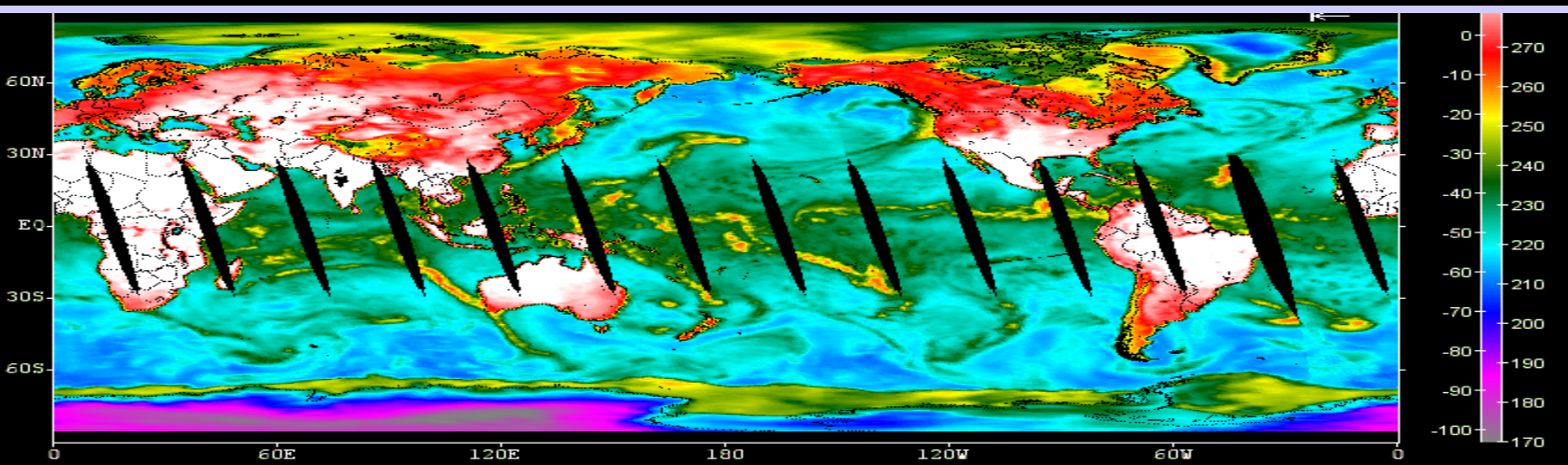




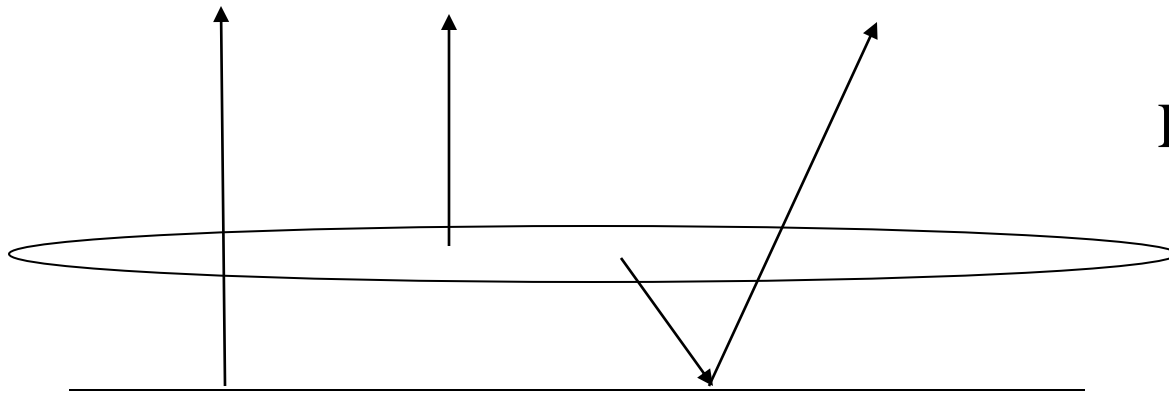
AMSU
23.8
dirty
window



atm Q
 warms
 BT
31.4
window



50.3
GHz



Low mist over ocean

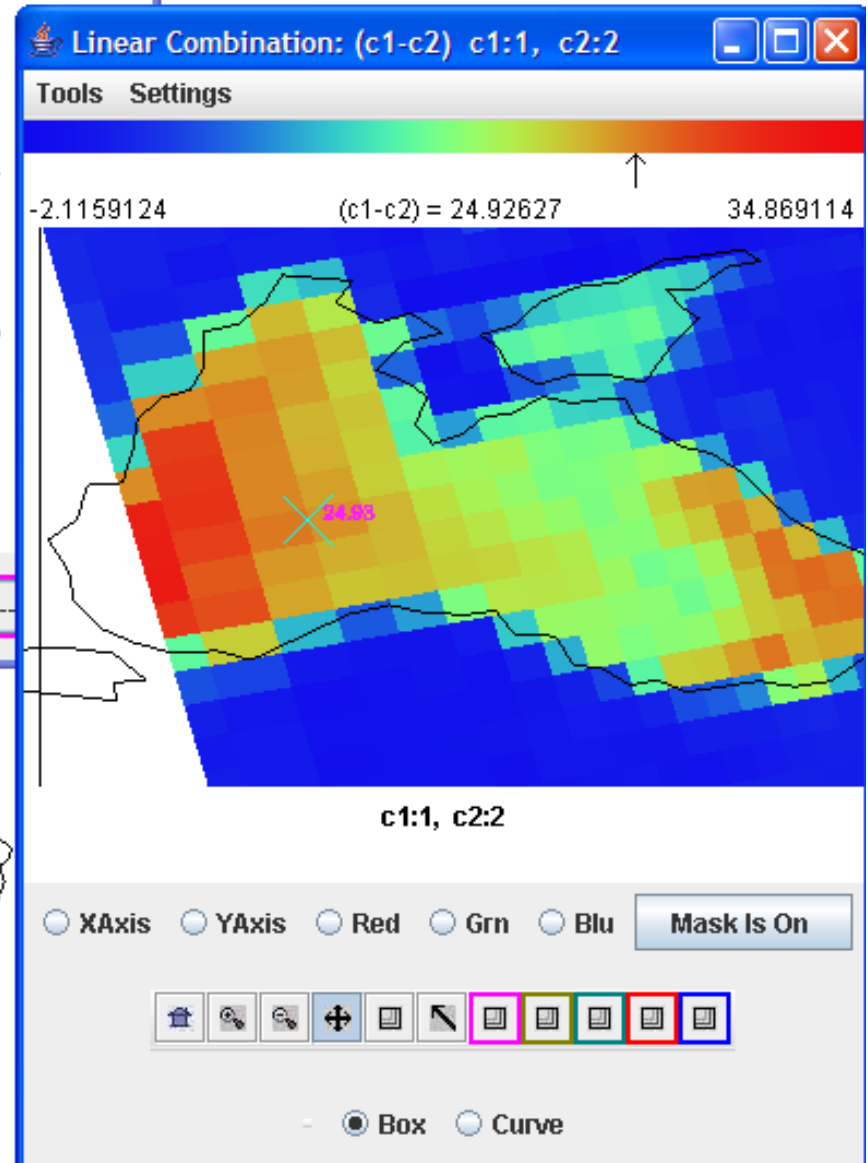
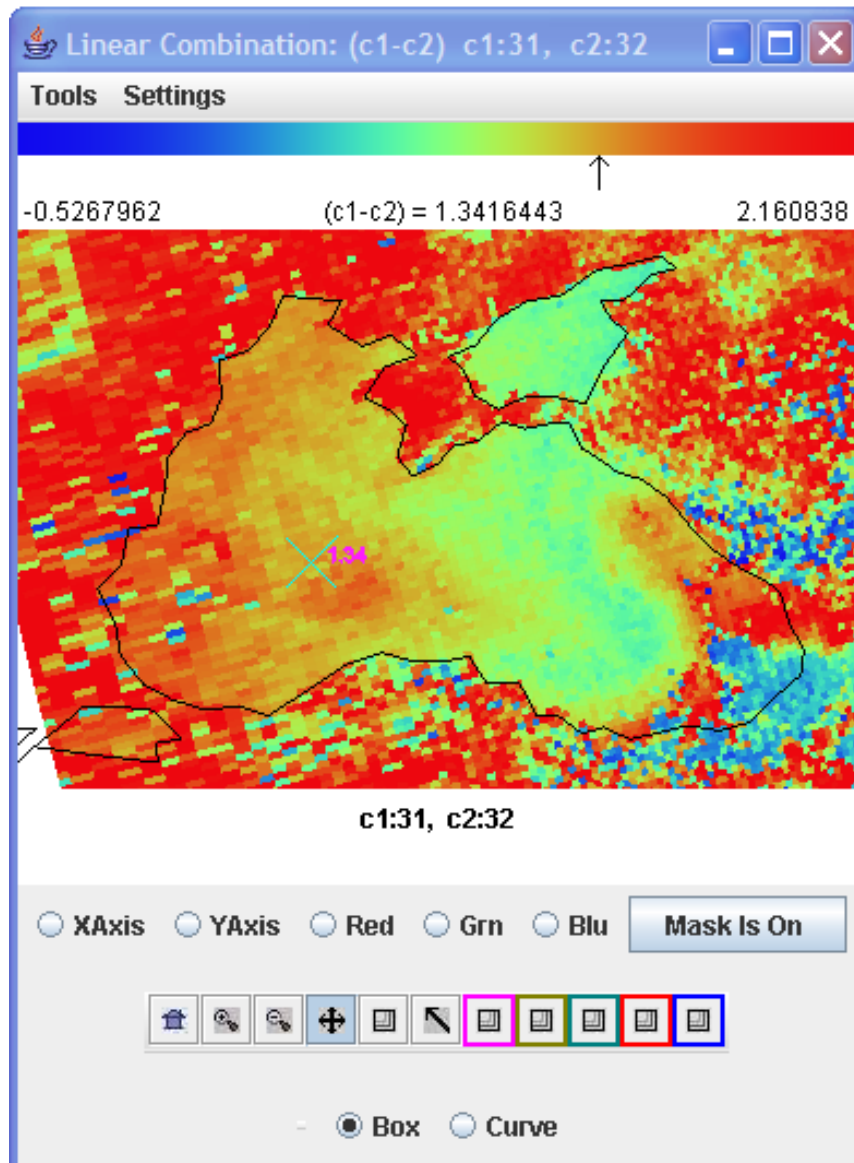
$$T_b = \epsilon_s T_s (1 - \sigma_m) + \sigma_m T_m + \sigma_m (1 - \epsilon_s) (1 - \sigma_m) T_m$$

So

$$\Delta T_b = - \epsilon_s \sigma_m T_s + \sigma_m T_m + \sigma_m (1 - \epsilon_s) (1 - \sigma_m) T_m$$

For $\epsilon_s \sim 0.5$ and $T_s \sim T_m$ this is always positive for $0 < \sigma_m < 1$

MW split window has larger signal for low level moisture than IR split window



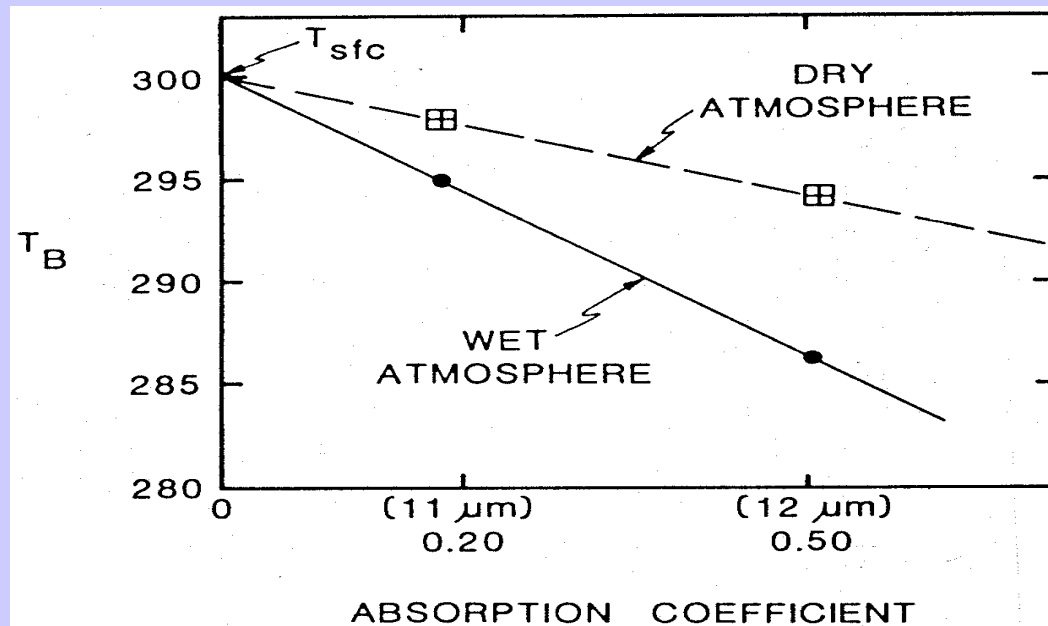
Moisture

Moisture attenuation in atmospheric windows varies linearly with optical depth.

$$\tau_\lambda = e^{-k_\lambda u} \approx 1 - k_\lambda u$$

For same atmosphere, deviation of brightness temperature from surface temperature is a linear function of absorbing power. Thus moisture corrected SST can be inferred by using split window measurements and extrapolating to zero k_λ .

Moisture content of atmosphere inferred from slope of linear relation.



Accuracy of Satellite Derived Met Parameters

T(p) within 1.5 C of raobs for 1 km layers

SST within 0.5 C of buoys

Q(p) within 15-20% of raobs for 2 km layers

TPW with 3 mm of ground based MW

TO3 within 30 Dobsons of ozone profilers

LI adjusted 3 C lower (for better agreement with raobs)

gradients in space and time more reliable than absolute

AMVs within 7 m/s (upper trop) and 5 m/s (lower trop)

CTPs within 50 hPa of lidar determination

Geopotential heights within 20 to 30 m

for 500 to 300 hPa

For TC, Psfc within 6 hPa and Vmax within 10 kts

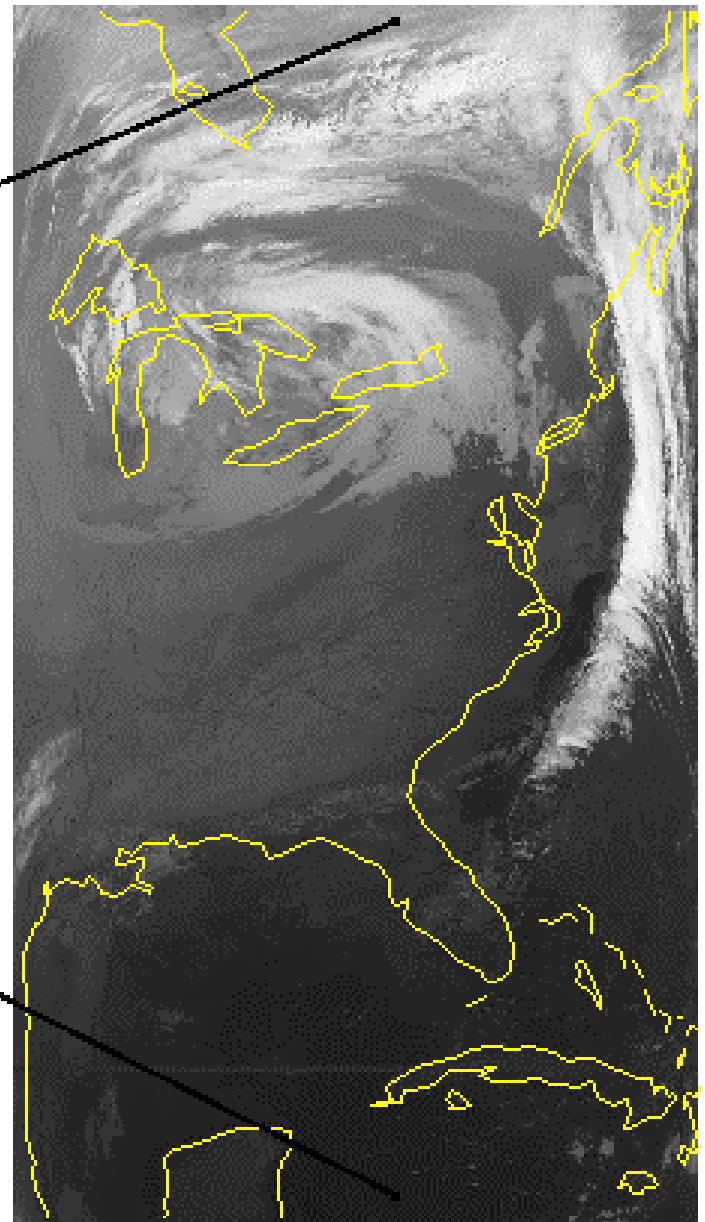
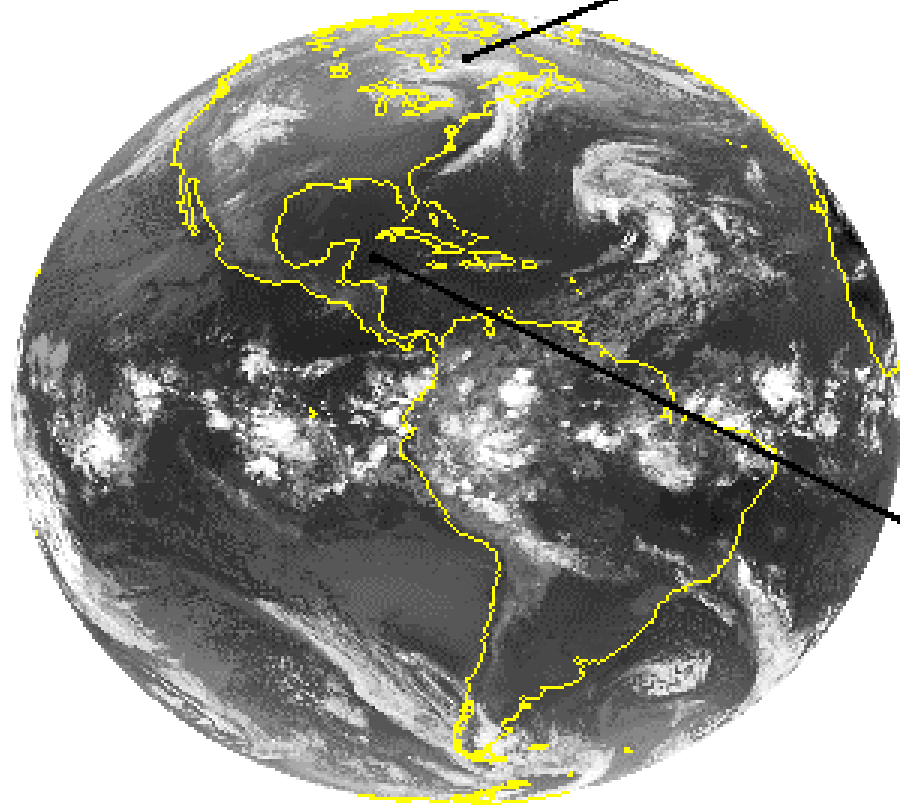
(from MW ΔT_{250})

Trajectory forecast 72 hour error reduction about 10%

Geo vs Leo

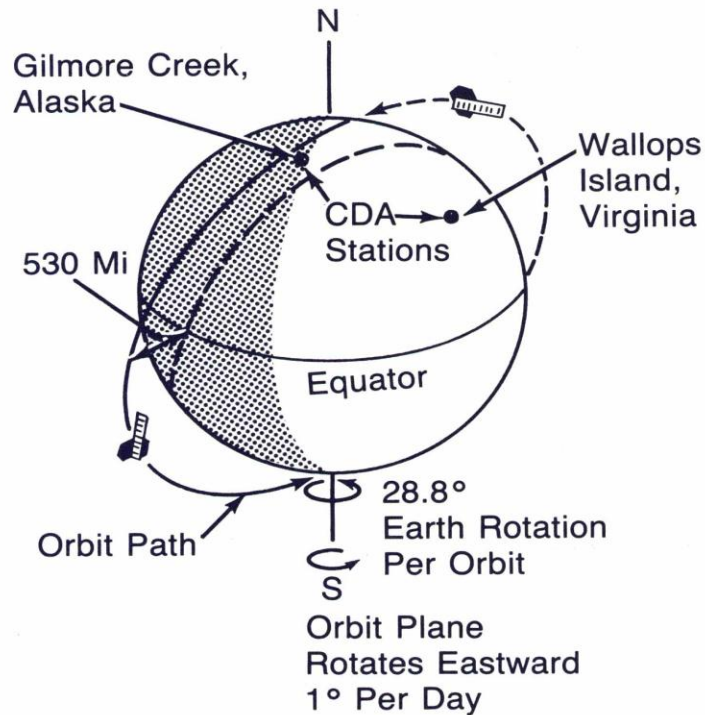


GEO vs LEO

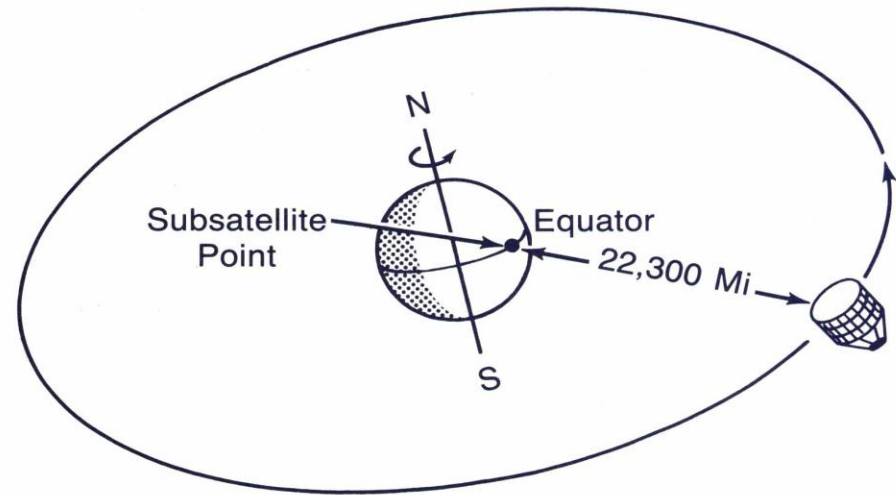


Polar (LEO) & Geostationary (GEO) Orbits

Polar Orbiting Satellites



Geostationary Satellites



Comparison of geostationary (geo) and low earth orbiting (leo) satellite capabilities

Geo

observes process itself
(motion and targets of opportunity)

repeat coverage in minutes
($\Delta t \leq 15$ minutes)

near full earth disk

best viewing of tropics & mid-latitudes

same viewing angle

differing solar illumination

visible, NIR, IR imager
(1, 4 km resolution)

IR only sounder
(8 km resolution)

filter radiometer

diffraction more than leo

Leo

observes effects of process

repeat coverage twice daily
($\Delta t = 12$ hours)

global coverage

best viewing of poles

varying viewing angle

same solar illumination

visible, NIR, IR imager
(1, 1 km resolution)

IR and microwave sounder
(1, 17, 50 km resolution)

filter radiometer,
interferometer, and
grating spectrometer

diffraction less than geo

Access to Data and HYDRA

Access to visualization tools and data

For hydra2 <ftp://ftp.ssec.wisc.edu/rink/hydra2/>

For MODIS data and quick browse images

<http://rapidfire.sci.gsfc.nasa.gov/realtime>

For MODIS data <http://ladsweb.nascom.nasa.gov/>

For AIRS data <http://daac.gsfc.nasa.gov/>

For VIIRS, CrIS, and ATMS data, orbit tracks, guide

<http://www.nsof.class.noaa.gov>

<http://www.ssec.wisc.edu/datacenter/npp/>

http://www.class.ncdc.noaa.gov/notification/faq_npp.htm

See tutorial "How do I order NPP data in CLASS (11/28/11)"

The Big Picture

Key Areas of Uncertainty **in Understanding Climate & Global Change**

- * Earth's radiation balance and the influence of clouds on radiation and the hydrologic cycle
- * Oceanic productivity, circulation and air-sea exchange
- * Transformation of greenhouse gases in the lower atmosphere, with emphasis on the carbon cycle
- * Changes in land use, land cover and primary productivity, including deforestation
- * Sea level variability and impacts of ice sheet volume
- * Chemistry of the middle and upper stratosphere, including sources and sinks of stratospheric ozone
- * Volcanic eruptions and their role in climate change

Global Energy Flows $W m^{-2}$

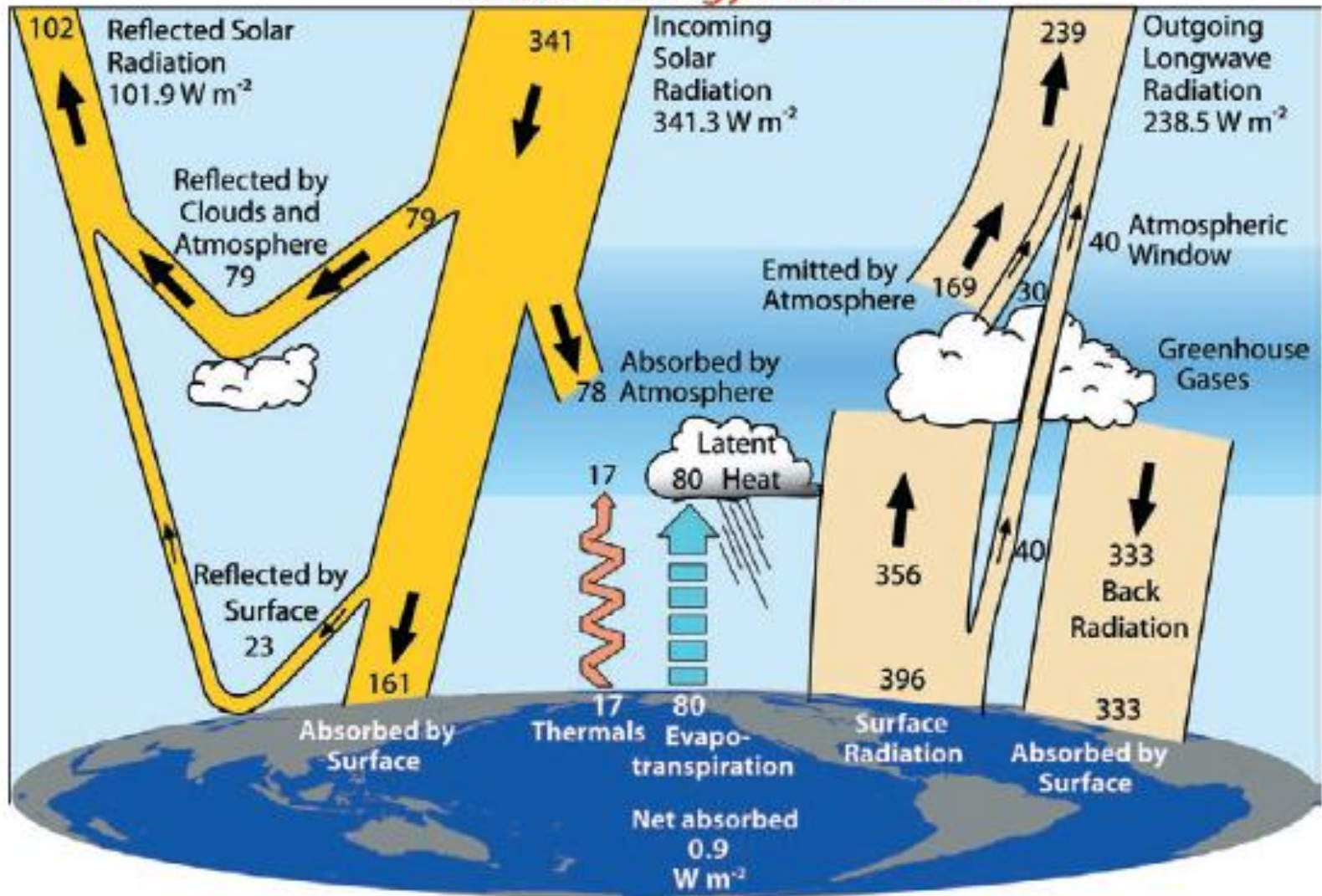
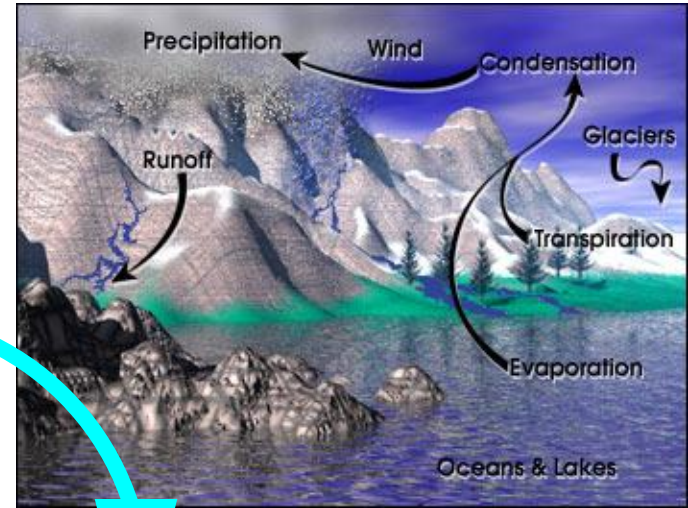
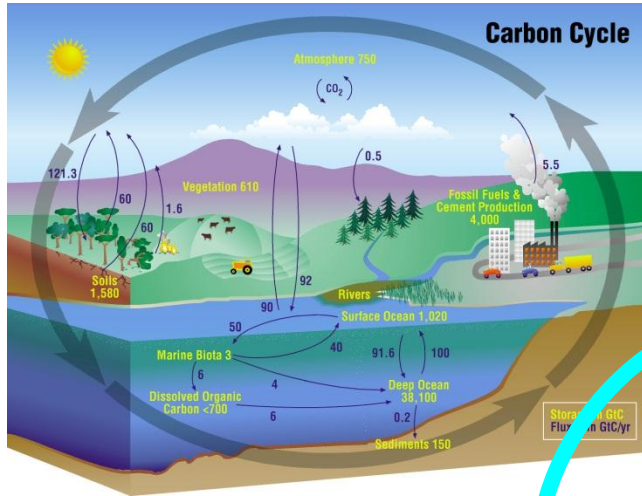


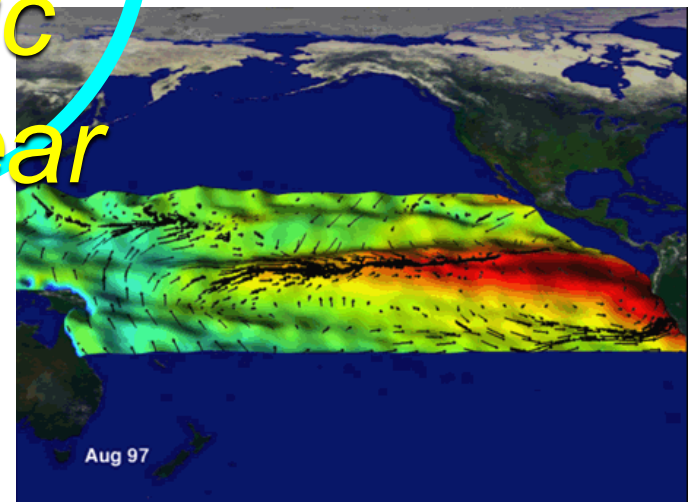
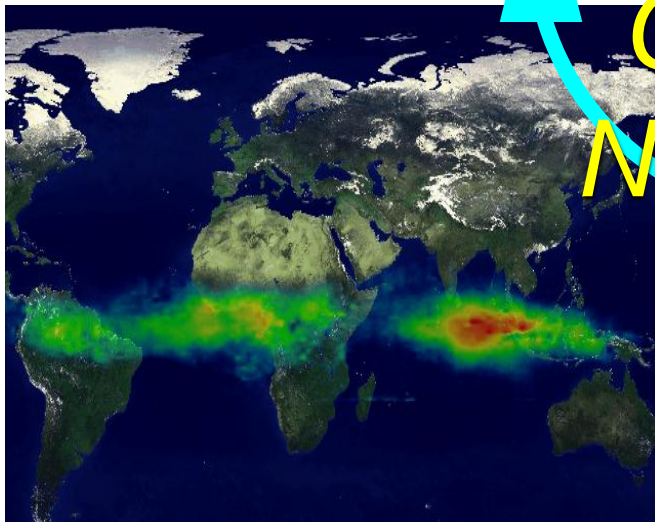
FIG. 1. The global annual mean Earth's energy budget for the Mar 2000 to May 2004 period ($W m^{-2}$). The broad arrows indicate the schematic flow of energy in proportion to their importance.

Major Climate System Elements



*Coupled
Chaotic
Nonlinear*

Atmosphere and Ocean
Dynamics



Spectral Signatures